University of Huddersfield Repository

Markham, H.M.

Determination of Accurate Temperature and Enthalpy Measurements using Differential Scanning Calorimetry

Original Citation

Markham, H.M. (2014) Determination of Accurate Temperature and Enthalpy Measurements using Differential Scanning Calorimetry. Masters thesis, University of Huddersfield.

This version is available at http://eprints.hud.ac.uk/id/eprint/28697/

The University Repository is a digital collection of the research output of the University, available on Open Access. Copyright and Moral Rights for the items on this site are retained by the individual author and/or other copyright owners. Users may access full items free of charge; copies of full text items generally can be reproduced, displayed or performed and given to third parties in any format or medium for personal research or study, educational or not-for-profit purposes without prior permission or charge, provided:

- The authors, title and full bibliographic details is credited in any copy;
- A hyperlink and/or URL is included for the original metadata page; and
- The content is not changed in any way.

For more information, including our policy and submission procedure, please contact the Repository Team at: E.mailbox@hud.ac.uk.

http://eprints.hud.ac.uk/

Determination of Accurate Temperature and Enthalpy Measurements using Differential Scanning Calorimetry

Hayley Marie Markham

September 2014

Department of Chemical and Biological Sciences

Queensgate Campus, Huddersfield. HD1 3DH

This thesis is submitted to the University of Huddersfield in fulfilment of the requirements for the degree of Master of Philosophy.

Acknowledgements.

It would not have been possible to write this thesis without the help, support, and guidance from those who have knowingly or otherwise been there when it was needed the most.

This Thesis would not have been possible without the support of my supervisors, Professor Edward Charsley and Dr Gareth Parkes, nor without the support of my work colleagues at the time; Professor Peter Laye, and James Rooney a.k.a ‘Jim’.

A final word of thanks should go to the University of Huddersfield for providing the opportunity to further my education as part of their staff development programme.

Part of this work was also supported by the UK Ministry of Defence through contracts with QinetiQ Ltd, and by armasuisse, Switzerland.

Abbreviations

Acronym	Definition
TA	Thermal analysis
ASTM	American Society for Testing and Materials
DSC	Differential Scanning Calorimetry
DTA	Differential Thermal Analysis
DSC_{std}	DSC standard reference material
endo	Endothermic event
exo	Exothermic event
GEFTA	Die Gesellschaft für Thermische Analyse e.V.
HF-DSC	Heat flux DSC
ICTAC	International Confederation for Thermal Analysis and Calorimetry
ISO	International Organisation for Standardisation
ITS-90	International Temperature Scale 1990
LGC	Laboratory of the Government Chemist
NIST	National Institute for Standards and Technology
Organic Material $_{(D)}$	Indicates organic material is a DSC reference material
Organic Material $_{(Mpt)}$	Indicates organic material is a melting point reference material
PC-DSC	Power Compensated DSC
UFO	Unidentified Flying Object

Symbol	Definition
°C	Degrees celsius (Temperature)
C_p	Heat capacity
$dT_e / d\beta$	Heating rate dependence
R_{th}	Thermal resistance
t	Time
T_{cert}	Certificate temperature
T_e	Extrapolated onset temperature
T_o	Onset temperature
T_p	Peak temperature
T_R	Reference temperature
T_S	Sample temperature
T_{std}	Temperature standard reference material
T_{step}	Equilibrium temperature using stepwise isothermal method
$T_{\beta=0}$	Equilibrium temperature using zero heating rate (extrapolated) method
$T_{\beta=0\ (FHR)}$	Equilibrium temperature using extended zero heating rate method
ΔP	Change in power
ΔT	Change in temperature
κ	Calibration factor
Φ	DSC signal

List of Figures

List of Tables

Abstract

This thesis shows that the equilibrium transition temperatures of materials can be accurately determined using two developed methodologies designed to be used with differential scanning calorimeters. These methods are the extrapolation to zero heating rate and a stepwise isothermal method. The use of these methods allows for the instrument, which is typically scanning in nature to produce accurate temperature values under near equilibrium conditions. By employing the DSC methodologies for accurate temperature measurements it has been possible to determine a range of temperatures of transition and fusions under near equilibrium conditions for inorganic potassium salts (nitrate, perchlorate, and dinitramide), and rubidium salts (nitrate, and dinitramide) all of which have transitions of pyrotechnic interest. In cases where decomposition occurs at slower heating rates, the modification of the extrapolation to zero heating method to incorporate the use of faster heating rates above 10°C min^{-1} has enabled accurate temperatures of transition to be determined. In addition, this thesis also explores the use of materials with solid-solid transitions susceptible to thermal history such as potassium nitrate and re-evaluates the suitability for use in DSC calibration.

The close proximity in temperature of the LGC Limited DSC standards indium and diphenylacetic acid, has enabled a direct assessment to be made of any differences resulting from the use of a metal or an organic substance in the calibration of DSC equipment. These measurements clearly established that indium may be used as a calibrant when making accurate equilibrium temperature and enthalpy measurements on organic materials in the same temperature range. Accurate enthalpy measurements have also been made on the above inorganic nitrates and perchlorates and measurements on the transitions of rubidium nitrate have established that equivalent values are given by heat flux and power compensated instruments. Enthalpy measurements on organic DSC calibration standards in the range 42-147 °C using a power compensated instrument demonstrated that there was no significant error in using indium as a single point calibrant for measurements on the fusion of organic materials at lower temperatures.

Chapter 1 Introduction

1.1 Project Aims

The aim of the project is to provide an evaluation of two methods designed to determine accurate temperatures of transition under near equilibrium conditions. Since DSC is a relative technique because of its dynamic temperature characteristics the measurements are not typically made in thermal equilibrium. The two methods for accurate temperature measurement include the extrapolation to zero heating rate and the isothermal stepwise heating methods.

To validate the two methods the equilibrium temperature of fusion of commercial forms of indium will be measured using two independent heat flux DSC systems. Once validated more accurate values for the equilibrium temperatures of transition for solid-solid transitions of inorganic substances spanning the temperature range 160-300°C will be measured. These materials which include $RbNO_3$, KNO_3 and $KClO_4$ exhibit one or more transitions of interest.

Organic DSC standards provide the opportunity of calibrating DSC equipment in a temperature range for which there are no suitable metal calibrants. A range of materials will be measured spanning the temperature range 40-150°C and with this the temperature dependence of the calorimetric results can be assessed. In the measurement of the fusion of diphenylacetic acid its close proximity to the fusion of indium will enable a direct assessment to be made of any differences resulting from the use of a metal or an organic substance in the calibration of DSC equipments.

An extended extrapolation to zero heating rate study to include faster heating rates in the range 10-50°C min^{-1} will be made to provide a more accurate measurement of equilibrium temperatures of transition for materials which are susceptible to decomposition under slow heating rates.

In addition to accurate temperature measurements, attempts have also been made to improve the accuracy of measured enthalpic determinations using DSC.

1.2 Thermal Analysis

Thermal analysis (TA) is defined as the study of the relationship between a sample property and its temperature as the sample is heated or cooled in a controlled manner.[1]

In thermal analysis a property or a range of properties of interest are monitored as a sample is heated or cooled at a linear rate. There are several thermal analysis techniques that lend themselves to measure specific properties, with some of the more common place ones being listed in Table 1. These can be used to study specific properties exhibited by samples either independently such as thermogravimetry (TG) or in conjunction with other techniques such as thermogravimetry-evolved gas analysis (TG-EGA).

Table 1. ***A list of common thermal analysis techniques and the sample properties for which they are used to measure.***

Sample Property	Technique	Abbreviation
Temperature Difference	Differential Thermal Analysis	DTA
Heat Flow	Differential Scanning Calorimetry	DSC
Mass	Thermogravimetry	TG
Gas Flow	Evolved Gas Analysis	EGA
Dimensional and Mechanical	Dynamic Mechanical Analysis	DMA
	Thermomechanical Analysis	TMA
Optical	Thermooptometry	Hotstage

Differential scanning calorimetry (DSC) is by far the most widely used of the thermal analysis techniques in both academia and industry. It can, in principle, study any reaction that takes place with a change in enthalpy and is relatively easy to use.

These reactions include, but are not limited to solid-solid phase transitions, fusion, crystallisation, curing and decomposition reactions. Some of the more important

areas of application for DSC are in the routine study of pharmaceuticals and polymers, however, the technique is extensively used in the study of a wide range of materials.

The fundamental attributions of a DSC measurement are in the determination of temperature and enthalpy changes of a reaction, however, the accuracy and precision of the measurements made are entirely dependent on both the availability of suitable materials and the experimental protocols for the calibration of the equipment.[2]

DSC has been increasingly implemented for use as a quality assurance technique with an increasing emphasis on the need for improved calibration techniques. Methods and materials for calibration have developed over time from metal to inorganic materials however, problems arising in the suitability of the calibration material in relation to the sample to be measured can result in the rejection of an otherwise satisfactory material. In an industrial setting this may lead to cost penalties and loss of credibility for the manufacturer.[3]

1.3 History of the Differential Scanning Calorimeter

The theory of the heating rate change curve was first introduced by LeChatelier providing foundation blocks from which thermal analysis techniques would stem from. Early works into melting point determinations of some of the materials studied in this thesis can be dated as far back as 1880.[4]

Advancements in knowledge and the design of more sophisticated instrumentation, thermal analysis expanded quite swiftly from simple temperature measurements into systems that could provide more in-depth information into a samples' thermal behaviour. In 1945 early development work by Speil on the DTA of clays led to the considerations of obtaining meaningful enthalpic data from a DSC curve.[5] But it wasn't until the development of DSC in the early 1960's that the direct calorimetric measurement of the energies of transition of a sample were measured which meant that quantitative data was obtainable for much smaller sample sizes at much faster heating rates.[6]

Of the many manufacturers and models on the market there are in principle only two types of commercial DSCs available; these are the heat flux DSC (HF-DSC) and the power compensated DSC (PC-DSC). What differentiates between the HF-DSC and the PC-DSC systems is the method in which they derive a heat flow signal. This is discussed further in Sections 1.4.2 and 1.5.2.

Regardless of its operating principle a DSC system can be broken down into three major components, a source of heat (the furnace), a measurement source (thermocouples) and controllers (software).

1.4 Heat Flux DSC

Heat flux DSC is a widely accepted term used in modern day thermal analysis to describe a variant of DSC instrumentation. Sometimes it is referred to as quantitative DTA.

1.4.1 Heat Flux Furnace Design

The main identifying component of a DSC that differentiates between the operating principles of HF-DSC and PC-DSC systems is its measurement cell, how its furnace is constructed and how it controls the application of heat to both the sample and reference materials. The principle behind the heat flux DSC measurement system is such that it is able to derive the heat flow signals of both a sample and a reference material by measuring a temperature differential between thermocouples and mathematically converting the signals into heat flow data. A typical schematic representation of the measuring cell of a HF-DSC is given:

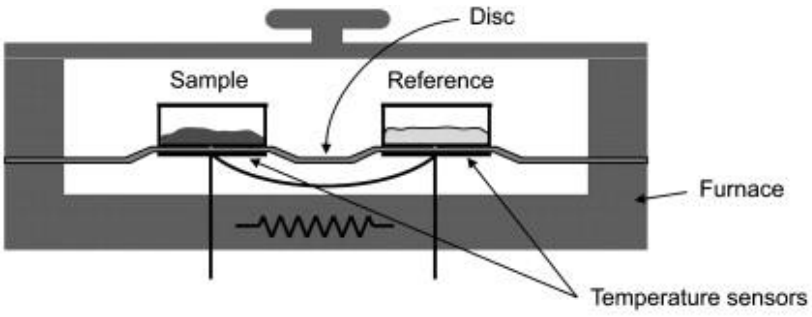

Fig. 1. ***A cross section of a heat flux DSC measuring cell from a TA Instruments DSC2920.***[7]

Within the measurement cell of a heat flux DSC heat is supplied from a single furnace generally constructed of a highly conductive metal such silver that encapsulates the DSC head, forming a chamber. A continuous flow of an inert gas is also used to purge the measurement cell which facilitates in the conduction of heat.

The measurement source (thermocouples) in a heat flux system are arranged so that they are located directly on or under a plate on which the sample and reference crucibles are placed. This is also referred to as the DSC head. The design of the DSC head can differ greatly amongst manufacturers although the method of deriving the raw signal remains the same.

1.4.2 Heat Flux DSC Signal Generation

Signals are generated when a sample is heated (or cooled). Heat is continually applied at a linear (or programmable) rate to the furnace until changes in temperature (ΔT) between the sample thermocouple (T_S) and reference thermocouple (T_R) are recorded. At the point of change the system will always try to maintain a thermal equilibrium between both T_S and T_R and will either supply more heat to the furnace or stop heating in an attempt to return T_S and T_R to equilibrium.

In general T_R is either an inert material such as alumina powder or a clean empty crucible.

The changes in temperature ($\Delta T = T_S - T_R$). are subsequently converted to a DSC signal (Φ) by dividing ΔT by the thermal resistance of the system R_{th} and applying a calibration factor κ. The DSC signal is then either plotted out in relation to temperature or time to produce a DSC curve.

The thermal resistance R_{th} is a factor that is predetermined by the cell design (amongst other contributing factors) and is a fixed value incorporated into the measurement software which cannot be modified by the operator. The calibration factor κ however, is changeable by the operator and can be accountable for many errors observed in DSC measurements due to poor calibration practices. The factor κ is generated mathematically by calculating differences between true values relating to a reference material which are stored within the software to those measured and inputted by the operator.

1.5 Power Compensated DSC

The power compensated DSC (PC-DSC) was first developed by M. J. O'Neill and the Perkin Elmer Corporation in the early 1960's after which an article on the development of a scanning calorimeter was published, entitled 'The Analysis of a Temperature-Controlled Scanning Calorimeter'.[8] This paper showed that the control of heat to and from individual furnaces containing the sample and reference allowed a much higher degree of control in maintaining thermal equilibrium during enthalpy changes.

1.5.1 Power Compensated Furnace Design

The measurement cell of the power compensated system is arranged so that the reference and sample measuring cells have separate heaters as opposed to the single heater design of the heat flux DSC.

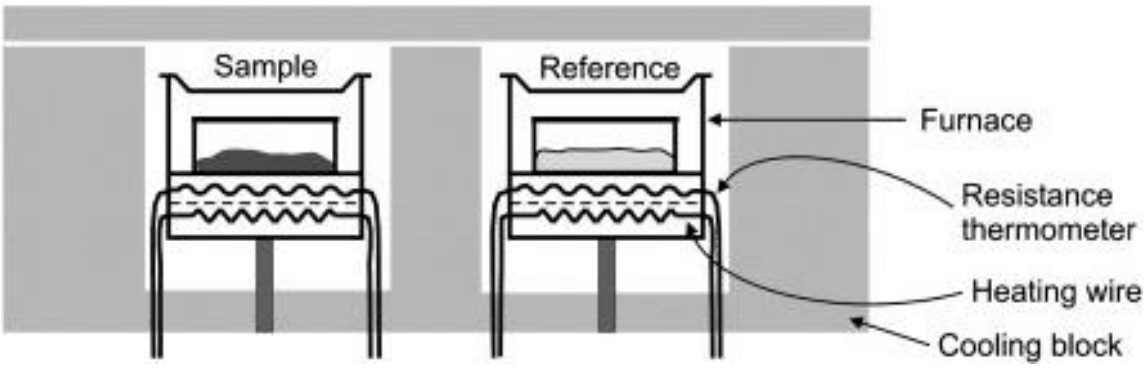

Fig. 2. ***Cross sections of power compensated DSC measuring cells.***[7]

1.5.2 Power Compensated Signal Generation.

During an experiment, the power supplied to each heater is continually adjusted so that the temperature difference ΔT between the sample and the reference is kept at zero (the “thermal null state”).[9]

The amount of power required to compensate the system ΔP is proportional to the calculated temperature ΔT therefore no complex calculations are necessary. The DSC signal (Φ) is then determined from $\Phi = \kappa . \Delta T$, where κ is a predetermined calibration constant from prior calibration of the machine.

1.6 DSC Curve Interpretation

When a sample is analysed using DSC, a thermal analysis curve is generated showing enthalpy and other changes as a function of time or temperature. The curve can indicate a range of thermal properties as a combination of peaks, troughs and deflections and are often discussed in the terms of an ‘event’.

These ‘events’ can either be in the form of a positive deflection (above the baseline) or a negative deflection (below the baseline).

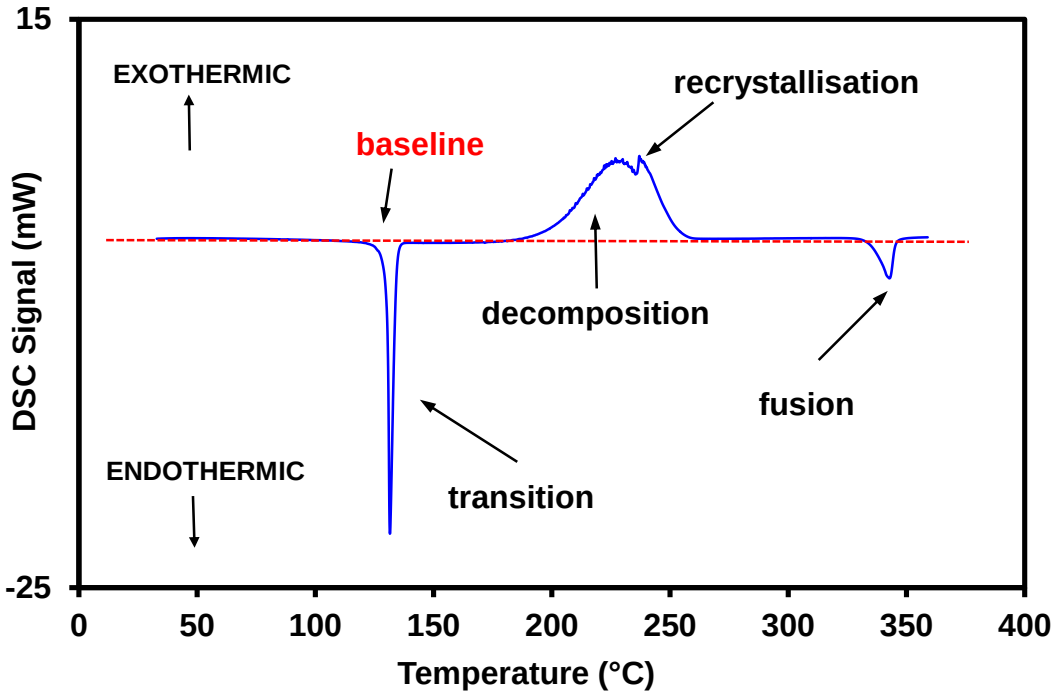

Fig. 3. ***The use of KDN-1 (Fig. 7273) to illustrate events observed on a DSC curve.***

Positive deflections seen in a DSC curve are attributed to exothermic changes whereby the change in the sample results in the emission of heat into the surroundings i.e. ΔT is +positive. Examples of exothermic events include decomposition reactions, recrystallisation, and freezing.

Negative deflections are attributed to endothermic changes in the sample where heat is absorbed from the surroundings in order for changes to occur i.e. ΔT is -negative. Examples of endothermic events include melting, vaporisation, and also solid-solid phase changes.

When interpreting a DSC plot it is important that the direction of the endotherm or the exotherm is noted to avoid confusion as different software programmes have their own preferences as to whether the exotherm is displayed either up or down. The area of a peak is directly proportional to the energy required or released by a process however, accurate measurement of this area relies on the construction a suitable baseline.

1.6.1 Baseline Construction

The term “baseline” is used to describe the response of the instrument without any sample influence. In the determination of accurate temperatures the choice of the initial baseline style is less critical, however, in the determination of accurate enthalpies the suitability of the baseline placement and its construction is paramount.[10-11] Some of the baseline constructions available within the commercial software which were used include:

Line (linear): A straight line connecting the two limits on the measurement curve. Used typically for reactions which do not produce abrupt c_p changes.

Integral Tangential: A baseline is generated in an iteration process in which the integral between the curve and baseline is calculated. The conversion calculated from the integration between the evaluation limits on the measured curve is normalised. This bow-shaped or s-shaped baseline is based on the tangents made on the left and the right of the event. The Integral tangential construction is typically used in the measurement of events with significant C_p changes.

Integral Horizontal: Measured in a similar way to the integral tangential baseline, however, horizontal lines at the left and right limits on the measurement curve are used as the tangents for the baseline. This construction is generally used in the event of a considerable heat capacity change such as decomposition or vaporisation.

The change in the baseline before and after a process often relates to the heat capacity of the sample which can change on melting, decompositions, etc., although often to only a small extent. It is sometimes necessary to magnify the curve to enable the correct baseline construction to be used. An example of the errors inherent in enthalpy measurements when selecting baseline constructions is given below.

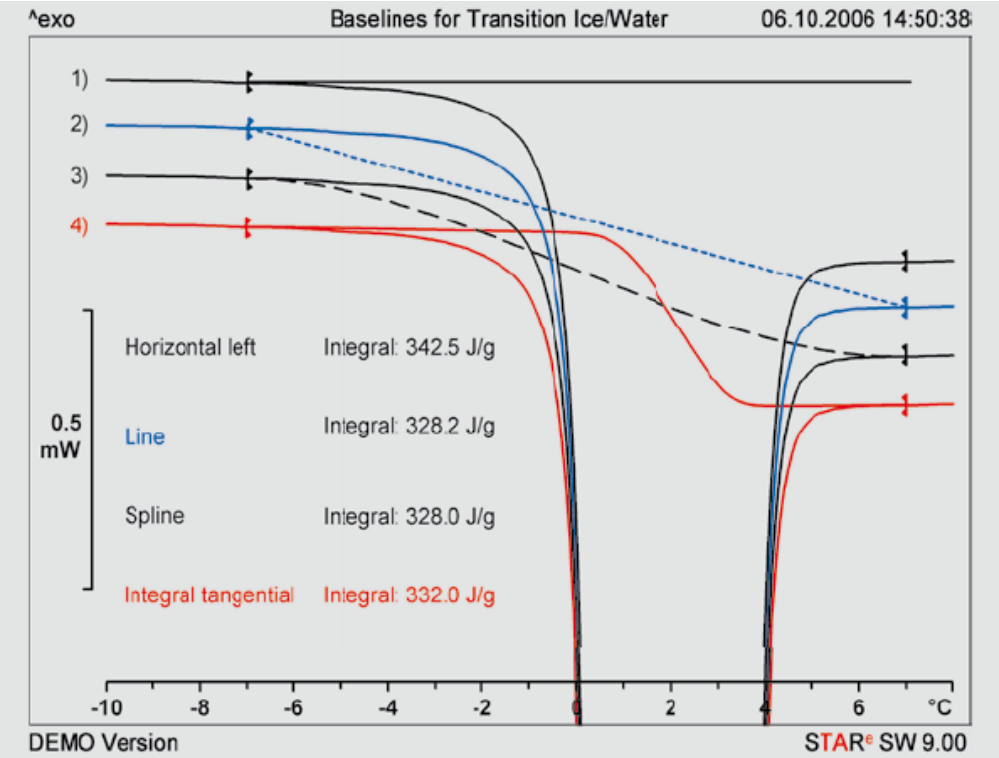

Fig. 4. ***The influence of baseline construction on the enthalpy determination of the transition of ice/water measured using DSC.***[12]

1.6.2 Regions of Interest

Constructions specific for temperature measurements (regions of interest) related to a DSC curve are shown below in Fig 5. These include:

(a) T_o Onset Temperature: The temperature at which the DSC curve begins to deviate from the initial baseline. This point of deflection from the baseline is often misinterpreted and its construction often down to individual judgement.

(b) T_e Extrapolated Onset Temperature: The temperature at which an auxiliary line through the steepest part of the peak to be measured intersects the initial baseline. This is the main construction that forms the basis of the extrapolation to zero heating rate measurements.

(c) T_p Peak Temperature: The temperature at which the absolute maximum of the peak occurs.

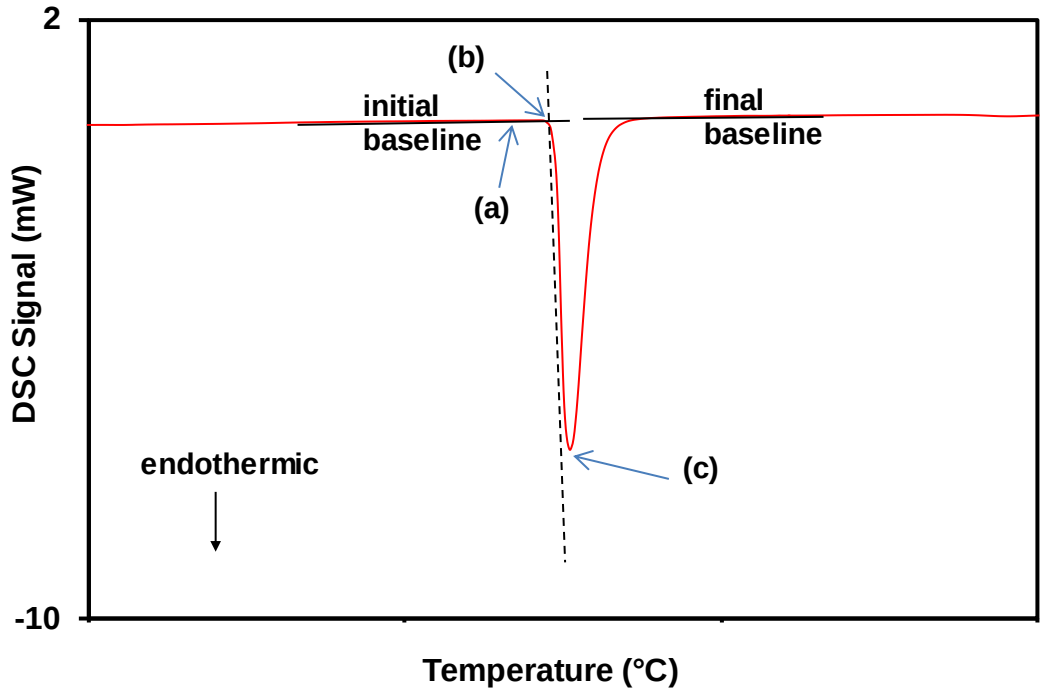

Fig. 5. ***Characteristic temperatures of interest of a peak observed using DSC.***

1.7 Determination of Accurate Temperatures

Recent studies have discussed two possible approaches for the determination of the equilibrium temperature of transition.[13] These methods have been adopted for the accurate measurement of equilibrium temperatures of transitions by DSC. The methods include the extrapolation to zero heating rate ($T_{\beta=0}$) and the isothermal stepwise heating (T_{step}) methods.

1.7.1 Extrapolation to Zero Heating Rate $T_{\beta=0}$ Method

In the first method, the extrapolated onset temperature (T_e) of the melting peak of a material is measured at a range of heating rates. The method of extrapolation was initially proposed by Höhne et al[14] and utilises the DSC in its conventional dynamic mode. Based on an elaboration of the recommended procedure of calibration by Gesellschaft für Thermische Analyse e.V. (GEFTA), it set out to derive the equilibrium temperature of a material at "zero heating" using a linear correction so that it was comparable to temperatures on the fixed scale ITS-90.[15]

$T_{\beta=0}$ is calculated by measuring the extrapolated onset temperature of transition over a range of heating rates (typically 1 to 10°C min^{-1}). The resultant T_e of the material is then plotted against its respective heating. The equilibrium temperature of the material being studied is calculated by mathematically extrapolating to a zero heating rate ($T_{\beta=0}$) using a first order line of y = mx + c.

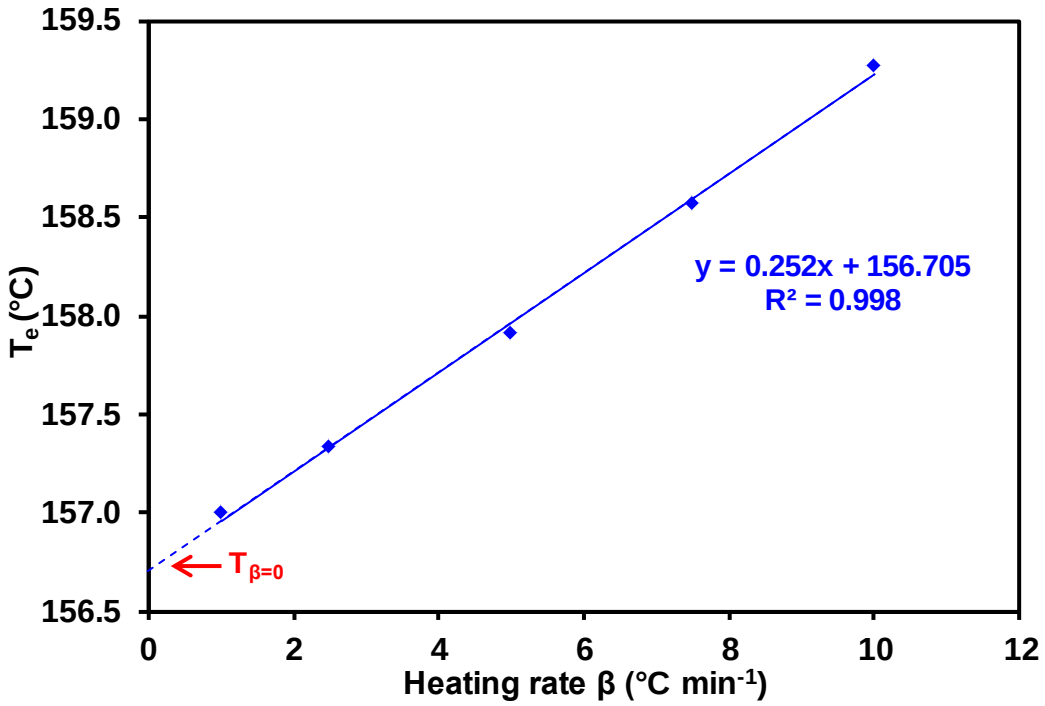

Fig. 6. ***A plot of extrapolated onset temperature versus heating rate for a sample of indium described later in the Thesis but used here to illustrate the extrapolation to zero heating rate construction.***

Regressional analysis is a statistical method for modelling the linear relationship and allows the quantification of the errors associated with the construction of the slope and the calculated intercept. For calculating regressional analysis it is assumed that the error in the measurement of the extrapolated onset temperature (y) and the values of the heating rate (x) are known precisely.

Calculated using y = mx + c the intercept c ($T_{\beta=0}$ of transition for a material) is calculated using:

$$c = \frac{[\sum x^2 \sum y - \sum x \sum xy]}{[N \sum x^2 - (\sum x)^2]} \qquad \textit{Equation 1}$$

Where x is the chosen heating rate (β), and y the measured extrapolated onset (T_e) from the DSC heating curve.

N is the number of heating rate determinations.

The error associated with the equilibrium temperature can then be determined using the following equation:

$$(\sigma_c)^2 = \frac{\left[(\sigma_y)^2 \sum x^2\right]}{[N\sum x^2 - (\sum x)^2]} \qquad \textit{Equation 2}$$

Where

$$(\sigma_y)^2 = \frac{\sum(y - c - mx)^2}{(N-2)} \qquad \textit{Equation 3}$$

The gradient of the linear plot can then be calculated using:

$$m = \frac{[N\sum xy - \sum x \sum y]}{[N\sum x^2 - (\sum x)^2]} \qquad \textit{Equation 4}$$

And the errors associated with the gradient considered using:

$$(\sigma_m)^2 = \frac{[N(\sigma_y)^2]}{[N\sum x^2 - (\sum x)^2]} \qquad \textit{Equation 5}$$

Finally an overall error calculation for the equilibrium transition temperature using the above method is then stated as a least square fit of summative errors associated with the intercept ($T_{\beta=0}$) and the error associated with the primary calibration of the instrument.

The ITS-90 is a temperature scale of high purity metals which have been certified using platinum resistance thermometers, the values of which are used as reference points in the primary calibration of temperature in TA methods. As DSC is a dynamic technique an evaluation of this method of determining equilibrium

temperatures was performed by Charsley et al using certified organic melting point temperature standards.[13] The results provided experimental confirmation that the $T_{\beta=0}$ was equivocal to the certified liquefaction temperature of the standards.

1.7.2 Isothermal Stepwise Heating T_{step} Method

The second method of deriving equilibrium temperatures of transition is to use isothermal stepwise heating (T_{step}). This process of determining equilibrium temperatures has evolved from methods used previously for determining purity measurements using adiabatic calorimetry which have been implemented for use on differential scanning calorimeters.[16]

In the T_{step} method the transition temperature of interest is determined using stepwise heating conditions where the temperature of the sample is raised in small increments (typically 0.1°C). The small temperature increments are then combined with periods of isothermal holds (typically 20 minutes) to enable the sample to equilibrate at the new temperature so that any transition takes place under near equilibrium conditions similar to those of adiabatic calorimetry.

The equilibrium melting temperature (T_{step}) is then obtained from an average temperature of the final steps in the process (Fig. 7). The final steps being identified as the temperatures immediately prior (T_1) and following (T_2) a notable transition for which there are no further deflections upon heating and the baseline remains constant during the following isothermal period.

In situations where the transition occurs over a wide temperature range location of T_1 and T_2 can be difficult and therefore best studied using much larger temperature increments or by using the $T_{\beta=0}$ method. In contrast to the $T_{\beta=0}$ method the use of T_{step} is laborious if the behaviour of the sample during a transition is not fully known.

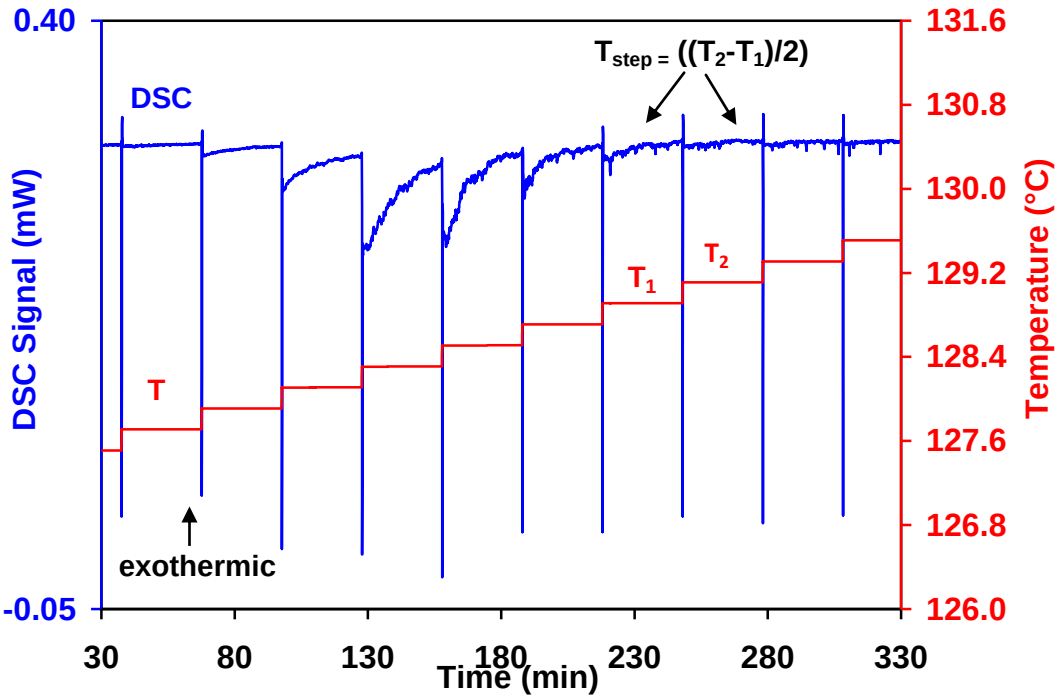

Fig. 7. ***Results of a stepwise heating plot of the solid-solid transition of potassium nitrate (Section 4.6) to demonstrate the placement of temperatures T_1 and T_2 required to measure T_{step}.***

The errors reported on the T_{step} are derived from propagating the errors of half of the temperature increment along with the error associated with the initial calibration of the instrument using:

T_{step} error = $\sqrt{a^2 + b^2}$ Equation 6

Where (a) is half of the temperature increment as T_{step} is taken as an average temperature of two increments and (b) is the error associated with the initial temperature calibration.

1.8 Measurement of Enthalpy

To determine the enthalpy of transition, the conventional approach of using software provided by the instrument manufacturer has been used. This process requires the operator to draw a suitable baseline (baseline styles are discussed in

Section 1.6.1) across the region of interest which is then subsequently calculated by the software to provide heat flow data.

Comparison enthalpic measurements have also been shown in this thesis using calculations made by Professor Peter Laye. These are measured using an approach adapted from one recommended by Richardson[17] and is discussed in detail in the publication on rubidium nitrate[18] which is given in Appendix 2.

1.9 Calibration

1.9.1 Introduction

Calibration can be summarised as all of the operations required for the purpose of determining the values of errors of measuring instruments, material measures, and measurement standards. As a DSC provides information on both the temperature and heat flow of a sample the calibration should result in the following:

1 The temperature of an event can be measured in the absolute sense to a traceable standard.

2 The associated enthalpy can also be measured in the absolute sense to a traceable standard.

The traceable standard being a material used in the calibration process for which has traceable certificates and measurements from a national standards body such as the National Physical Laboratory.

The materials typically used in the calibration of DSCs display sharp first order transitions, generally those attributed to the melting of high purity metals listed in the ITS-90.[19] Other alternative calibrants include both inorganic and organic salts and will be explored later in the thesis.

As DSC is increasingly used as a quality assurance tool the role of calibration is important for ensuring that reproducible data can be produced regardless of location i.e. round robin testing.

In most accredited laboratories the following of a protocol for instrument calibration is set out by a recognised international standard such as the International Organisation for Standardisation (ISO) or the American Society for Testing and Materials (ASTM). The more familiar ones for DSC users being:

- ISO 11357-1:2009, Plastics-Differential scanning calorimetry (DSC)-Part 1: General principles.
- ASTM E967-08, Standard Test Method for Temperature Calibration of Differential Scanning Calorimeters and Differential Thermal Analyzers.
- ASTM E968-02, Standard Practice for Heat Flow Calibration of Differential Scanning Calorimeters.

The benefit of having recognised calibration procedures in place is paramount in order to guarantee that the services provided are fit for purpose, however the subject of calibration and research into calibration procedures are continually occurring as companies seek to refine procedures and ultimately to reduce costs[20-24].

Whilst the outcome of this thesis provides a means of determining much more accurate temperature measurements of transition (±0.05°C) using DSC the development of the two procedures and the materials studied, equally serve as a means to both reduce the time spent on a calibration procedure and the type of materials used.

For the purpose of calibration whether it be for temperature or enthalpy, the materials used need to be of a high quality. The materials are, in general, originally certified using highly precise thermal methods such as adiabatic calorimetry and their values utilised as fixed reference points in the calibration process.

There are several organisations that are dedicated to the testing, production, and supply of reference materials suitable for calibration of temperature and enthalpy of thermal equipment. These include:

(a) The International Confederation for Thermal Analysis and Calorimetry (ICTAC). A confederation of national or regional thermal analysis and calorimetry societies. The aim of ICTAC is to promote international understanding and cooperation in thermal analysis and calorimetry through the organisation of international congresses and the work of its scientific committees.

(b) National Institute for Standards and Technology (NIST). Founded in 1901 NIST is one of the oldest physical science laboratories whose mission is to promote innovation and industrial competitiveness by advancing measurement science, standards and technology.

(c) LGC Ltd formerly known as the Laboratory of the Government Chemist (LGC). LGC Standards provides products and services to inspire measurement and quality control within the laboratory, and is part of LGC Science and Technology Division which acts as the UK National Measurement Institute for chemical and bio-analytical measurements.

More detail on the origin of the calibration materials used in this study can be found in Section 2.3.1.

1.9.2 Calibration Process

The procedure involved in the calibration of DSC instruments involves two processes. The initial calibration (primary calibration) and calibration checks (secondary calibration).

1.9.3 Primary Calibration

The primary calibration of a DSC is the initial procedure used to modify any current or factory settings in place for enthalpy and temperature measurements using fixed point reference materials. The calibration of a DSC is traditionally carried out using the fusion of high purity metals with well-defined melting points on the

International Temperature Scale (ITS-90). The most commonly used metals are indium, tin, and lead.

Table 2. ***Calibration materials on the ITS-90 fixed temperature scale.***

Material	Temperature / °C	Material	Temperature / °C
Mercury	-38.83	Lead	327.46
Water	0.01	Zinc	419.53
Gallium	29.76	Aluminium	660.32
Indium	156.60	Silver	961.78
Tin	231.93	Gold	1064.18
Bismuth	271.40		

In the older style DSCs only a single calibration factor (κ) (whether determined from a single or multi point calibration) can be stored within the software making the calibration process cumbersome when wanting to interchange measurement conditions. With the more modern equipment it is now possible to store several calibrations making it easier to swap between the calibration requirements of several methodologies without the need of fully recalibrating the system from scratch each time. Of the DSCs used in this study both the Mettler Toledo DSC822^e and the Perkin Elmer Diamond DSC were capable of storing multiple calibration data. However, the Thermal Instruments TA2920 could only store one current calibration.

1.9.4 Secondary Calibration and Long Term Monitoring

The secondary calibration (sometimes called the calibration check) is the frequent measurement of the temperature and enthalpy of a substance at regular intervals during experimentation. The substance measured must fall within the ranges (temperature and enthalpy) of calibration, however, independent of that used in the primary calibration i.e. a fresh sample.

By performing regular calibration checks an assessment of the primary calibration can be made. This provides a traceable performance indicator of the instrument ensuring reproducible results are achieved with confidence. This is an important measure when performing experiments over an extended period of time, especially if routine, to show that the instrument has not changed from the limits originally defined in the primary calibration. The frequency of the secondary calibration is user defined, however, for most analytical laboratories this is set out by a quality assurance protocol.

Secondary calibration data collected during this study is provided in Appendix 3.

Chapter 2 Experimental

The following section outlines the main experimental variables and methods used within this Thesis.

2.1 Instrumentation

2.1.1 Heat Flux DSC

Two heat flux DSCs were used as part of the project

(a) Mettler Toledo DSC822^e This comprises a fully enclosed heat flux system that has a unique circular thermocouple arrangement located on a ceramic DSC head.

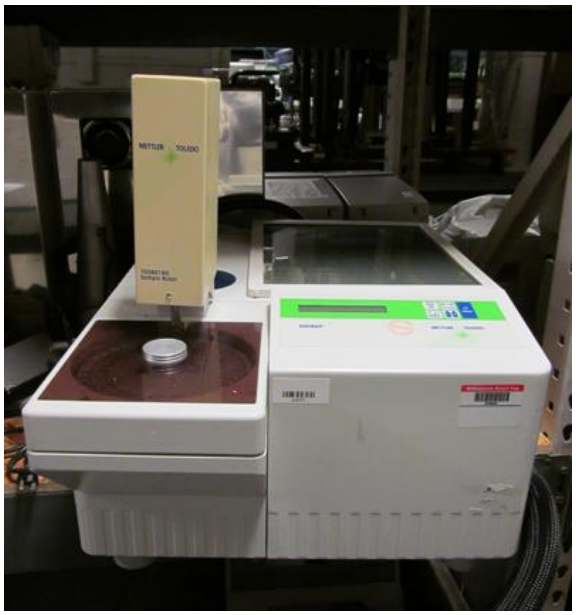

Fig. 8. ***The Mettler Toledo DSC822^e***

The Mettler Toledo DSC822^e features an integrated robot for automated sampling and reproducible sample positioning. Due to its inherent reproducibility over manual placement of the crucible the robot was used throughout the experiments

unless otherwise stated. The STAR^{e} (Version 9) software was used for the manipulation of the data. The Mettler has a "tau lag" function built into the software which corrects for influences on temperature measurements caused by changes in heating rate. For this study this feature was disabled to ensure additional software corrections did not influence the results obtained.

A cross section of the Mettler Toledo DSC822^{e} measuring cell and thermocouple arrangement are given in Figs 9 and 10 below.

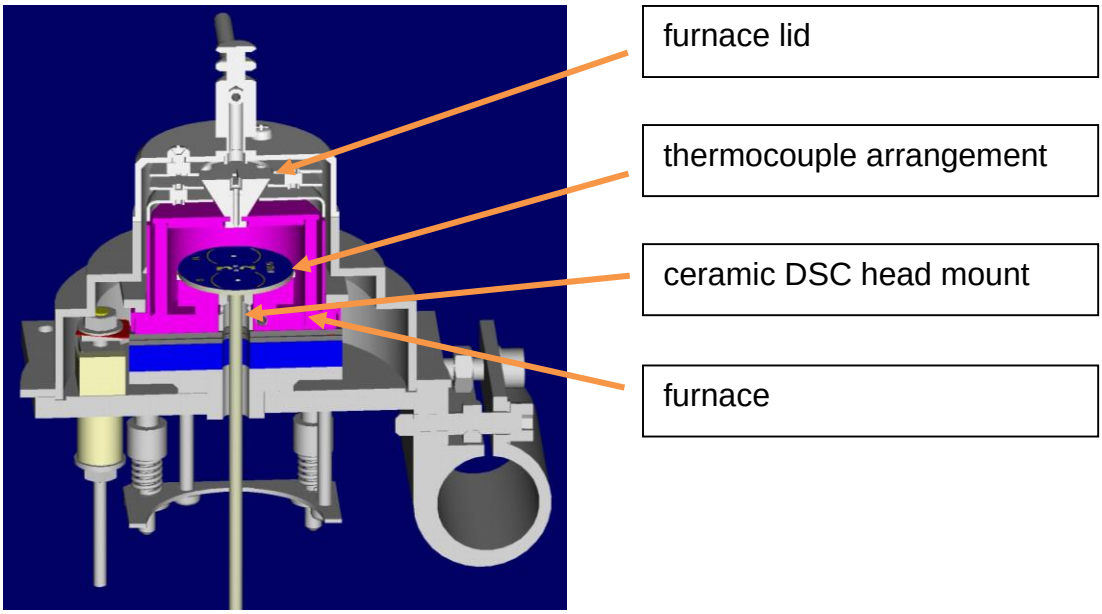

Fig. 9. ***A cross section of the Mettler Toledo DSC 822^{e} measuring cell.***[25]

The Mettler DSC head has a unique arrangement of 56 thermocouples in a circular design around both the sample and reference positions instead of a single point of contact under each sample position.

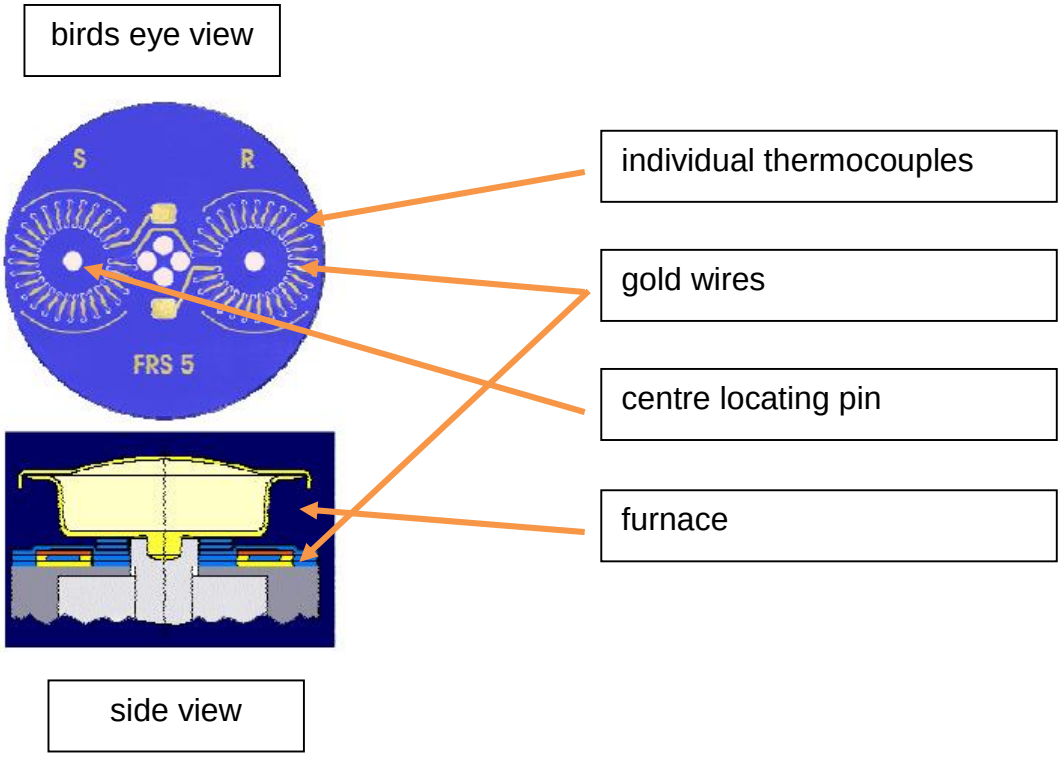

Fig. 10. ***An illustration of the Mettler Toledo DSC822^{e} thermocouples.***[25]

(b) Thermal Instrument TA2920 DSC This comprises of a manually operated DSC where the sample and the reference are located on raised platforms on a constantan (copper/nickel alloy) disk.

Fig. 11. ***A Thermal Instruments TA2920DSC***

Thermal Instrument TA2920s' software Universal Analysis 2000 was used for both the control of the DSC and the manipulation of data. The glass bell jar is used to maintain the atmosphere around the furnace and measuring cell.

Unlike the Mettler DSC822^{e}, the differential heat flow is monitored by thermocouple wires welded to chromel (nickel-chromium alloy) wafers located under the sample and reference housing positions.

A cross section of the TA2920 measuring cell and thermocouple arrangement is shown in Fig.12 below.

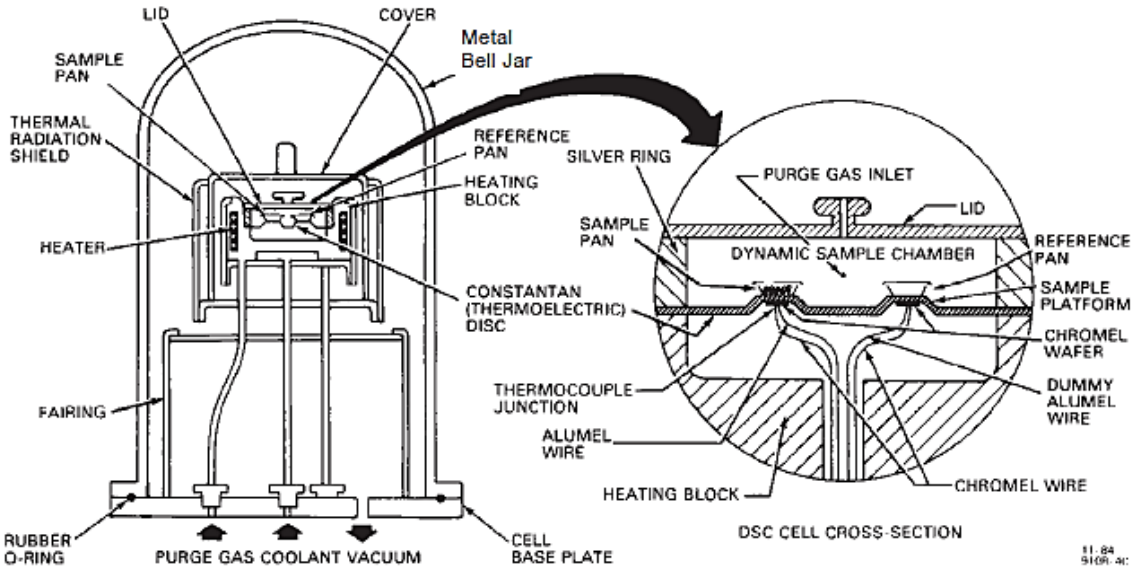

Fig. 12. ***A TA Instruments TA2920 measuring cell cross section.***[26]

Measurements made under near equilibrium conditions using the contrasting cell types and thermocouple arrangements are discussed further in Section 3.3.1.

The primary temperature calibration was performed in light of the proposed experimental method to be used and the temperature range over which materials were to be studied. For the majority of this study, the DSCs were calibrated using the equilibrium temperature values obtained using T_{step} measurements of high purity indium, tin, and lead as either single or multiple temperature points. The

crucible type and atmospheric conditions in which subsequent experiments were performed were also used in the calibration process.

The enthalpy was adjusted using factory settings. This was achieved by recording the heat flow of three independent high purity LGC indium samples at 3°C min^{-1} and allowing the software to make the necessary adjustments. For example, if the average heat of fusion for three independent runs was 28.6 Jg^{-1} this would be input into the calibration software and related to the factory setting of 28.4 Jg^{-1}. The software would then automatically apply a correction to all subsequent heats of fusion measurements by multiplying their values by a correction constant of 0.993. (28.4/28.6 = 0.993)

2.1.2 Power Compensated DSC Instrumentation

The Perkin Elmer Diamond DSC was the only power compensated DSC used in this study. The Pyris (version 11) software was used for both the control of the instrument and the manipulation of data.

Fig. 13. ***A Perkin Elmer Diamond DSC***

It is a manually operated machine with ultra-light weight (1g) furnaces in comparison those used in heat-flux systems (30-200g). The size difference results in faster heating and cooling rates and allows direct heatflow determination, eliminating the need for complex mathematics.

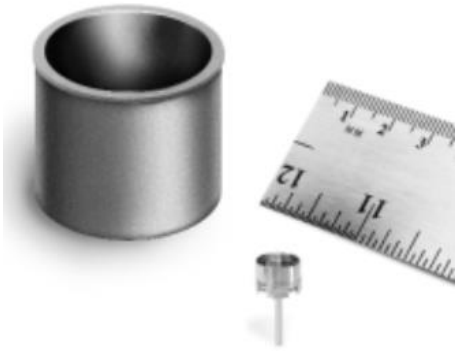

Fig. 14. ***A Perkin Elmer Diamond DSC furnace.[9]***

2.2 Additional Thermal Analysis Techniques

2.2.1 Hot Stage Microscopy

A Stanton Redcroft HSM-5 hot stage with a manual Linkam temperature programmer was used.

A hot stage microscope comprises of a heated chamber with a single furnace and temperature sensor on which a crucible is placed and the sample observed through a glass window. The use of a camera and a microscope enables the recording and playback of any changes that might occur within the sample when heated or cooled which cannot be observed using techniques such as DSC. Images or “stills” can be captured at specific temperatures and used in technical reports where a descriptive may not suffice.

A cross section of the measuring chamber is shown in Fig 15.

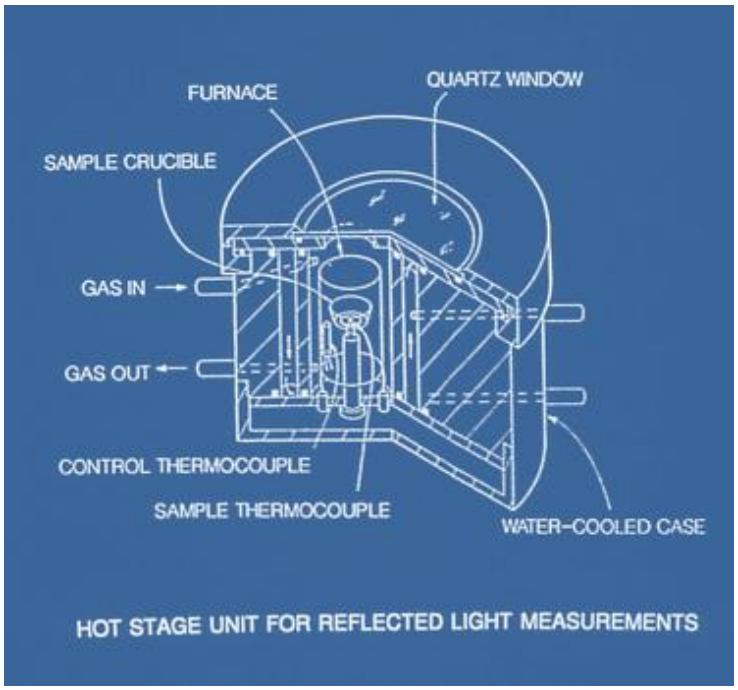

Fig. 15. ***A cross section of a Stanton Redcroft hot stage HSM-5.***[27]

2.2.2 Thermogravimetry

A Mettler Toledo TGA851[e] was used to assess the volatility of the organic samples prior to use. The instrument was controlled using the same version of STAR[e] software provided with the Mettler Toledo DSC822[e].

Fig. 16. ***A Mettler Toledo TGA851[e].***[28]

2.3 Materials Used

Sample preparation can be a time consuming part of setting up for an analysis but is essential for ensuring reproducible work and so is discussed here in detail.

2.3.1 Calibration Metals

The calibration metals indium, tin, and lead have been used in various forms. For the primary calibration of the DSC, high purity metals supplied by the Laboratory of the Government Chemist (LGC Ltd) were used for both the enthalpy of fusion and the melting temperature measurements.

For the powdered samples, the highest purity available through generic chemical suppliers was used, the details of which are listed in Table 3.

Table 3. ***High purity metal materials and their supplied form***

Supplier	Sample	Supplied state	Purity / %	Referred to in the text as:
LGC2601	Indium	0.5g tear drops	99.99998	LGC indium, solid indium
Alfa Aesar	Indium	Finely divided powder	99.99999	Indium powder
LGC2609	Tin	0.5g tear drops	99.9996	LGC tin, solid tin
Alfa Aesar	Tin	Finely divided powder	99.99999	Tin powder
LGC2608	Lead	0.5g tear drops	99.9995	LGC lead, solid lead
Alfa Aesar	Lead	Finely divided powder	99.99999	Lead powder

Sample preparation of solid metal materials

The following steps were used for the preparation of solid metal materials for analysis by DSC:

1. Prepare two clean cutting surfaces by wiping down glass plates with a 10% isopropyl-90% water solution. The choice of cutting surface is important to avoid future cross contamination and should not score easily. *The cutting surface used in this preparation was a couple of plain ground glass drinks coaster of about 10cm^2*.
2. Remove a sample of the desired metal standard using a pair of clean tweezers and place onto the glass surface. *The LGC metals were supplied as "tear drop" shaped approximately 3mm in size.*
3. Using the tweezers to hold the sample, take a clean scalpel blade and slice off a slither of the metal approximately 1mm thick. *More effort is required to slice both tin and lead in comparison to the malleable indium*.
4. Place the remainder of the sample in a clean closable sample container labelled up correctly for future use. *A 3ml stoppered glass vial with a push fit lid was used.*
5. Cut and weigh a section of the slither to the desired mass for analysis. *For example 10mg.*
6. Using the end of the scalpel blade lift the cut slither and place ~1cm away from the corner of the cutting surface. Using the other clean cutting surface to sandwich the metal slither apply a small amount of pressure at the same time as rotating the top plate through a quarter turn to produce a flat disc of your metal sample. *Glass is ideal to use as a cutting surface as it also acts as a window to see how well your sample has been reshaped. However, do not be tempted to flatten your material too much as a too thin sample will in fact weld itself to the cutting plates. The diameter of the disc of material should also not exceed the size of the base of the DSC pan.*
7. Using the scalpel blade, lift the metal disc off of the cutting plate and into the DSC pan of choice. Using the end of a flat faced rod lightly tamp the sample into the base of the pan to maximise the contact between the pan and the sample. *A ground glass rod was used here*.

Sample preparation for powdered metals:

The powdered materials were used as received. The metal was weighed directly into the crucible and an even layer distributed across the base using gentle tapping.

2.3.2 Organic DSC Certified Reference Materials

Certified organic DSC reference materials were provided by LGC Ltd. Table 4.

Previous studies have shown that particle size can influence DSC results.[29] therefore, as a precaution, the samples that were supplied as crystals were reduced in size to provide a more homogeneous sample. This was done by lightly crushing the crystals in the crucible using the end of a glass rod.

Table 4. ***Organic certified reference materials supplied for the use in DSC calibration***

Supplier	Sample	Supplied state	Purity / %	Referred to in the text as:
LGC2613	Phenyl salicylate	Crystals <710µm	99.994	$PSal_{(D)}$
LGC2610	Biphenyl	Crystals <710µm	99.992	$Biphenyl_{(D)}$
LGC2603	Naphthalene	Crystals <710µm	99.97	$Naphthalene_{(D)}$
LGC2604	Benzil	Finely divided powder	99.996	$Benzil_{(D)}$
LGC2605	Acetanilide	Crystals <710µm	99.996	$Acetanilide_{(D)}$
LGC2606	Benzoic acid	Finely divided powder	99.994	$Benzoic\ acid_{(D)}$
LGC2607	Diphenylacetic acid	Crystals <710µm	99.98	$DAA_{(D)}$

2.3.3 Organic Melting Point Certified Reference Materials

In addition to the organic DSC certified reference materials at the time this project work commenced, the same reference materials (with exception to biphenyl) were also supplied as melting point reference standards. These materials are intended for use in the calibration of melting point apparatus. Table 5.

The thermodynamic melting points provided on the certificates are based upon the melting point that would be observed under equilibrium conditions (i.e. zero heating rate). The purity of each material supplied was given and had been measured by DSC. The preparation of the samples before use on the certificate is given as follows: " A sample sufficient for measurement should be taken from the screw-cap vial supplied, lightly crushed in an agate mortar to produce a fine powder and dried, for example by storage for 48 hours over P_2O_5 in a dessiccator".[30]. To stay consistent with the DSC reference materials, those supplied with large variations in crystallanity were lightly crushed in the crucible before use.

Table 5. ***Organic certified reference materials supplied for the use in melting point apparatus calibration***

Supplier	Sample	Supplied state	Purity / %	Referred to in the text as:
LGC2411	Phenyl salicylate	Crystals <710µm	99.57	$PSal_{(T)}$
LGC2402	Naphthalene	Crystals <710µm	99.97	$Naphthalene_{(T)}$
LGC2403	Benzil	Crystals <710µm	99.996	$Benzil_{(T)}$
LGC2404	Acetanilide	Crystals <710µm	99.996	$Acetanilide_{(T)}$
LGC2405	Benzoic acid	Finely divided powder	99.994	$Benzoic\ acid_{(T)}$
LGC2406	Diphenylacetic acid	Finely divided powder	99.98	$DAA_{(T)}$

2.3.4 Materials used in Pyrotechnic Compositions

Inorganic oxidants used in pyrotechnic compositions of interest were potassium and rubidium nitrates, potassium perchlorate and potassium dinitramide. The samples and their preparation are described below:

Potassium Nitrate

Potassium nitrate (KNO_3) (AlfaAesar) was supplied in the form of a crystalline powder with a purity of 99.997%. Samples of KNO_3 that were studied as received in the crystalline form without any pre-treatment are referred to in the text as KNO_3-C.

Potassium nitrate which had been pre-treated before use is referred to in the text as KNO_3-SD and was prepared by taking crystalline KNO_3 (~1g) and lightly triturating it in an agate pestle and mortar before being passed through a 150µm brass sieve and collected. The crystals that passed through the sieve were placed on to a watch glass and dried at 105°C for 2 hours before being transferred to a separate sample vial for storage. All samples were stored in a desiccator when not in use.

Rubidium Nitrate

Rubidium nitrate ($RbNO_3$) (AlfaAesar) was supplied in the form of a crystalline powder with a purity of 99.975%. The crystals were crushed and stored the same as KNO_3.

Potassium Perchlorate

Potassium perchlorate ($KClO_4$) (Sigma Aldrich) was supplied in the form of a crystalline powder with a purity of 99.99%. Additional measurements were also made on an ICTAC reference material of unknown purity. Both materials were used as received with no pre-treatment.

Potassium and Rubidium Dinitramide

Samples of potassium dinitramide (KDN) and rubidium dinitramide (RbDN) were supplied by QinetiQ and armasuisse, Switzerland. The samples provided were in the form of white crystals with varying morphology between batches and are listed in Table 6.

Table 6. ***Potassium and rubidium dinitramides***

Sample	Supplied state	Purity / %
KDN-1	crystalline powder	unknown
KDN-Bofors	crystalline powder	unknown
KDN-2	crystalline powder	unknown
RbDN-1	crystalline powder	unknown
RbDN-2	crystalline powder	unknown

Unless otherwise stated the materials were used as received. Due to the photosensitive nature he samples were kept in darkness and handled inside a custom made dark box.

2.4 Experimental Conditions

2.4.1 Sample Mass

The mass of the sample to be studied has been shown to have a significant influence on the structure of a DSC curve.[31] Masses of between 2.5 and 5mg were used when studying the inorganic and organic materials as with these small quantities the possibility of large thermal gradients across the sample were greatly reduced. A greater mass of 10mg for indium was used when studied with the organic materials because of its considerably smaller enthalpy of fusion.

2.4.2 Sample Crucible

The crucible or pan used in DSC is to contain the sample to be measured so that it does not come into contact with the measuring plate as it is subjected to its thermal programme. The crucible material used should be one that does not react with the sample over the temperature ranges to be studied. The sample pans used in this study were constructed of aluminium and had internal volumes of 20µl (non hermetically sealable pan base) and 40µl (hermetically sealable pan base). Aluminium pans were chosen for the majority of this study unless otherwise stated. There are relatively inexpensive, conduct heat efficiently and were not reactive with the samples and temperature ranges used in this study. All pans were used as supplied and were not pre-treated prior to use.

The aluminium pans used consist of two pieces, the base and the lid and were sealed using the tooling supplied by the manufacturers to ensure reproducible crimping. The following three configurations were used:

1. Open pan

This configuration is used when a sample exhibits little or no physical change during its thermoanalytical measurement. The open pan is simply the base of a crucible that is open to the atmosphere without a lid.

2. Non-hermetically sealed pan

Used for samples whereby the maximum contact with the base of the crucible is achieved. This configuration involves a flat circular crucible with a lid that is pressed directly on top of the sample using a tool supplied by the pan manufacturer. A self-generated atmosphere is created when using this type of crucible.

3. Hermetically sealed pan

This is used for a range of samples and is particularly effective for samples that are liable to “creep”. The base of the crucible often has a well and when cold welded using the tool provided is UFO shaped. Fig. 17 below.

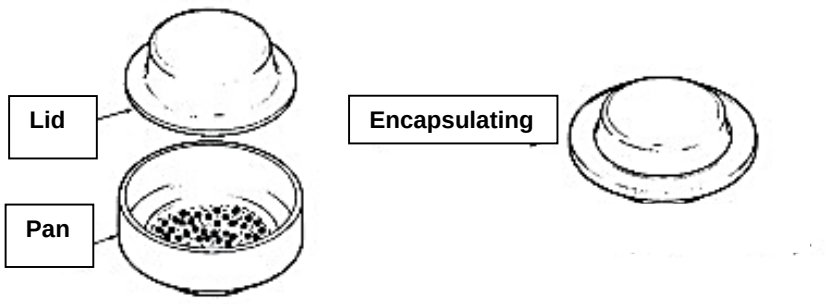

Fig. 17. ***An example of a hermetically sealed crucible.***[26]

The cold weld seal of a hermetically sealed pan is susceptible to rupture if a large amount of volatiles are produced therefore it is almost always used with a pin hole made in the lid prior to welding so not to disturb the seal. Although pans made by different manufacturers are similar they are not always interchangeable. It was found however, that the Mettler Toledo 40µl pan could be used in any of the DSCs used in this study. Ceramic crucibles manufactured by Mettler Toledo with an internal volume of 70µl were also used in measurements made on the hot-stage microscope.

Aluminium crucibles used in the study are given in Figs 18-20 below.

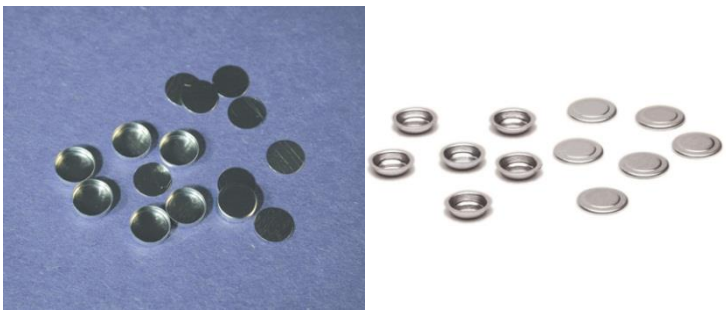

Fig. 18. ***Perkin Elmer non-hermetic (left) and hermetic (right) Al pans.***[32]

Fig. 19. ***TA Instruments non-hermetic (left) and hermetic (right) Al pans.***[33]

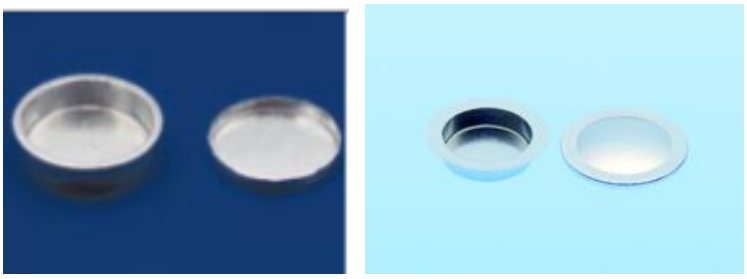

Fig. 20. ***Mettler Toledo 20µl (left) and 40µl (right) Al pans.***[34]

2.4.3 Atmosphere

Argon or nitrogen were used in the DSC experiments at a continuous flow of 80cm^3min^{-1}. For enthalpy measurements performed using the Perkin Elmer Diamond DSC a flow rate of 20cm^3min^{-1} was used. The decreased flow rate was a recommendation of the manufacturer possibly in light of the considerably smaller volume of the furnace.

Where materials of pyrotechnic interest were studied, such as potassium nitrate, an argon atmosphere was chosen due to the implications of possible unwanted reactions in a nitrogen atmosphere.

Chapter 3 Studies on Indium

3.1 Introduction

This chapter includes information on the choice and preparation of high purity metal standards used in the DSC calibration with the main focus of the study looking at the most popular metal used in DSC calibration; indium.

Indium is available to purchase in several forms such as powder, pellet and wire. It is a popular calibrant of choice due to its sharp fusion peak, its compatibility with a wide range of crucible materials, and its relatively low fusion temperature. The ITS-90 value for its freezing point is 156.5985°C but is globally recognised as 156.6°C although the information available about its reusability is limited.

Unless otherwise stated high purity powdered indium and LGC indium were used as prepared in Section 2.3.1.

3.2 Influence of Pre-treatment on Indium.

It is often advised that before using a metal sample for calibration it is pre heated through its fusion temperature and cooled sufficiently before use in order to achieve the maximum contact with the base of the crucible. This sometimes is referred to as the “bedding down” of a sample however, the problem is this approach does not apply to the majority of samples studied by DSC which can only be heated once.

This section aims to evaluate whether it is necessary to bed in samples before use and whether this process indeed influences the resultant temperature of fusion. Studies in which samples of both powdered and LGC indium have been measured and compared are discussed.

3.2.1 Visual Observations of the fusion of Indium

Samples of both indium powder and LGC indium were studied using a Stanton Redcroft Hot Stage Microscope HSM-5 to observe and record the melting behaviour when undergoing a temperature programme similar to that which is used in DSC. 2mg samples of both materials were heated at a rate of 10°C min^{-1} using ceramic crucibles in a flowing nitrogen atmosphere. Once fused the samples were allowed to cool to room temperature and then re heated.

Playback of the powdered indium showed that it was possible to observe movement within the sample at the temperature of fusion where a radial band glistened from the edge to the centre of the crucible at the point of fusion.

The material stayed as a powdered form and did not appear to “fuse”.

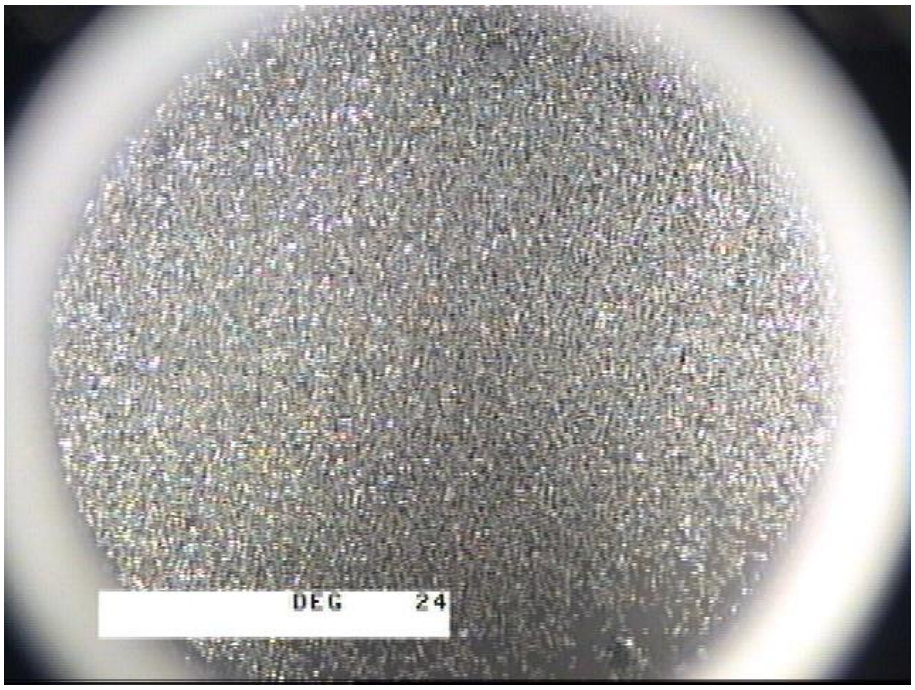

Fig. 21. ***A hot stage image of indium powder before fusion at 24°C (sample mass, 2mg; heating rate, 10°C min^{-1}; atmosphere, nitrogen)***

The melting behaviour of LGC Indium was very different to that of its powdered counterpart.

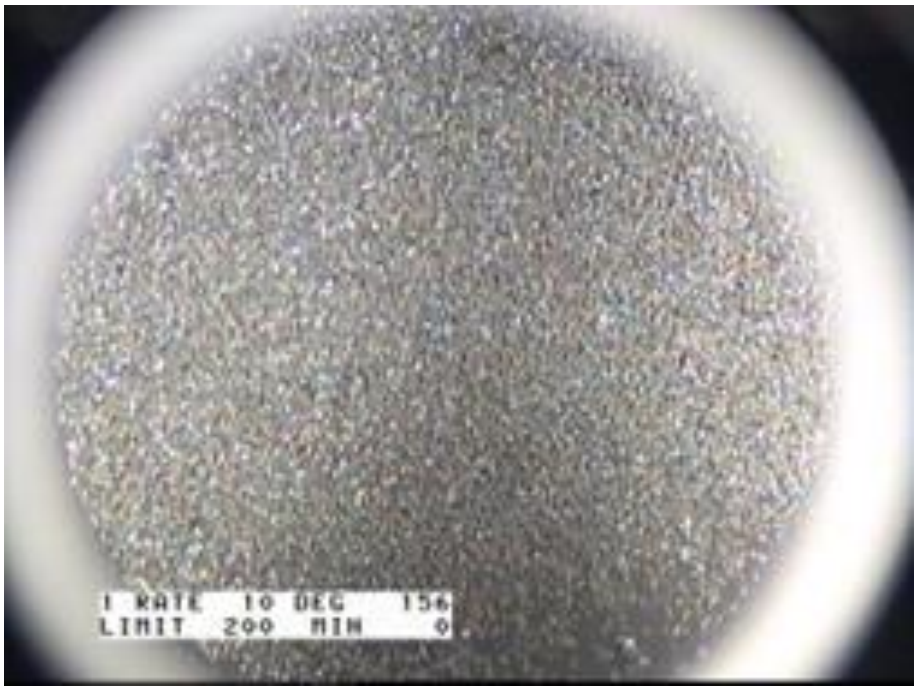

Fig. 22. ***A hot stage image of indium powder after fusion at 156°C (sample mass, 2mg; heating rate, 10°C min^{-1}; atmosphere, nitrogen)***

There was a significant change that occurred during fusion, with the sample forming a small spheroid in the base of the crucible. This is a significant observation as it shows that once “pre melted” the contact surface area between the sample and the crucible base is reduced, a contrast to the principle that metal calibrants are pre melted before use in order to improve the reliability of subsequent measurements by bringing about a better thermal contact between the sample and crucible.

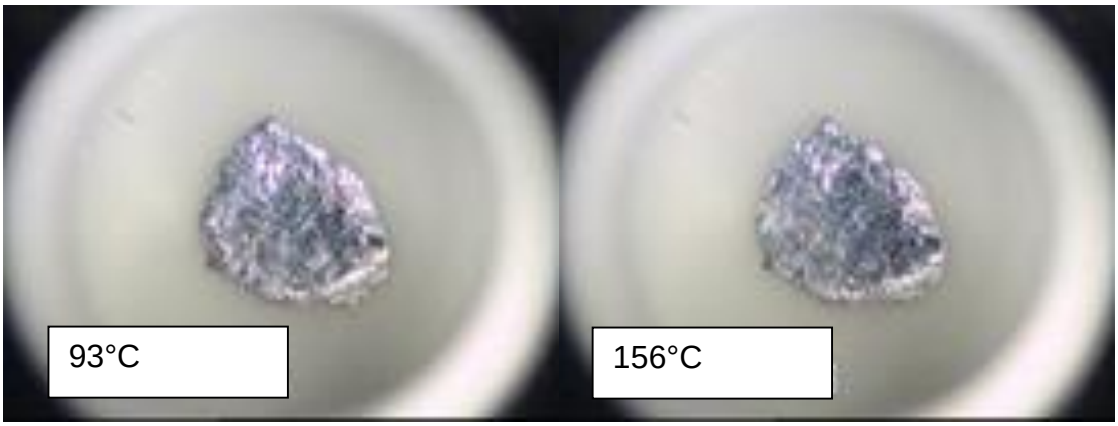

Fig. 23. ***Hot stage images of LGC indium during fusion at 93°C and 156°C (sample mass, 2mg; heating rate, 10°C min^{-1}; atmosphere, nitrogen)***

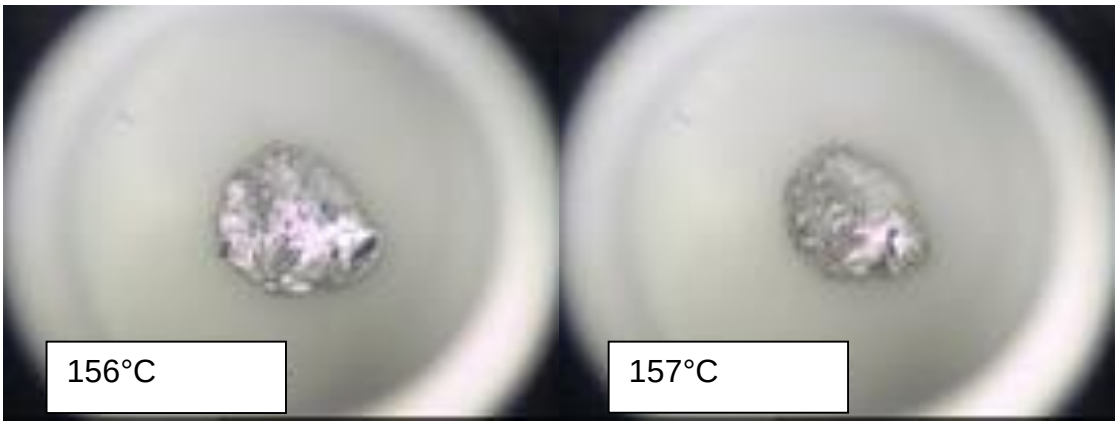

Fig. 24. ***Hot stage images of LGC indium during fusion at 156°C and 157°C (sample mass, 2mg; heating rate, 10°C min^{-1}; atmosphere, nitrogen)***

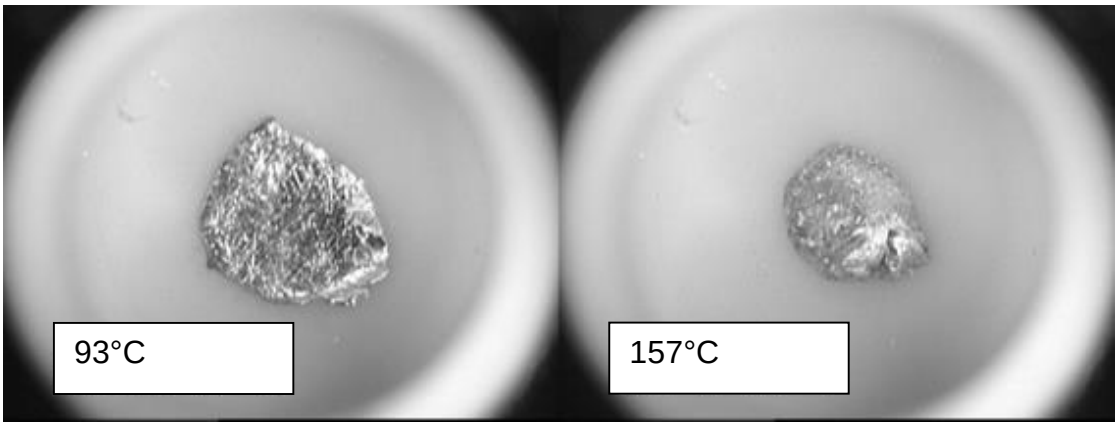

Fig. 25. ***Hot stage images of LGC indium before and after fusion (sample mass, 2mg; heating rate, 10°C min^{-1}; atmosphere, nitrogen)***

Further heating of both the LGC and powdered indium through the fusion temperature indicated that there were no more significant changes in the samples.

When selecting a metal calibrant there are no set rules as to which form of metal to use and it generally falls down to personal preference, and to others, cost. Having observed differences in the behaviour of indium samples upon heating the "bedding in" process was studied further.

3.3 Influence of Indium Form on the Temperature of Fusion

Having observed differences in melt behaviour using the hot stage microscope the influence of the form of indium on its temperature of fusion has been studied by DSC. Preliminary measurements were made using a Mettler Toledo 822^e with the tau lag function disabled using a heating rate of 3°C min^{-1}. The heating rate was chosen based on the methodology used for secondary calibrations of the DSCs. 10mg samples of both powdered and LGC indium were encapsulated in 40µL aluminium pans with a pin hole in the lid and the experiments performed in a flowing nitrogen atmosphere (80cm^{3}min^{-1}). The measurements were made in triplicate and cycled twice in order to make an assessment of the effect of pre heating indium.

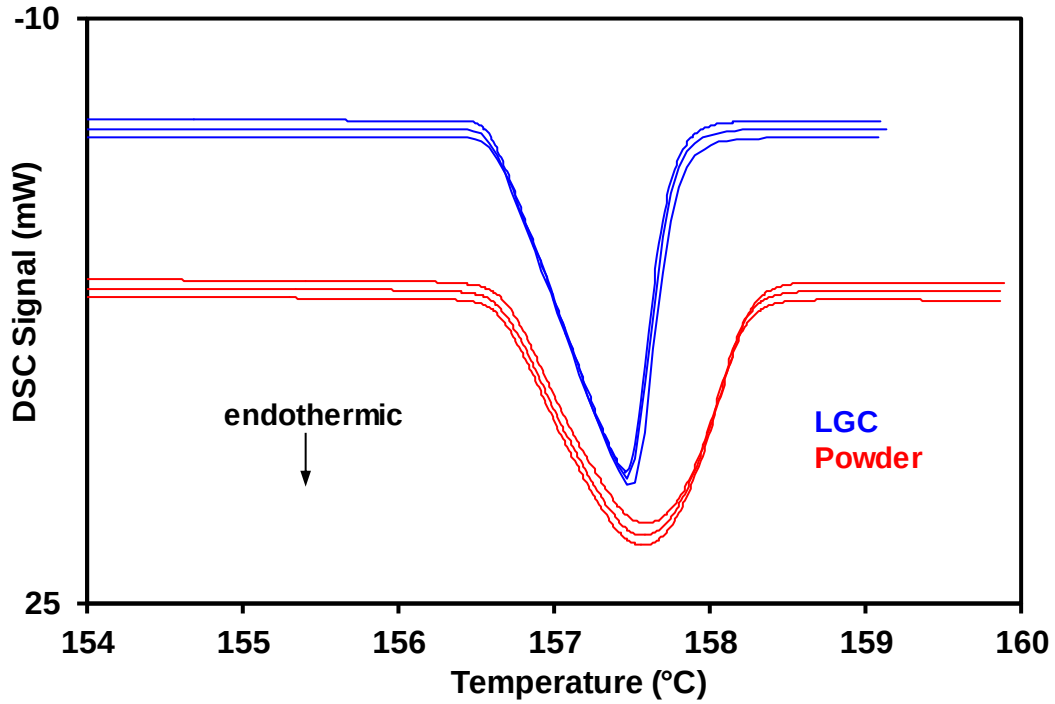

Fig. 26. ***DSC curves for indium powder and LGC indium cycled (sample mass, 10mg; heating rate, 3°C min^{-1}; atmosphere, nitrogen)***

The results showed that at a heating rate of 3°C min^{-1} there is no significant difference between the initial and subsequent measured extrapolated onset temperatures (Fig. 26) although differences seen in the sharpness of the endotherm may suggest a difference in enthalpy and will be investigated further.

It was found during preliminary work on the sample preparation protocol in Section 2.3.1 that if the solid indium sample was neither sufficiently thin nor pressed firmly into the base of the crucible that there was a small change in the melting temperature from the first and second heating. It would be, therefore, a sensible precaution to bed in a metal sample before use.

3.3.1 Accurate Equilibrium Temperature of Fusion Measurements of Different Indium Forms.

Previous results showed that when heating at a dynamic rate of 3°C min^{-1} there was no significant differences between the initial and subsequent heats of powdered and LGC indium. However, assumptions should not be made that the materials behave the same under the influence of different heating rates. Triplicate samples of indium were measured at a variety of heating rates using the $T_{\beta=0}$ method in order to evaluate their behaviour. A new sample for each experiment was used in order to enable an accurate assessment to be made of any effects of pre-heating.

Table 7. ***Equilibrium temperatures of LGC indium using the $T_{\beta=0}$ method (sample mass, 10mg; atmosphere, nitrogen)***

Experiment	$T_{\beta=0}$ / °C	$(dT_e / d\beta)$ / min
First Heating	156.52 ± 0.03	0.074 ± 0.006
Second Heating	156.51 ± 0.03	0.072 ± 0.005
Third Heating	156.49 ± 0.03	0.075 ± 0.004
Mean Value	156.51 ± 0.02	0.074 ± 0.003
Certified Value	156.61 ± 0.01	-
Calibration correction	0.10 ± 0.02	

A linear correlation was found between the measured T_e and heating rate β for both forms of indium and is shown in Fig. 27. The dT_e / dβ value for LGC Indium given in Table 7 is the same as that previously reported for indium in 1990 by Höhne.[14]

Corresponding extrapolation to zero heating rate experiments were also carried out on indium powder and the results are summarised in Table 8. It can be seen that the equilibrium fusion temperature is unchanged by melting and that the value agrees well with that obtained for the LGC sample.

Table 8. ***Equilibrium temperatures of indium powder using the $T_{\beta=0}$ method (sample mass, 10mg; atmosphere, nitrogen)***

Experiment	$T_{\beta=0}$ / °C	(dT_e / dβ) / min
First Heating	156.50 ± 0.02	0.054 ± 0.003
Second Heating	156.48 ± 0.02	0.053 ± 0.003
Third Heating	156.47 ± 0.01	0.053 ± 0.002
Mean Value	156.48 ± 0.01	0.053 ± 0.002

Although a linear correlation was found again between the T_e and the heating rate β, the magnitude of the gradient $dT_e/d\beta$ from the extrapolation to zero heating rate experiments for the powder is significantly smaller than those obtained for the LGC sample.

The differences in slope ($dT_e/d\beta$) between the powder and the LGC indium indicate that at the slower heating rates the values are likely to converge, with small errors of 0.05°C to much greater temperature errors at more elevated heating rates where the values for the onset of fusion diverge. This implies that when fully calibrating a DSC; unless the same form of calibrant is used to both calibrate and to carry out secondary checks on the system then operation under dynamic conditions will incur significant errors which may amount to a perfectly viable sample being discarded.

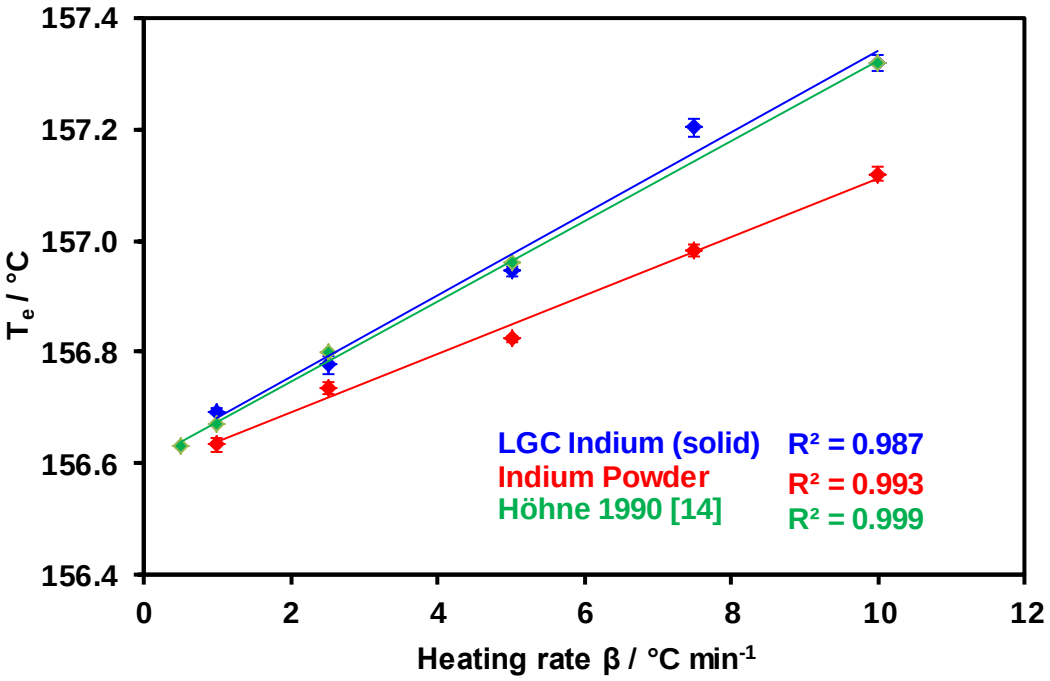

Fig. 27. ***Influence of heating rate on the extrapolated onset temperature of various indium samples***

The agreement between the initial and subsequent fusion experiments within the limits of experimental error also show that it is possible to make temperature measurements using indium to a high degree of precision.

Stepwise heating experiments were also performed using the same sample preparation described in Section 2.3.1, indium was heated in 0.05°C temperature increments with 20 min isothermal periods between steps. Where possible initial shorter isothermal periods were used in order to hasten the duration of the experiment.

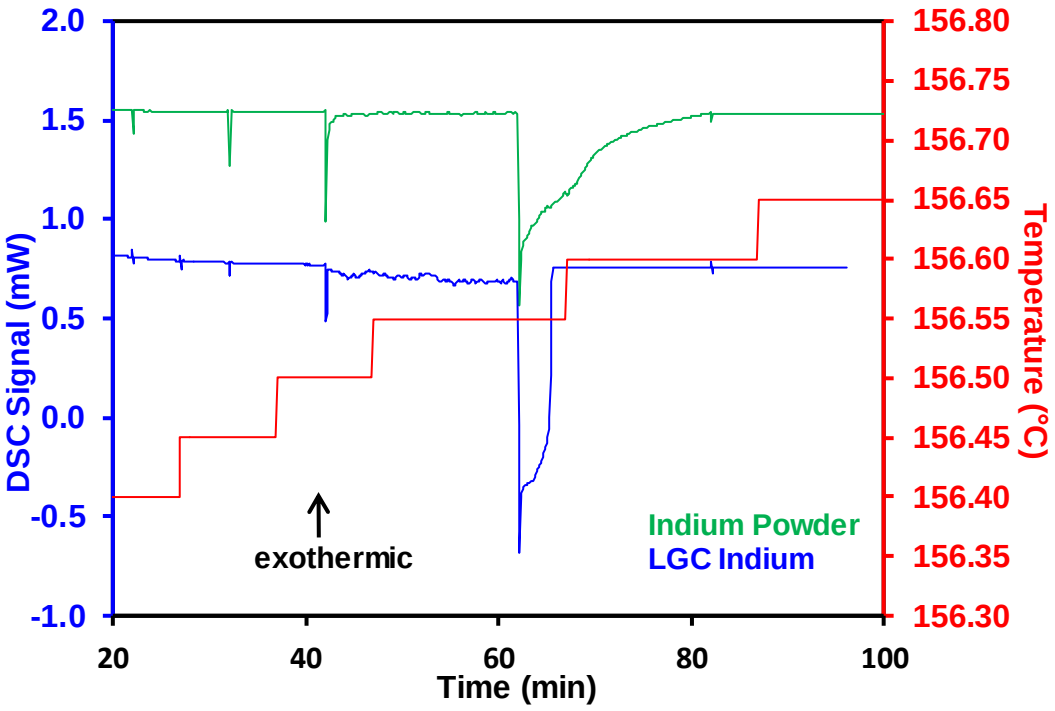

Fig. 28. ***Stepwise heating DSC curves for LGC indium and indium powder (sample mass, 10mg; step size 0.05°C; atmosphere; nitrogen)***

The stepwise measurements were performed in triplicate with a new sample for each experiment and are summarised in Table 9.

Table 9. ***Equilibrium temperature of fusion for indium samples using the T_{step} method (sample mass, 10mg; step size 0.05°C; atmosphere; nitrogen)***

Experiment	LGC T_{step} / °C	Powder T_{step} / °C
First Heating	156.52 ± 0.05	156.50 ± 0.03
Second Heating	156.51 ± 0.05	156.52 ± 0.05
Mean Value	156.52 ± 0.04	156.51 ± 0.03
Calibration Correction	0.09 ± 0.04	
Corrected Mean Temp.	156.61 ± 0.04	156.60 ± 0.03
Certified Value	156.61 ± 0.01	-

The agreement between the results for LGC indium and indium powder obtained by extrapolation to zero heating rate and stepwise heating clearly establishes the equality of the two methods for the determination of accurate equilibrium temperatures and confirm that under equilibrium conditions there are no differences in the fusion temperature of indium regardless of its form.

3.4 Cycling of Indium

An encapsulated indium sample is often used as a secondary standard to periodically check the calibration of a DSC for both temperature and enthalpy. There is no limit set as to how often a sample can be re-cycled through its fusion temperature before it is no longer considered reliable; however, some manufacturers suggest a limit of 10 cycles before discarding the sample.

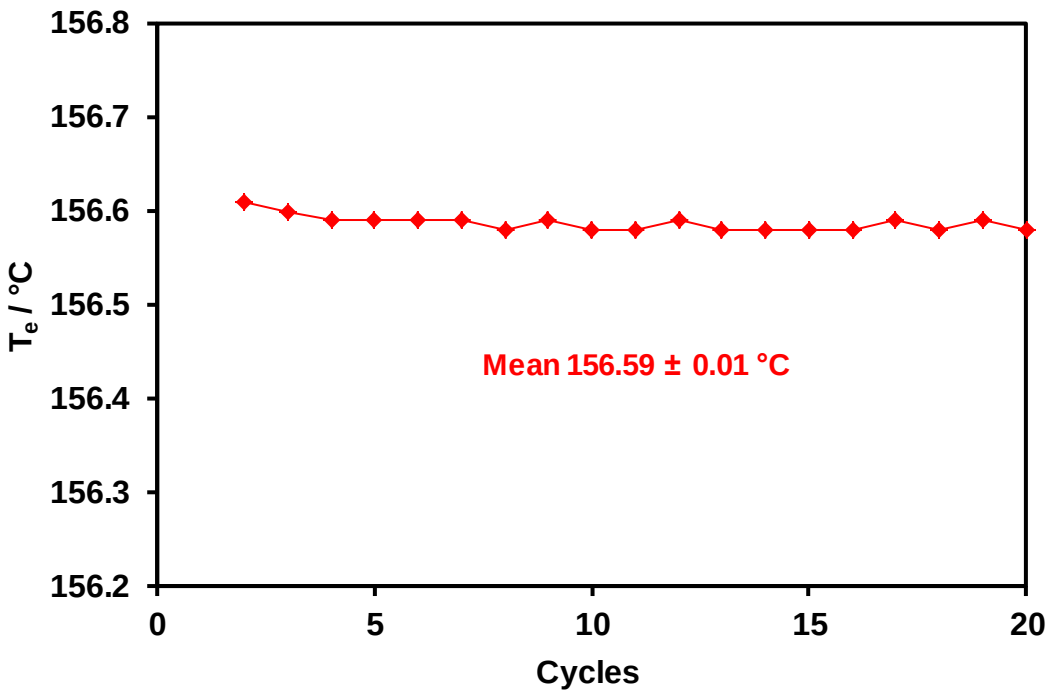

Fig. 29. ***Cycling of LGC Indium (Sample mass, 10mg; heating rate, 10°C min^{-1}; atmosphere, nitrogen)***

In order to check that the DSC remains within the calibration specified, it is good practice to bracket the batch of work with runs on a calibrant and periodically in

between if, for example, the work exceeded 10 consecutive runs. In the case of a continual programme of work a limit of 10 cycles would lead to the calibrant being discarded on almost a daily basis.

By cycling samples of indium an assessment of its suitability as a recycled secondary calibrant can be made. An example of the repeatability of the extrapolated onset of a sample of LGC Indium is shown in Fig. 29. The sample was both heated and cooled at a controlled rate of 10°C min^{-1} to and from ambient temperature before repeating. This was performed up to twenty cycles; double that of the recommendations.

3.5 Studies on Tin

3.5.1 Accurate Equilibrium Temperature of Fusion Measurements on Various Forms of Tin.

In addition to indium, the equilibrium temperatures of various forms of tin were studied. Tin itself is less frequently used in the secondary calibration process as it is believed to react with the aluminium crucible upon multiple use. However, it is required when making a multiple point primary calibration for higher temperature measurements. Mirroring the experimental conditions used in Section 3.3.1, the $T_{\beta=0}$ were determined for both the LGC and powdered forms of tin and their results given in Tables 10 – 11.

Table 10. ***Equilibrium temperature of LGC tin using the $T_{\beta=0}$ Method (sample mass; 10mg, atmosphere; nitrogen)***

Experiment	$T_{\beta=0}$ / °C	$(dT_e / d\beta)$ / min
First Heating	232.03 ± 0.05	0.070 ± 0.009
Second Heating	232.00 ± 0.03	0.065 ± 0.004
Third Heating	231.95 ± 0.06	0.081 ± 0.009
Mean Value	231.99 ± 0.08	0.072 ± 0.013

The linear relationship of dT_e / dβ for the powdered and LGC samples of tin are similar in gradient to those obtained for indium and indicate that the differences in slope observed could be attributed to the differences in heat transfer.

Table 11. ***Equilibrium temperature of high purity tin powder using the $T_{\beta=0}$ method (sample mass; 10mg, atmosphere; nitrogen)***

Experiment	$T_{\beta=0}$ / °C	(dT_e / dβ) / min
First Heating	231.66 ± 0.05	0.048 ± 0.008
Second Heating	231.61 ± 0.05	0.050 ± 0.007
Third Heating	231.59 ± 0.06	0.038 ± 0.009
Mean Value	231.62 ± 0.09	0.045 ± 0.014

Unlike the studies performed on indium there is a minor temperature difference in the equilibrium transition temperatures for the tin forms. The reason for this is unclear however, by performing T_{step} measurements this should provide experimental confirmation of the equilibrium temperature for tin.

Using the experimental conditions from Section 3.3.1 the equilibrium temperature for tin powder and LGC tin were determined using the T_{step} method.

Table 12. ***Equilibrium temperature of fusion of tin using the T_{step} method (sample mass; 10mg, atmosphere; nitrogen)***

Experiment	LGC T_{step} / °C	Powder T_{step} / °C
First Heating	232.03 ± 0.03	232.01 ± 0.01
Second Heating	232.01 ± 0.03	231.99 ± 0.03
Mean Value	232.02 ± 0.03	232.00 ± 0.03
Certified Value	231.92 ± 0.02	-
Calibration Correction	0.10 ± 0.04	-

The results are given in Table 12 and Fig 30 and confirm that they are directly comparable to the certified liquid temperature of tin and there are indeed no differences observed between the two sample forms when heated under near equilibrium conditions.

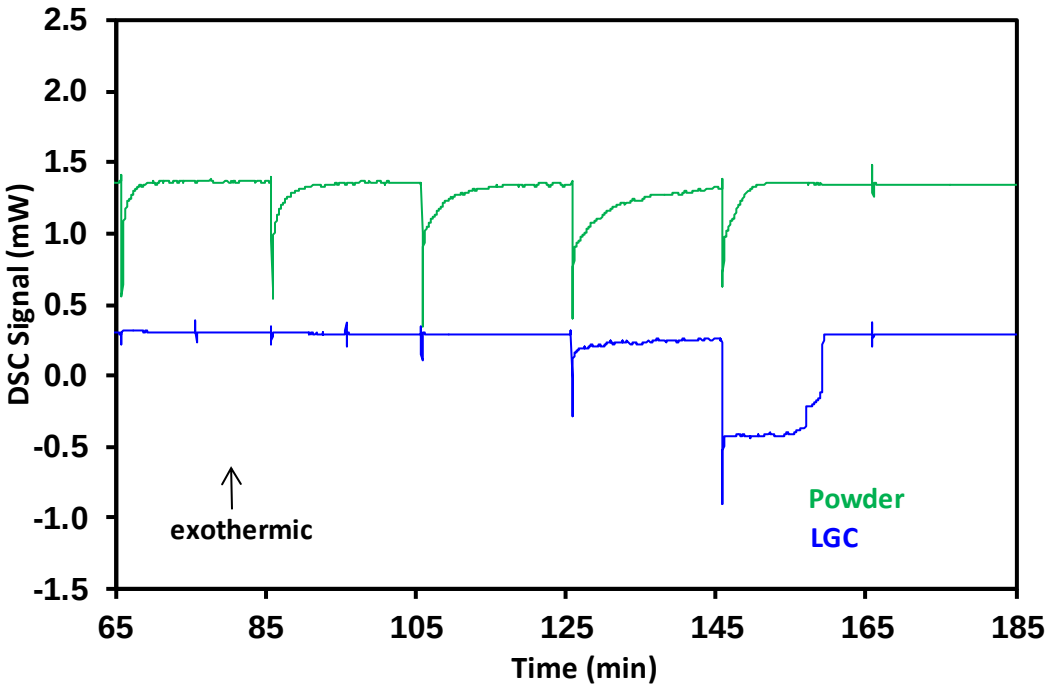

Fig. 30. ***An example of the stepwise heating of tin samples (sample mass; 10mg, step size 0.05°C, atmosphere; nitrogen)***

3.6 Conclusions for the accurate equilibrium temperatures of high purity metals

Measurements have been made to determine the equilibrium temperature of fusion of high purity indium and tin using the extrapolation to zero heating rate and isothermal stepwise heating rate methods and compared with their certified liquefaction values.

Indium is the calibration material of choice due to its well defined low temperature of transition at 156.6°C. It is taken for granted that indium regardless of it form will arrive at the same extrapolated onset temperature, however this thesis has shown that this only stands when measured under equilibrium temperatures. Should

powdered and solid (LGC) forms be measured dynamically in the conventional manner of operation i.e. at 10°C min^{-1} temperature differences of up to 0.2°C can be observed due to the differences in heat transfer across the sample. Whilst this may be considered a small difference, when determining accurate temperatures under equilibrium conditions these differences have been reduced to ±0.05°C using two independent heat flux DSC systems allowing a greater deal of confidence in the reported transition temperature(s).

Indium is often used as a secondary standard to periodically check the calibration of a DSC for temperature and enthalpy compliance. Whilst there is no limit set as to how often a sample can be re-cycled some manufacturers suggest a limit of 10 cycles before discarding the sample. It was found during preliminary work on the sample preparation protocol in Section 2.3.1 that if the solid indium sample was neither sufficiently thin nor pressed firmly into the base of the crucible that there was a small change in the melting temperature from the first and second heating. It would be, therefore, a sensible precaution to bed in a metal sample before use. Preliminary work has shown that samples of indium still provide reproducible extrapolated onset temperatures some 20 cycles later.

In addition to measurements on indium preliminary measurements were made on the equilibrium temperature of fusion of high purity tin. Whilst measurements under isothermal stepwise heating provided confirmation of the equilibrium temperature using DSC regardless of form, the extrapolation to zero heating rate method for the powdered material did not mirror this and would require further investigation.

Chapter 4 Solid-Solid Transitions of Inorganic Nitrates and Perchlorates

4.1 Introduction

The aim of this chapter is to implement the methods outlined in Section 1.7 to provide more accurate, equilibrium temperature values for the solid - solid transitions of the following inorganic compounds: potassium nitrate, rubidium nitrate, and potassium perchlorate. All of these compounds have one or more solid-solid transitions prior to fusion which have potential for use as low temperature calibration standards.

These materials are also of interest since they are used as oxidants in pyrotechnic systems. The word pyrotechnic translates from the Greek language “pyr” (fire) and “techne” (an art) which loosely describes the visual effects of a pyrotechnic composition when burning. Pyrotechnic compositions are designed to produce effects such as noise, bright coloured light, coloured smoke and heat; and can be incorporated into items such as fireworks, munitions or even safety devices.

A pyrotechnic composition in its simplest form is as a bi-component system that contains a fuel in the form of finely divided metal powder and an oxidiser. A large variety of inorganic oxidants are incorporated into the making of pyrotechnic mixtures and are typically used in the form of either a perchlorate or nitrate salt of a group 1 element. In order to develop new compositions the thermal behaviour of the intended oxidant has to be fully assessed to predetermine transitional and fusion behaviours which may influence the pyrotechnic reaction.

4.2 Rubidium Nitrate

4.2.1 Introduction

Rubidium Nitrate ($RbNO_3$) exhibits three reversible solid-solid phase transitions prior to fusion which takes place in the region of 310°C. The three transitions of $RbNO_3$ are given below with the temperatures in brackets representing the temperature ranges found in literature.

Transition 1 (160-166°C)	trigonal to CsCl (cubic)
Transition 2 (219-228°C)	CsCl (cubic) to rhombohedral
Transition 3 (278-291°C)	rhombohedral to NaCl (cubic)

$RbNO_3$ has been investigated as a possible temperature calibration standard since its transitions span the melting points of indium, tin and lead.[35]

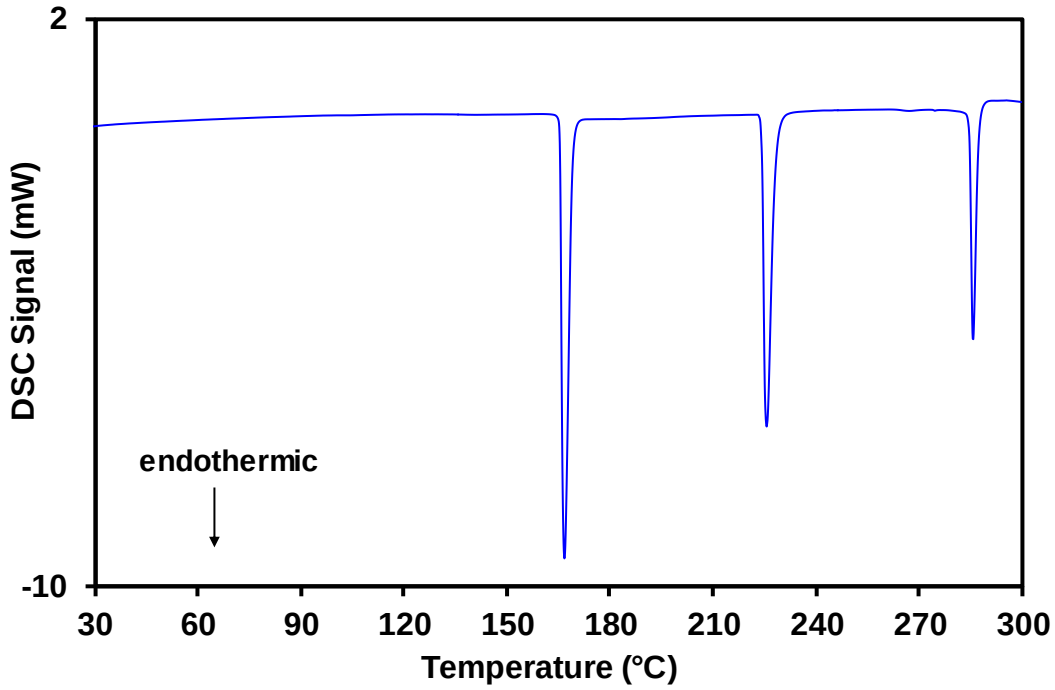

Fig. 31. ***DSC curve showing the solid-solid transitions of rubidium nitrate prior to fusion (sample mass, 5 mg; heating rate, 10°C min^{-1}; atmosphere, argon)***

An assessment of the stability of the three transitions has been made to determine whether it is possible to replace multiple sample calibrations spanning the temperature range 150°C to 300°C with a single inorganic substance.

An extensive literature review into the accurate onset temperature of transitions of $RbNO_3$ showed great variation, the reason for which remains uncertain.

Table 13. ***Literature temperature values for the solid-solid transitions of rubidium nitrate.***

First Author	Year	Temperature / °C			Ref.	Method
		T_1	T_2	T_3		
Rostkowski	1930	166	229	-	36	Heating curve
Plyushcev	1956	164	219	291	37	Heating curve
Mustajoki	1958	160	218	281	38	Calorimetry
Arell	1961	164.4	219-220.7	-	39	Calorimetry
Brown	1962	160	220	290	40	Microscopy
Rao	1966	166	228	278	41	DTA
Protsenko	1973	164	220	285	42	DTA
Secco	1999	166	222	285	43	DSC
Hichri	2002	164	227	282	44	DSC
Wacharine	2011	166	228	287	45	DSC
Jendoubi	2013	166	234	285	46	DTA/DSC
Average		164 ± 2	224 ± 5	285 ± 4		

$RbNO_3$ is reported to be stable to temperatures well above the transition temperatures and although thermal history was found to influence the temperature of Transition 2, Transitions 1 and 3 were reported to be free from such effects.[47] In view of the discrepancies in the literature, accurate values have been

determined for the equilibrium transition temperatures using DSC instrumentation described in Section 2.1. In addition, the enthalpies of the transitions have also been measured. Previous enthalpy measurements are few in number and are summarised later in Table 18.

4.3 Determination of Accurate Transition Temperatures of $RbNO_3$

A high purity rubidium nitrate (Alfa Aesar 99.975%) was used in these studies and was prepared as described in 'Materials Used' Section 2.3.4.

Accurate temperature measurements were made using two heat-flux DSCs; a Mettler Toledo DSC822^e (operated with the tau lag function disabled) and a Thermal Instrument TA2920. The instruments were calibrated for temperature using the T_{step} of high purity solid metals; LGC indium, tin and lead. For the measurements using lead, the crucibles were pre-oxidised by heating in air at 550°C for two hours to minimise reaction between the sample and the crucible.

Measurements were made using 5mg of sample in non-hermetically sealed 20µL crucibles in a flowing atmosphere of argon. Regular performance checks were carried out during the work to ensure consistency in the results.

4.3.1 Determination of $T_{\beta=0}$ for $RbNO_3$ Solid-Solid Transitions

The $T_{\beta=0}$ method was used over the range 1-10°C min^{-1} to determine accurate temperatures of transition for Transitions 1-3 of $RbNO_3$. The samples were heated through all transitions and a new sample used for each heating rate determination.

4.3.2 Transition 1

The influence of heating rate on the first transition of $RbNO_3$ using the Mettler Toledo DSC 822^e is shown in Fig. 32 and the $T_{\beta=0}$ constructions for both DSC instruments plotted in Fig. 33.

It can be seen that the peaks remain well defined and smooth during the heating rate measurements.

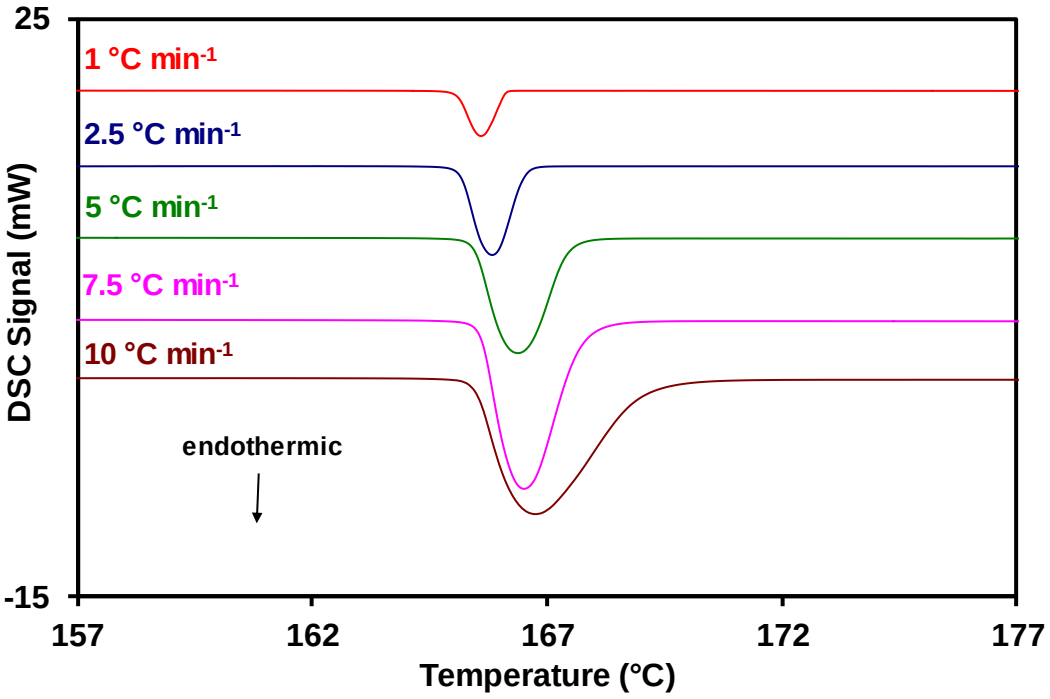

Fig. 32. ***Mettler Toledo DSC curves showing the influence of heating rate on transition 1 of rubidium nitrate. (sample mass, 5 mg; atmosphere, argon)***

The equilibrium transition temperatures obtained by extrapolating the values of T_e to a zero heating rate using two independent HF-DSCs are summarised in Table 14 below and show excellent reproducibility irrespective of the machine used.

Table 14. ***Extrapolation to zero heating rate temperatures for Transition 1 of rubidium nitrate.***

Instrument	$T_{\beta=0}$ / °C	(dT_e / $d\beta$) / min
Mettler Toledo DSC822^e	164.95 ± 0.05	0.08
Thermal Instrument TA2920	164.86 ± 0.03	0.08
Mean	164.91 ± 0.03	0.08 ± 0.00
Literature	164 ± 2	-

The uncertainties are the standard deviations and include the uncertainty in the calibration factor as described in Section 1.7.1

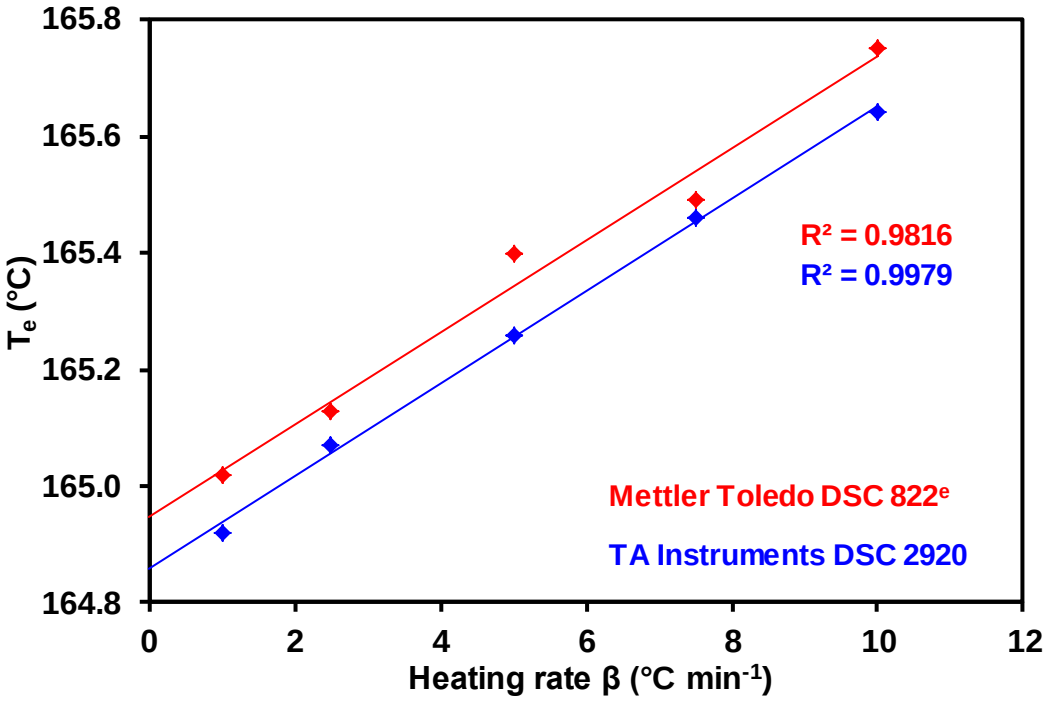

Fig. 33. ***Influence of heating rate on transition 1 of rubidium nitrate using two different heat flux DSC systems. (sample mass, 5 mg; atmosphere, argon)***

4.3.3 Transition 2

Unlike the first transition, transition 2 of $RbNO_3$ behaves in a different manner, especially when subjected to much slower heating rates. The peaks became less sharp, 'noisy', and broader as the heating rate decreased.

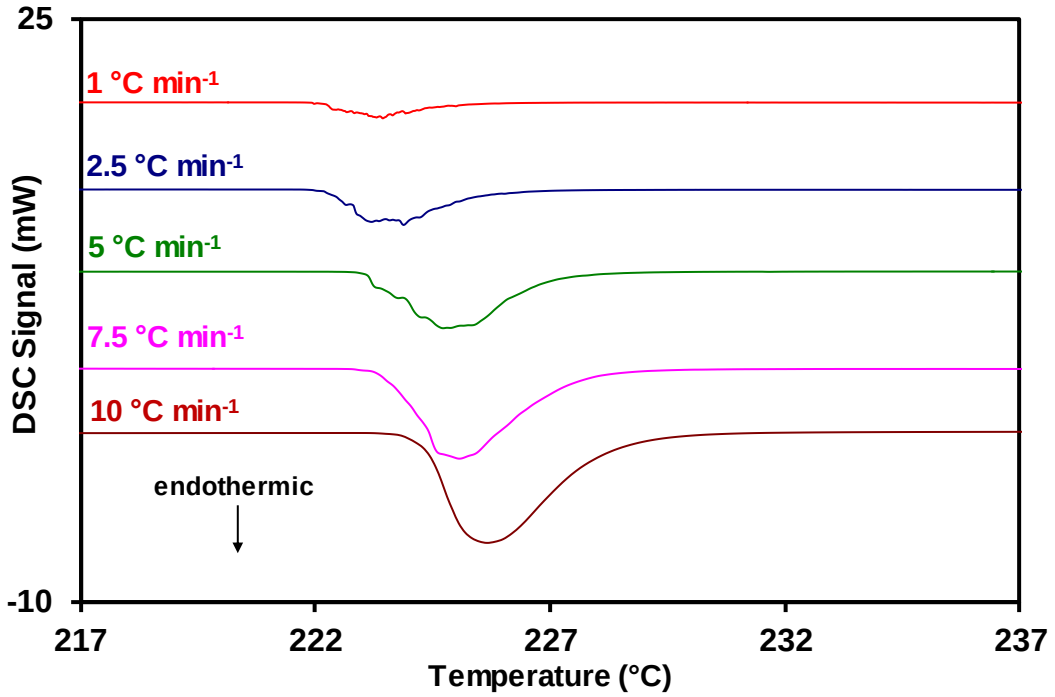

Fig. 34. ***Influence of heating rate on the Mettler Toledo DSC curves for transition 2 of rubidium nitrate (sample mass, 5 mg; atmosphere, argon)***

The noise was observed for both of the instruments used as is illustrated in Fig. 35 and shows the difficulty in making a T_e measurement. The peaks were therefore smoothed using the software provided by the instrument manufacturer. The smoothing option allows a regularly selected number of measurement points to be discounted to facilitate the smoothing of unwanted noise within a DSC measurement.

By implementing a 1:20 smoothing to the DSC raw data it was then possible to determine an extrapolated onset temperature for transition 2 without over compressing the data and compromising the peaks integrity.

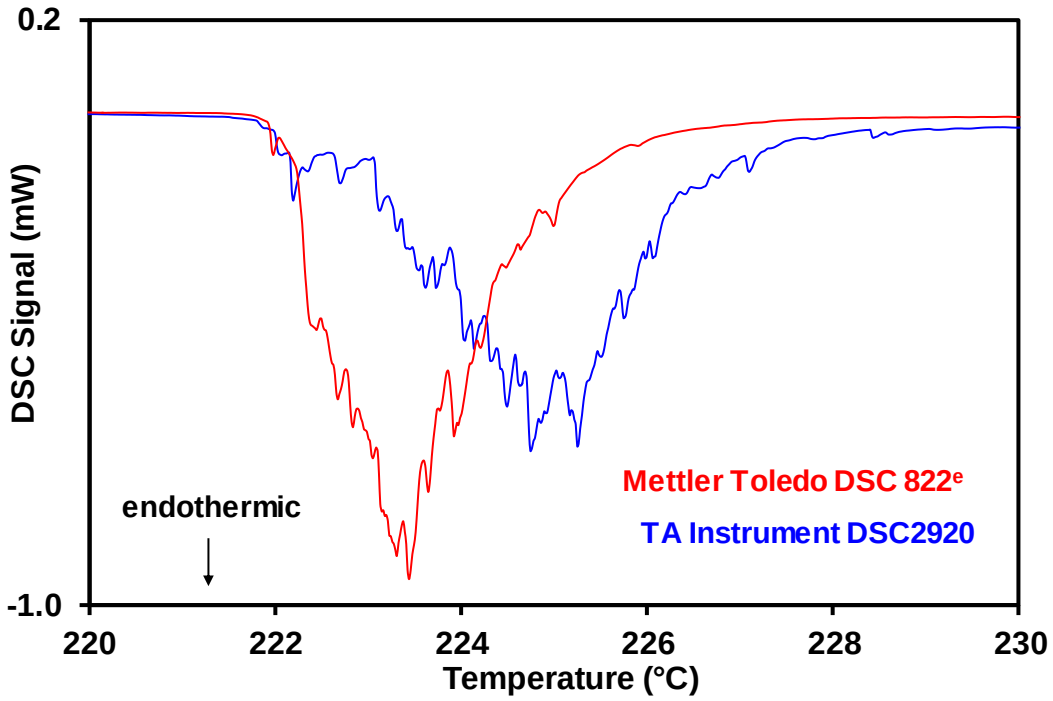

Fig. 35. *DSC curve during slow heating of transition 2 of rubidium nitrate (sample mass, 5 mg; heating rate, 1°C min^{-1}; atmosphere, argon)*

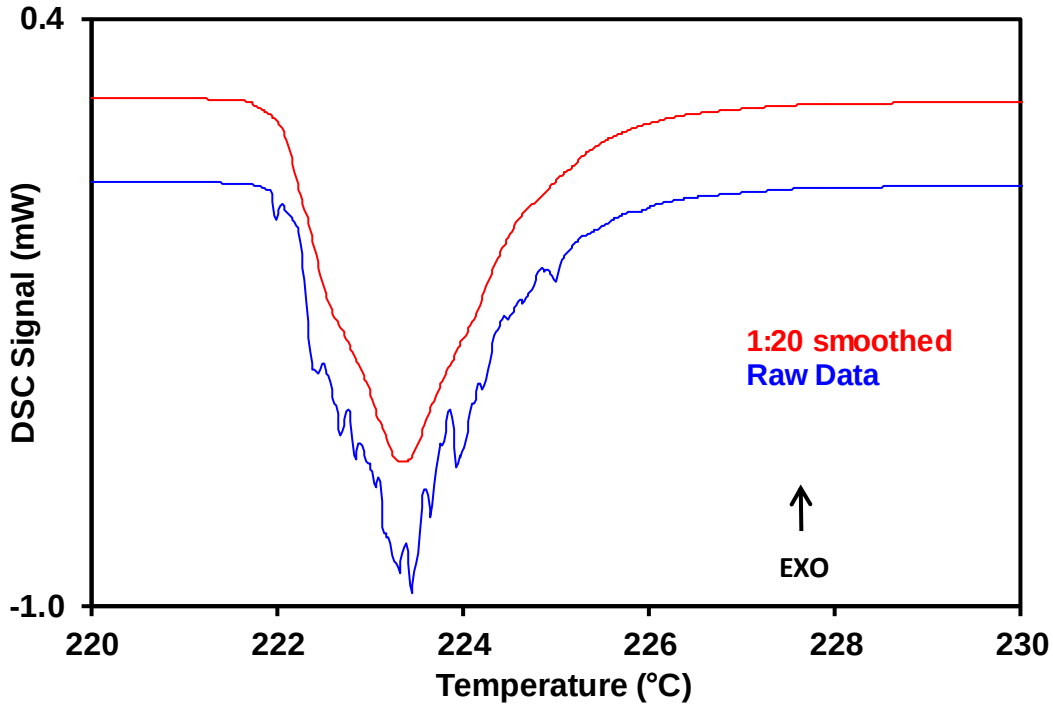

Fig. 36. *Mettler Toledo DSC curve for the slow heating of transition 2 of rubidium nitrate heated at 1°C min^{-1} before and after smoothing. (sample mass, 5 mg; atmosphere, argon)*

The equilibrium transition temperatures obtained by extrapolating the values of T_e to zero heating using the two HF-DSCs units are summarised in Table 15. The results show that a greater level of uncertainty in the measured $T_{\beta=0}$ temperatures than those observed for Transition 1. This is not unexpected in view of the noise observed.

Table 15. ***Extrapolation to zero heating rate temperature for transition 2 of rubidium nitrate (sample mass, 5 mg; atmosphere, argon)***

Instrument	$T_{\beta=0}$ / °C	$(dT_e / d\beta)$ / min
Mettler Toledo DSC822[e]	221.7 ± 0.4	0.27
Thermal Instrument TA2920	222.7 ± 0.5	0.27
Mean	222.2 ± 0.5	0.27 ± 0.0
Literature value	224 ± 5	-

4.3.4 Transition 3

Initial inspection of the DSC curve for Transition 3 appears to give a well defined peak (Fig. 31) however, when plotted at much higher sensitivities there was a noticeable endothermic baseline drift. This is illustrated in Fig. 37. It is also possible to see the presence of two endotherms which consistently appear at 265°C and 275°C. Thermogravimetric measurements showed that they were not associated with a mass change. These peaks were observed in all of the experiments and appeared to increase slightly in magnitude in repeated cycles of the sample through the transitions. The significance of these peaks is not clear and they have been ignored in obtaining the enthalpy values.

For the purpose of baseline consistence it was decided that all transitions were viewed initially on a 1mW scale (shown in Fig.37 in red). At 1mW scale it is a small enough zoom in which to establish any minor changes in heat capacity but not too much to exaggerate and possibly create digital artefacts.

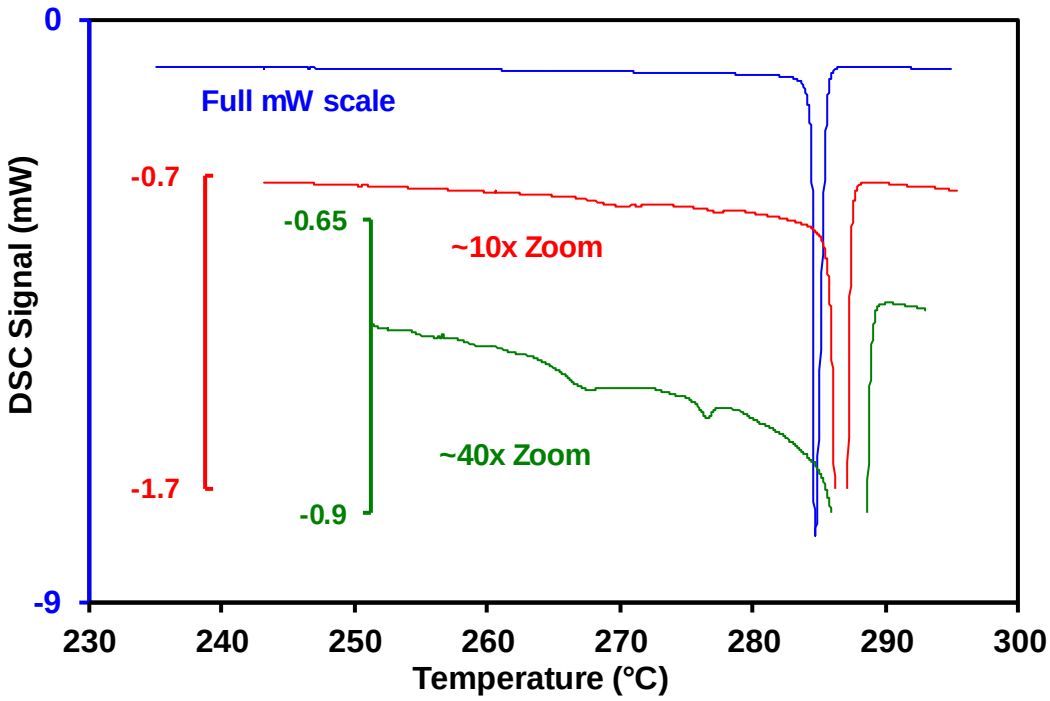

Fig. 37. *DSC curves plotted at different mW scale sensitivities for transition 3 of rubidium nitrate (sample mass, 5 mg; atmosphere, argon)*

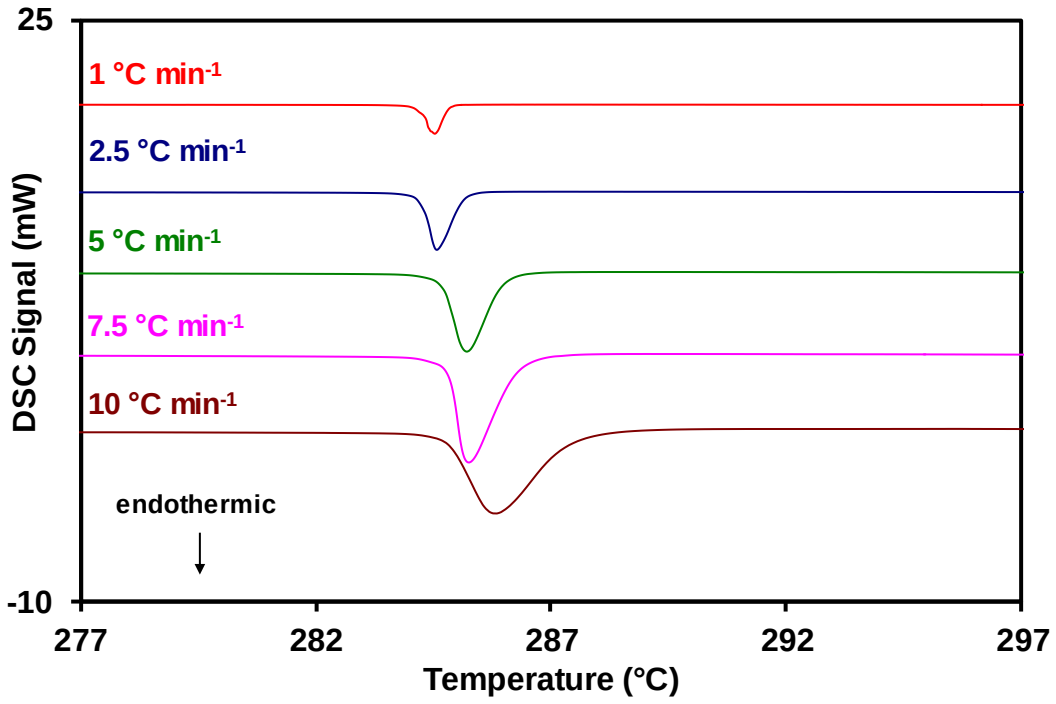

Fig. 38. *Influence of heating rate on the Mettler Toledo DSC curves for transition 3 of rubidium nitrate (sample mass, 5 mg; atmosphere, argon)*

As for the case with Transition 1 this also showed excellent reproducibility and the values obtained using the two DSC instruments were in close agreement.

Table 16. ***Extrapolation to zero heating rate temperatures for transition 3 of rubidium nitrate. (sample mass, 5 mg; atmosphere, argon)***

Instrument	$T_{\beta=0}$ / °C	(dT_e / $d\beta$) / min
Mettler Toledo DSC822[e]	283.98 ± 0.04	0.11
Thermal Instrument TA2920	284.07 ± 0.07	0.09
Mean $T_{\beta=0}$ of both instruments	284.03 ± 0.04	0.10 ± 0.01
Mean literature value	285 ± 4	-

The gradients of the curves obtained by plotting T_e against the heating rate β for the three transitions are markedly different. The mean values from the two instruments were 0.08 ± 0.00 min (Transition 1), 0.27± 0.03 min (Transition 2), and 0.11 ± 0.02 min (Transition 3). These uncertainties are estimates of the reliability of the results based on single standard deviations of the means of the experimental results and include an allowance for the uncertainty in assigning the onset temperature of melting and the error in the weighings.

4.3.5 Summary of $T_{\beta=0}$ Measurements for Transitions 1-3 of $RbNO_3$

Having calculated the calibration factor κ for each transition, errors that could be incurred when using a single point calibration at a heating rate β are shown in Fig. 39.

As the heating rate dependencies of Transitions 1 and 3 are very similar (dT_e / $d\beta$) the errors associated with the calibration correction at each heating rate would be minimal. However, in the measurement of Transition 2 (should either

Transition 1 or 3 been used as a single point calibration), the heating rate dependency is clearly different and would see errors up to 3.8°C when measured at 20°C min^{-1}

These variations within a single compound illustrate the potential errors in calibration at a single heating rate, more so when the calibrant and sample may have significantly different heating rate dependencies.

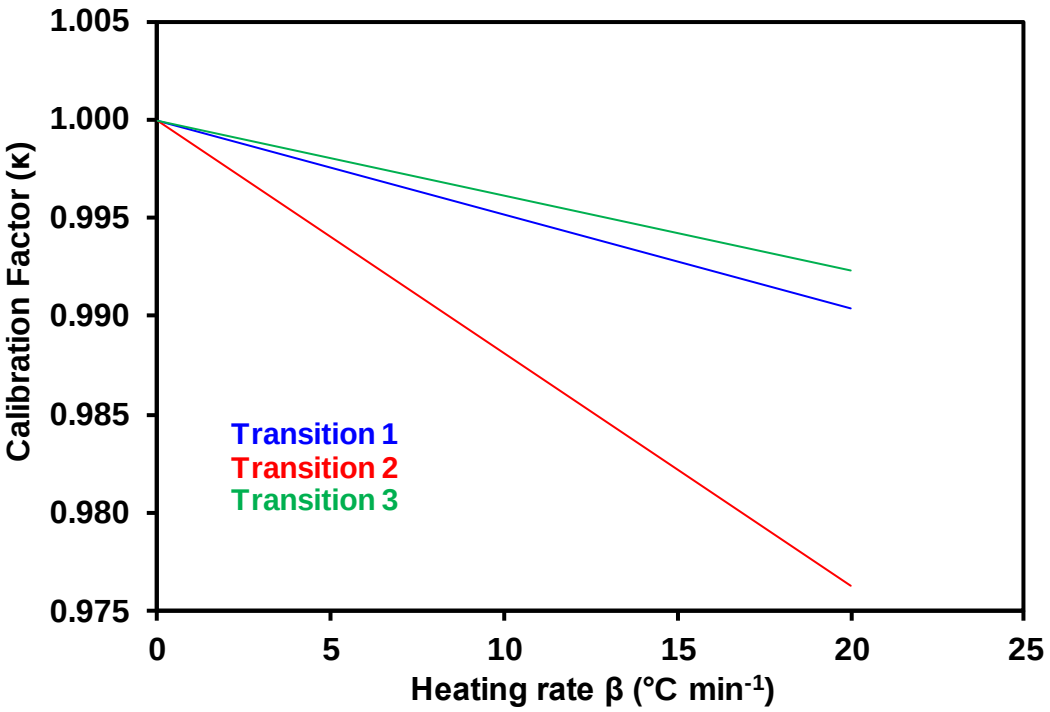

Fig. 39. ***Calculated calibration factor κ over a range of heating rates for the solid-solid transitions of rubidium nitrate.***

4.3.6 Determination of T_{step} for $RbNO_3$ Solid-Solid Transitions

Using the method described in section 1.7.2, stepwise equilibrium temperature measurements were made on both Transition 1 and Transition 3 of $RbNO_3$. It had been seen previously in the $T_{\beta=0}$ studies that Transition 2 of $RbNO_3$ would be unsuitable for this method of measurement due to the increasing amount of noise observed under slower heating rates. The standard increment of 0.05°C with an isothermal period of 20 minutes was used in these measurements.

A stepwise isothermal DSC plot for Transition 1 is shown in Fig. 40 and shows that the transitional change was complete within 120 minutes over a very narrow temperature range.

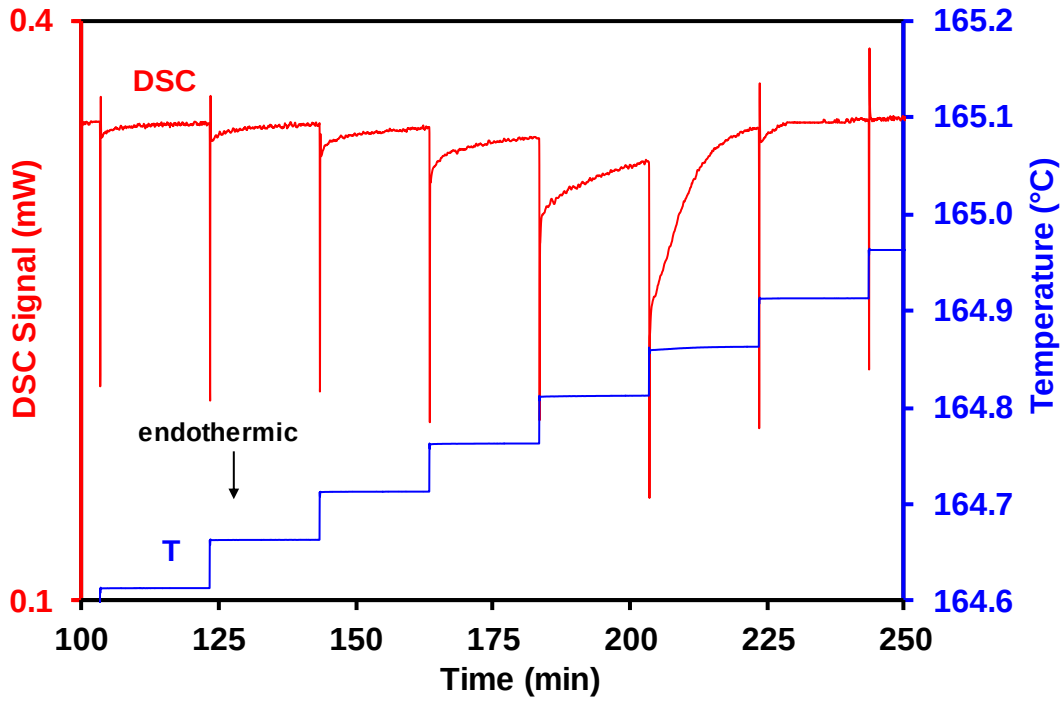

Fig. 40. ***DSC curve for transition 1 of rubidium nitrate obtained under stepwise heating conditions (sample mass, 5 mg; step size, 0.05°C; atmosphere, argon)***

By plotting the incremental enthalpy against temperature enables a direct comparison of the rubidium nitrate Transition 1 results from the stepwise and linear heating methods can be made. This is illustrated in Fig. 41 and discussed in the resulting publication.[18] By representing the data in this way it swiftly demonstrates the very narrow temperature range over which the transition takes place under stepwise heating conditions compared with heating under linear conditions.

The values obtained by the stepwise isothermal method for Transitions 1 and 3 are summarised in Table 17. Triplicate measurements were performed to ensure reproducibility. The results exemplify the excellent reproducibility that can be obtained using this technique.

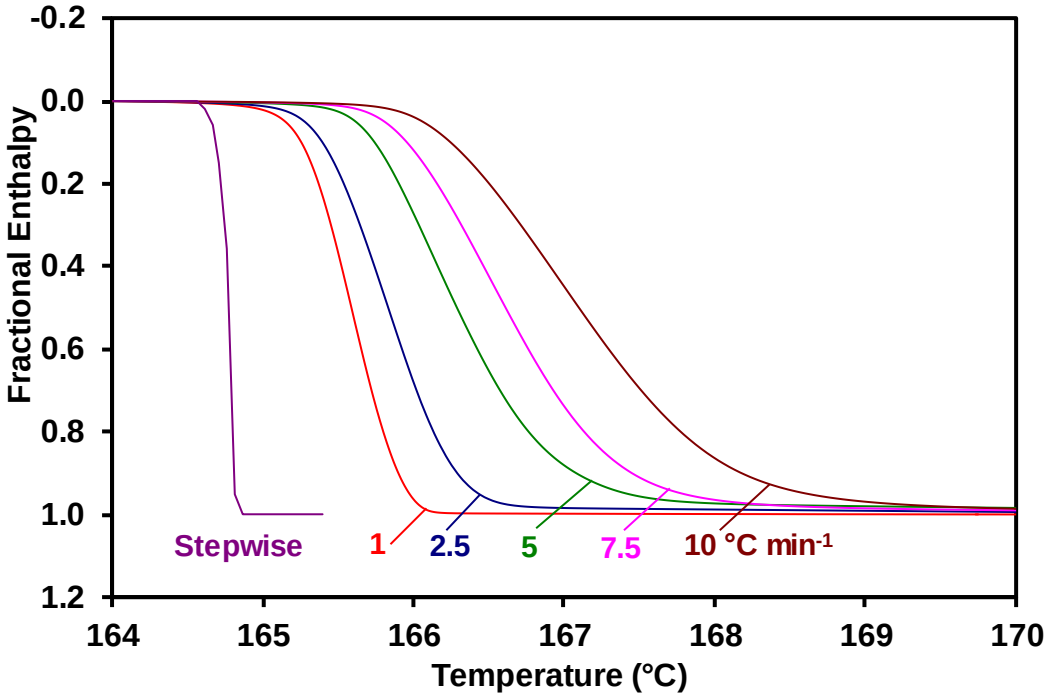

Fig. 41. ***A plot of fractional enthalpy against temperature for transition 1 of rubidium nitrate obtained under stepwise and linear heating conditions.***

Close agreement was again given between the values from the two DSC instruments and overall mean equilibrium temperature of 164.9 ± 0.1 °C and 284.1 ± 0.1 °C were obtained for Transitions 1 and 3 using both methods of determining accurate temperature measurements.

Table 17. ***Equilibrium temperature for the solid-solid phase transitions of rubidium nitrate obtained using the isothermal stepwise heating DSC method***

Instrument	Equilibrium Temperature / °C	
	Transition 1	Transition 3
Mettler Toledo DSC	164.90 ± 0.03	283.79 ± 0.03
TA Instrument TA2920	165.02 ± 0.04	283.84 ± 0.04
Mean T_{step} for both instruments	164.96 ± 0.05	283.82 ± 0.05
Mean literature value	164 ± 2	285 ± 4

4.4 Determination of Enthalpy for the Transitions of $RbNO_3$

In addition to accurate temperature measurements of transition, using an approach similar to that adopted by Richardson, enthalpies of the solid-solid transitions of rubidium nitrate have been determined. Like the temperature values, literature values for the transitions are scattered. Having observed small peaks within Transition 3 variation in the enthalpy measurements may be expected, however for transitions 1 and 2 the reason for this is unclear.

Table 18. ***Literature values for the enthalpies of the solid-solid transitions of rubidium nitrate.***

First Author	Year	Enthalpy (kJ mol^{-1})			Ref.	Method
		Transition 1	Transition 2	Transition 3		
Mustajoki	1958	3.90	3.21	0.96	38	Calorimetry
Arell	1961	3.86	3.24	-	39	Calorimetry
Rao	1966	3.97	2.72	1.26	41	DTA
Hohne	1983	3.82	3.15	1.37	48	DSC*
Hohne	1985	3.82	3.13	1.27	49	DSC±
Secco	1999	4.00	3.29	1.47	43	DSC
Mean Enthalpy		3.90 ± 0.08	3.12 ± 0.21	1.27 ± 0.19		

*Unweighted mean from 2 instruments

±Unweighted mean from round robin study. Value for transition 3 obtained using a linear baseline

The enthalpy determinations were carried out using a Mettler Toledo DSC 822[e] and a Perkin Elmer Diamond DSC. The measurements were made in triplicate at a heating rate of 3°C min^{-1} using an increased sample mass of 10mg.

The results obtained for the enthalpy measurements are given in Table 19. The calculations were made by Professor Peter Laye by adopting a linear temperature

extrapolation of the initial and final heat capacities. The aim in using this type of method for enthalpy measurements was to obtain values which have thermodynamic validity, therefore the assigned temperature (T_1) in the enthalpy determination was governed by that of the equilibrium transition temperatures previously measured in Section 4.3.

Table 19. ***Enthalpy values for the solid-solid phase transitions of rubidium nitrate using Richardson's method (sample mass, 10; heating rate, 3°C min^{-1}; atmosphere, argon)***

Instrument	Enthalpy / kJ mol^{-1}		
	Transition 1	Transition 2	Transition 3
Mettler DSC 822^e	3.83 ± 0.04	3.15 ± 0.04	1.74 ± 0.06*
Perkin Elmer Diamond	3.82 ± 0.02	3.13 ± 0.05	1.72 ± 0.06*
Mean	3.83 ± 0.02	3.14 ± 0.03	1.73 ± 0.04*

*These values were obtained by assigning T_1 to a temperature before the onset of C_p curvature.

It can be seen from Table 19 that there is no difference between the results obtained from either instrument which is of particular interest in view of their differences in operating principles. The superimposed peaks observed in Transition 3 and their associated enthalpies (~0.03kJ mol^{-1}) have been excluded from the final result. Using the commercial software provided by both DSC systems, calculations for enthalpy were made using suitable iterative baseline constructions and are summarised in Table 20.

Table 20. ***Enthalpy values for the solid-solid transitions of rubidium nitrate measured using two calculation methods.***

Instrument	Enthalpy / kJ mol^{-1}		
	Transition 1	Transition 2	Transition 3
Ricardsons' Method	3.83 ± 0.02	3.14 ± 0.03	1.73 ± 0.04*
Mean from DSC Software	3.83 ± 0.02	3.12 ± 0.02	1.73 ± 0.03

4.5 Conclusions for the Determination of Accurate Temperature and Enthalpy Values for the Solid-Solid Transitions of $RbNO_3$

Accurate values for the equilibrium temperatures of the three solid–solid phase transitions of high purity rubidium nitrate have been measured by two different experimental methods using two different types of heat flux DSC instruments. Transitions 1 and 3 showed good reproducibility and gave overall mean values of 164.9 ± 0.1 and 283.9 ± 0.1 °C, respectively. These values show a significant improvement in precision over those published previously and show potential for use as secondary calibrants for accurate temperature measurements.

The DSC peak for transition 2 was less well-defined at lower heating rates and the equilibrium temperature could not be measured using the stepwise technique. A value of 222.2 ± 0.5 °C was obtained by the extrapolation to zero heating rate method. In light of the difficulties in measuring the accurate temperature of Transition 2 and its significant difference in $dT_e/d\beta$, this transition would be an unsuitable candidate for use as a temperature calibrant for samples which exhibited similar heating rate dependencies to Transitions 1 and 3.

The enthalpies of the transitions have been measured at the equilibrium temperatures using both heat flux and power compensation DSC instruments. For Transitions 1 and 2 there was good agreement for the two sets of results and mean values of 3.83 ± 0.02 and 3.14 ± 0.03 kJ mol^{-1} respectively were obtained. For transition 3 there is greater uncertainty in the results because of the slow increase in the heat capacity before the main transition peak.

Similar results were given for the enthalpies of the three transitions using the dedicated software supplied by the instrument manufacturers.

4.6 Potassium Nitrate

4.6.1 Introduction

Potassium nitrate is an oxidant that when combined with a fuel is a gas producing composition generating an intense white light when ignited. In addition to its use as a pyrotechnic oxidant, the solid-solid transition of potassium nitrate was formerly recognised as a standard reference material for use in the calibration of DTA equipment.[50] Potassium nitrate has an aragonite structure at room temperature and has been reported to exhibit complex structural behaviour upon heating and cooling through the solid-solid transition.[51-54] Potassium nitrate exhibits a low temperature transition prior to the onset of melting in the region of 130°C and is shown below in Fig. 42.

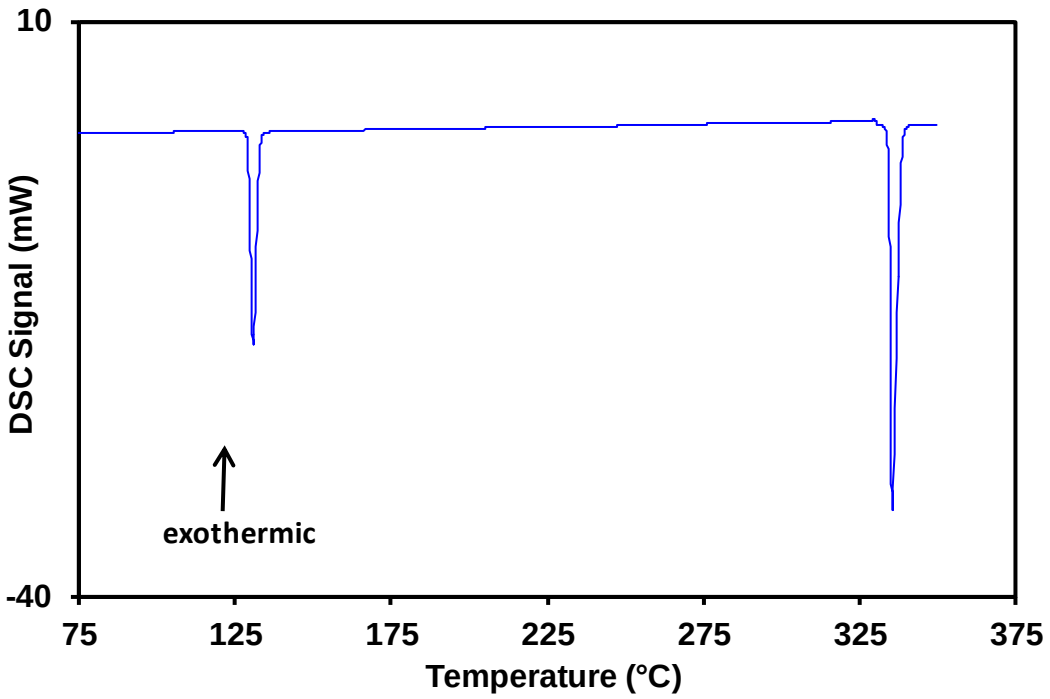

Fig. 42. ***Mettle Toledo DSC curve for potassium nitrate (sample mass, 5mg; heating rate, 10°C min^{-1}; atmosphere, argon)***

A literature review into the onset temperature of the solid-solid transition of KNO_3 has been made and is summarised in Table 21. Although widely studied, even the most recent of measurements show a variation of several degrees for its temperature of transition.

Table 21. ***Literature temperature and enthalpy values for the solid-solid transition of potassium nitrate***

First Author	Year	Temperature / °C	Area / Jg^{-1}	Ref
Gordon	1955	128	-	55
Garn	1969	128.9 – 129.3	-	56
Bridgeman	1916	127.9	49	57
Arell	1962	127.7	49	39
Deshpande	1974	129 ± 2	48	58
Wang	1976	128	53	59
Rojers	1982	130	50	60
Carling	1983	133	56	61
Takahashi	1988	129.9	51	62
Westphal	1993	129.4	50	63
Westphal	1993	122.9	26	63
Westphal	1993	117	21	63
Zamali	1995	131	50	64
Guizani	1998	130.4	-	65
Jendoubi	2012	128	49	46
	Average	128 ± 4		

The reason for the vast range of reported temperature values is due to the solid-solid transition occurring in several crystalline arrangements or “phases”. At ambient conditions KNO_3 is said to be in the α-phase (or transition II) and once heated through the solid-solid transition KNO_3 undergoes a structural change to form a rhombohedral structure,the β-phase (or transition I).[66-67]

In addition to the α and the β phases Deshpande[58] reported that when cooling from high temperatures a thermal hysteresis exists with an intermediate metastable phase, γ-phase (transition III), formed before reversing to its original structure Fig. 43.

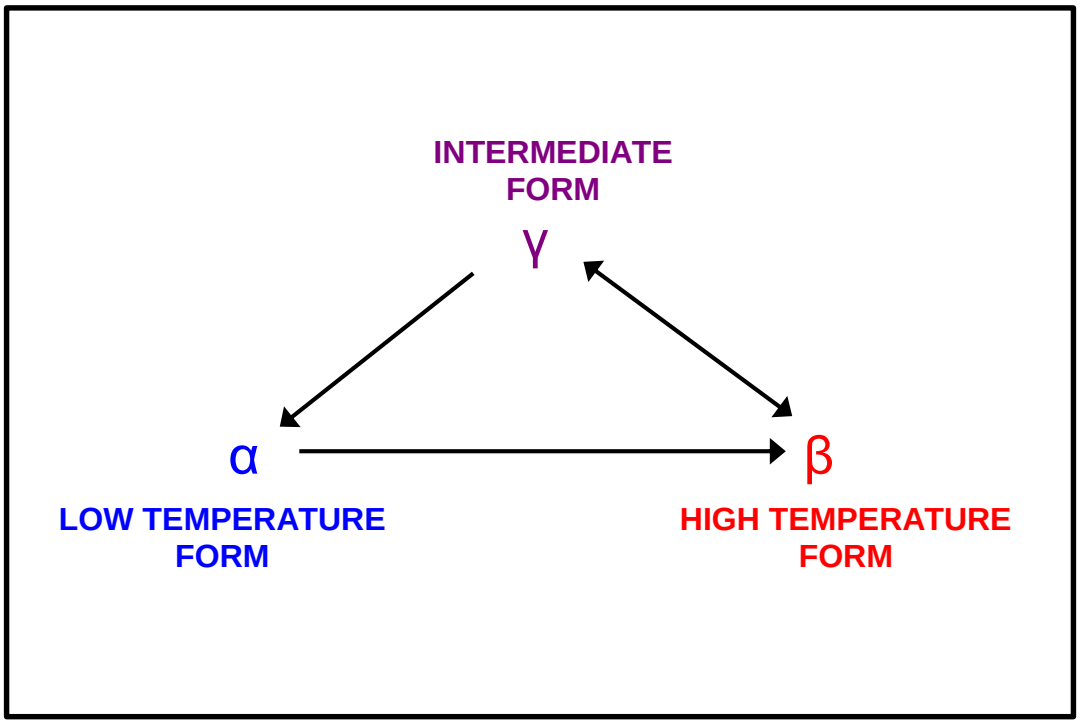

Fig. 43. ***Schematic of the structural forms undergone by the solid-solid transition of potassium nitrate.***

The thermal hysteresis surrounding the intermediate phase of the solid-solid transition of potassium nitrate is of great interest as it has been shown to portray ferroelectric properties[68, 51-52] and has potential for further investigation using TA techniques.

Samples which have ferroelectric properties possess a spontaneous electric polarisation that can be reversed by the application of an electric field; these are subjects of research interest due to their potential to be used in non-volatile random access memory devices. Implementing the methods successfully used to accurately determine temperatures of transition of $RbNO_3$ this section aims to re-measure and discuss the temperatures for the α→β, and the β→γ phases of KNO_3 with a much higher degree of accuracy than previously reported.

4.6.2 Preliminary Studies

Samples of KNO_3 were used and prepared as detailed in Section 2.3.

The Mettler Toledo 822^e DSC was calibrated using a triple point calibration with high purity indium, tin and lead using the T_{step} method. 20 µL aluminium pans were used and flowing atmosphere of argon used unless otherwise stated.

Measurements on the α→β phase for both KNO_3-C and KNO_3-SD at 10 °C min^{-1} are presented in Table 22. The measurements were made in order to establish whether the initial sample preparation contributed towards any changes in thermal behaviour as previously suggested by Westphal.[63]

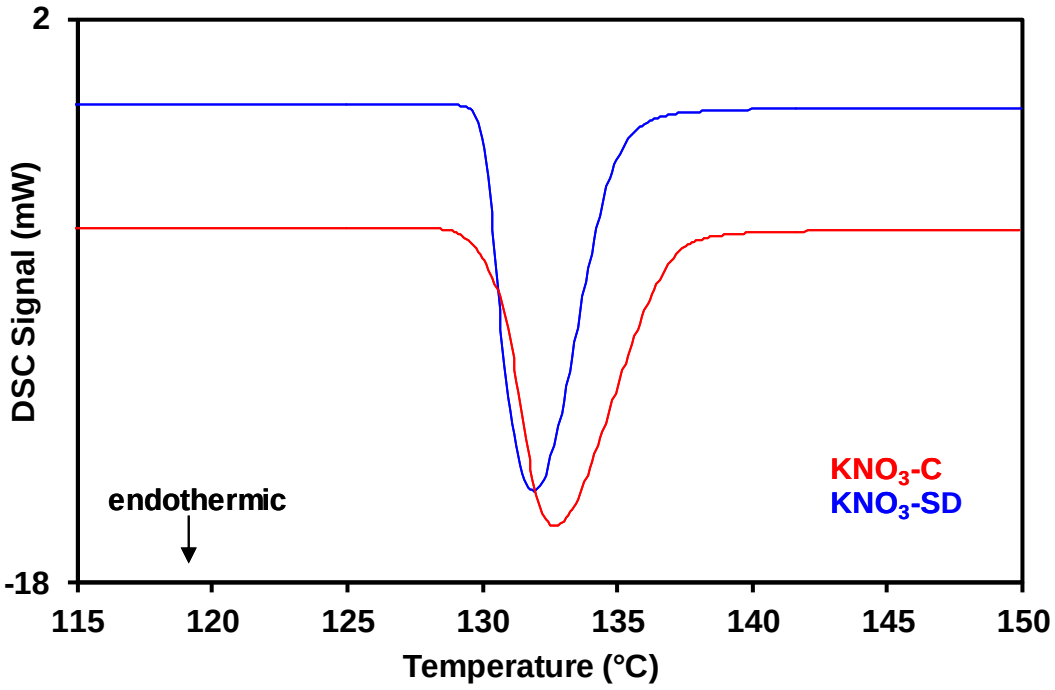

Fig. 44. ***Mettler Toledo DSC curves for the α → β solid-solid transition of potassium nitrate samples. (sample mass, 5mg; heating rate, 10°C min^{-1}; atmosphere, argon)***

The DSC results show that there is a significant temperature difference between the extrapolated onset of KNO_3-C and KNO_3-SD. Although a difference of 1°C of separation would not normally be up for discussion, when measuring temperature accuracies to better than ± 0.1 °C a degree would in fact amount to a significant

error. The ΔH values reported have been measured using the Mettler Toledo Star^{e} software using a linear baseline construction.

Table 22. ***Mettler Toledo DSC results for temperature and enthalpy of the α→β solid-solid transition of potassium nitrate. (sample mass, 5mg; heating rate, 10°C min^{-1}; atmosphere, argon)***

Sample	T_e / °C	ΔH / Jg^{-1}	Determinations
KNO_3 – C	130.7 ± 0.3	53.3 ± 1.3	16
KNO_3 – SD	129.7 ± 0.2	52.7 ± 1.1	11

Measurements on potassium nitrate which had had the drying stage omitted were also measured to confirm that the drying alone had not accounted for the temperature variance.

4.6.3 Identification of the Intermediate Phase γ

The identification of the intermediate γ-phase on heating using DSC has been reported to be dependent on its previous thermal history. Sawada[68] reported that the ferroelectric γ-phase *did not* appear if the sample were not heated to temperatures above 160°C, whilst in a more recent study[63] the identification of the γ-phase was only apparent once heated to temperatures above 150°C whilst cooled to temperatures no less than 135-105 °C.

With the method of preparation uncertain for the γ-phase both methods were explored and their resultant DSC curves analysed.

Method development: Pre-heating to 150°C

Triplicate (heat-cool-heat) DSC measurements were made on samples of KNO_3-C. The samples were heated to a maximum temperature of 150°C after which they were control cooled at 10°C min^{-1} to ambient prior to immediate re-heating. Controlled cooling was used in order to eliminate the potential for 'supercooling' to occur as the DSC chamber is returned to ambient conditions. It can be seen from

the DSC curve given in Fig. 45, that upon cooling re-crystallisation occurs from the β→α phase in two distinct regions. The majority of the recrystallisation occurs across a wide temperature range (105 – 45°C). The subsequent reheating of the KNO_3-C reveals small low temperature exotherms which were previously absent. These could be attributed to small solid-solid transitions of polymorphous KNO_3 continuing to return to its original crystalline structure but this would have to be confirmed using crystallographic methods.

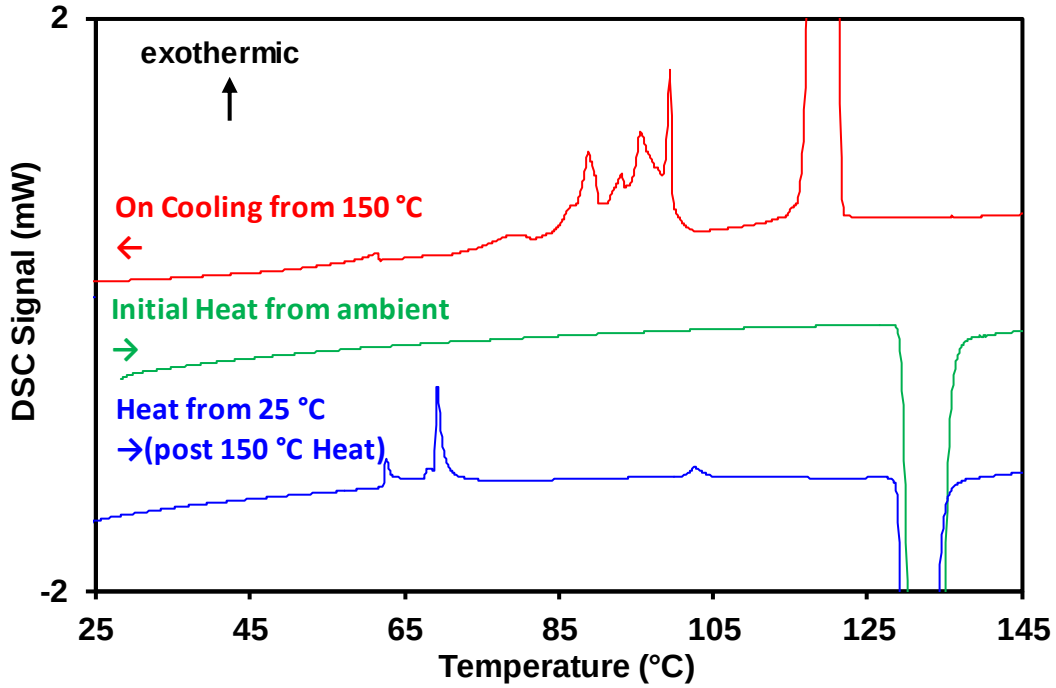

Fig. 45. ***Mettler Toledo DSC curves for the cycling of KNO_3-C heated to a T_{max} of 150 °C. (sample mass, 5mg; heating rate, 10°C min^{-1}; atmosphere, argon)***

It can be seen that the second heat through the solid-solid transition results in a transition with both a T_e and a ΔH similar to that of the initial α→β phase thus confirming that this was not the γ-phase transition being measured.

Method development: Preheating to 300°C

Triplicate (heat-cool-heat) measurements were made on samples of KNO_3-C. The samples were heated to a maximum temperature of 300°C before being cooled at a controlled rate of 10°C min^{-1} to ambient prior to re heating.

The initial heat through the solid-solid transition resulted in both temperatures and enthalpies associated with the α→β phase however, upon cooling from 300°C the re-crystallisation of KNO_3 occurs only in a single stage directly superimposable over one of the regions seen previously when conditioned to 150°C (Fig.46).

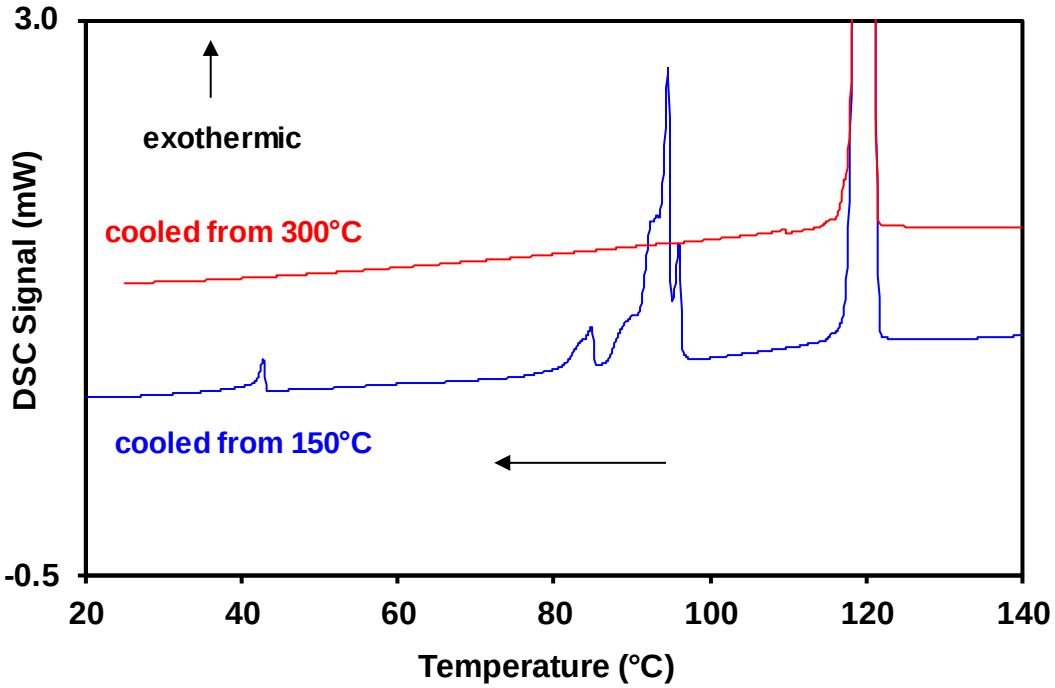

Fig. 46. ***Mettler Toledo DSC cooling curves for KNO_3-C (sample mass, 5mg; cooling rate, 10°C min^{-1}; atmosphere, argon)***

The subsequent baseline on the reheat of the sample is absent of any secondary recrystallisation and supports that the sample having being preconditioned to 300°C is in a stable crystal conformation.

The resultant peak for the solid-solid transition of the preconditioned KNO_3 is significantly different in appearance to that seen previously for the sample conditioned to 150°C (Fig.47).

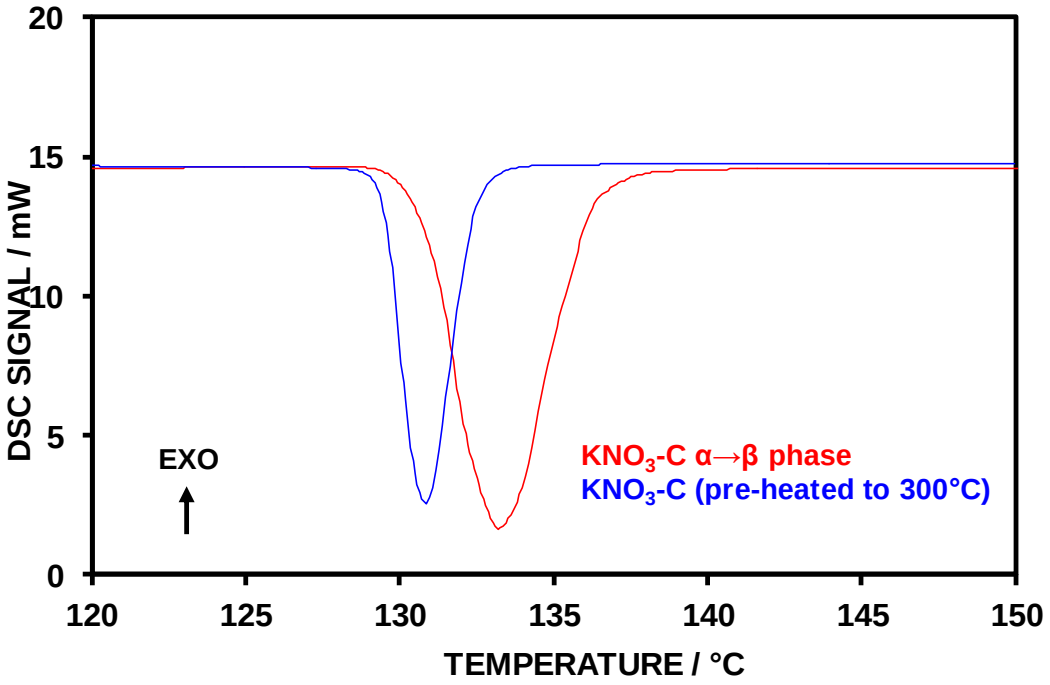

Fig. 47. ***DSC curves identifying the solid-solid transitions of KNO_3-C on heating (sample mass, 5mg; heating rate, 10°C min^{-1}; atmosphere, argon)***

With the heat of fusion approximately halved[63] literature supports that having preconditioned the sample initially to 300°C the subsequent reheat of the sample from ambient is through the γ→β phase.

Having established these conditions samples of KNO_3 in its various phases could now be isolated and measured under near equilibrium conditions.

4.6.4 Accurate Temperature Measurements.

Having established the preconditioning requirements to determine the γ→β phase for the solid-solid transition of KNO_3 using DSC, the extrapolation to zero heating rate method has been implemented to determine accurate equilibrium temperatures of transition for samples of KNO_3-C and KNO_3-SD.

4.6.5 Extrapolation to Zero Heating Rate $T_{\beta=0}$ Method

Both the Mettler Toledo DSC822^e and the TA Instruments TA2920 were used in determining the equilibrium temperature of transition for the α→β and γ→β phases of KNO_3. The instruments were calibrated using the T_{step} of high purity indium, tin, and lead in order to span the range of both the solid-solid transition and the fusion temperatures of the potassium nitrate. 5mg samples were encapsulated in non-hermetically sealed 20µl aluminium crucibles and measured in a flowing atmosphere of argon.

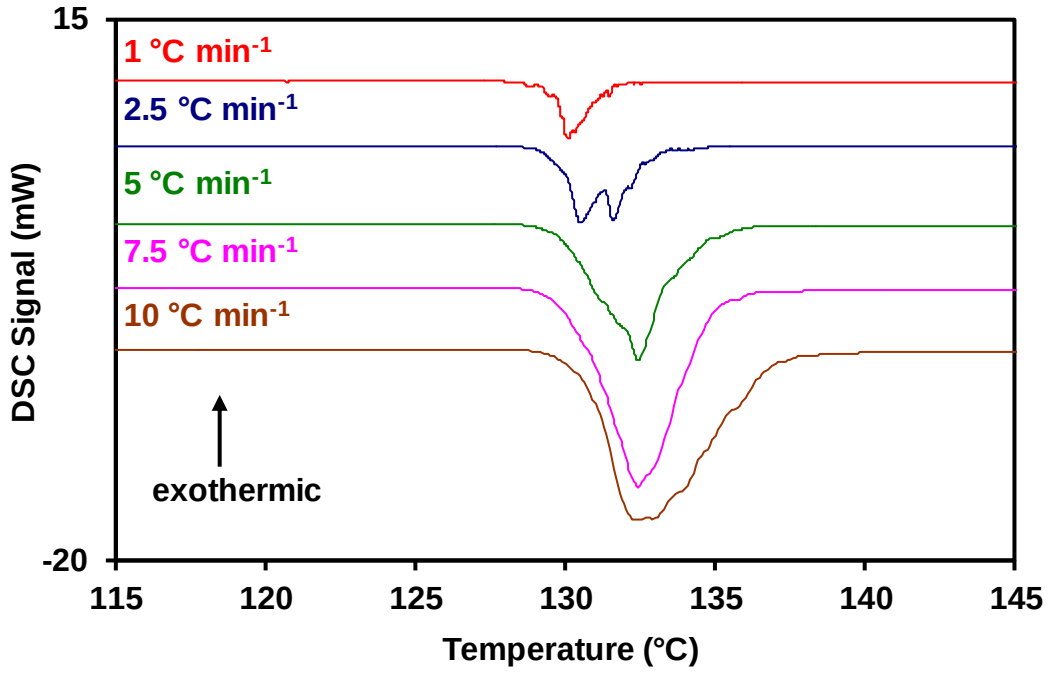

Fig. 48. ***Influence of heating rate on the solid-solid transition of KNO_3-C in the α→β phase. (sample mass, 5mg; heating rate, 10°C min^{-1}; atmosphere, argon)***

The stacked DSC plots for the influence of heating rate of both the α→β and γ→β phases of KNO_3-C are given in Figs 48 and 49.

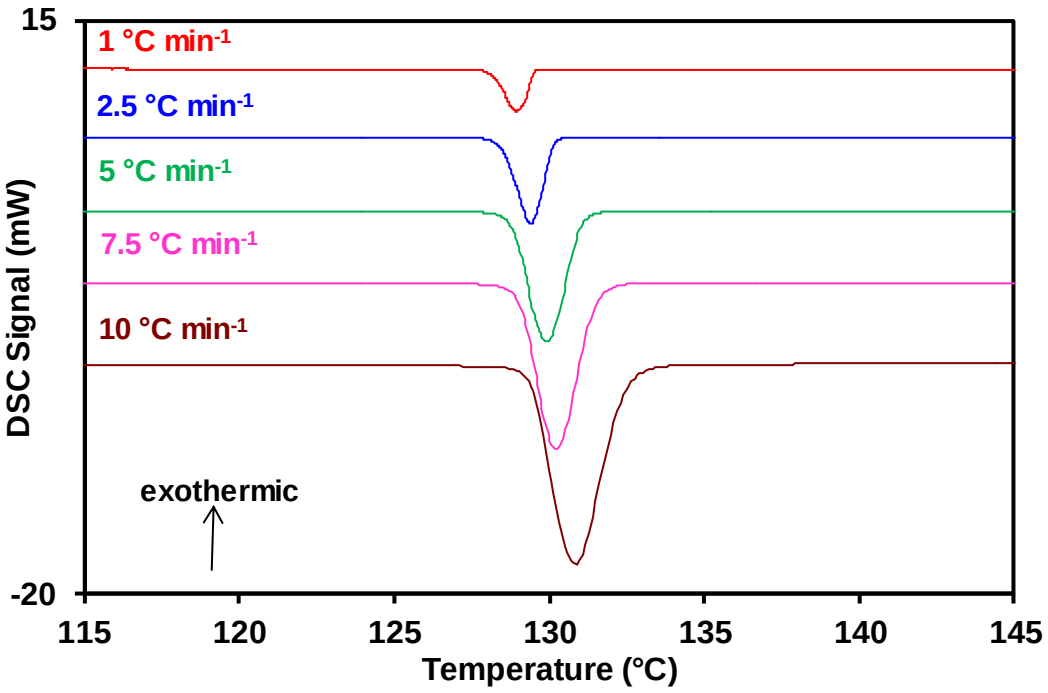

Fig. 49. ***Influence of heating rate on the solid-solid transition of KNO_3-C in the γ→β phase (sample mass, 5mg; heating rate, 10°C min^{-1}; atmosphere, argon)***

Notably the α→β phase of KNO_3-C has much more 'noisy' DSC traces than those of the preconditioned γ→β phase and it was observed under very slow heating rates KNO_3-C produced increasingly noise similar to that seen previously in Transition 2 of $RbNO_3$.

The noise was significantly reduced (Fig 50) in samples whose particle size had been initially reduced prior to measurement. As with the results of Transition 2 of $RbNO_3$ the DSC curves were smoothed using an integrated 1:20 smoothing operation.

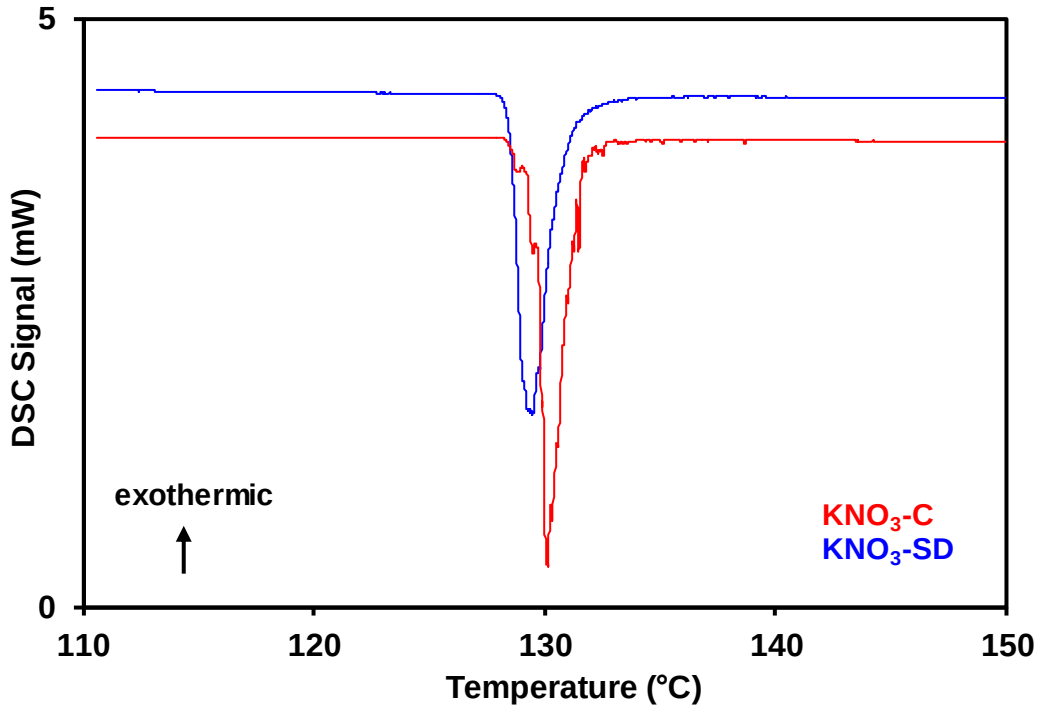

Fig. 50. ***Influence of slow heating on the solid-solid transition of KNO_3 in the α→β phase. (sample mass, 5mg; heating rate, 1°C min^{-1}; atmosphere, argon)***

The results for the extrapolated onset temperature for the α → β phase of both KNO_3-C and KNO_3-SD have been summarised in Table 23. Given the nature of the peak shape in the 'as received' crystalline form, future studies were performed on samples which had previously been reduced in size prior to aid in the correct allocation of T_e.

Table 23. ***Extrapolation to zero heating rate results for the equilibrium temperature of transition for the α → β phase of potassium nitrate. (sample mass, 5mg; atmosphere, argon)***

Sample	$T_{\beta=0}$ / °C	$dT_e/d\beta$ (min)
KNO_3 - C	129.6 ± 0.2	0.077
KNO_3 - SD	128.4 ± 0.2	0.168

Due to the difference in the heating rate dependence $dT_e/d\beta$ of the two samples KNO_3-SD and KNO_3-C it would be difficult to use the onset of the α→β phase as a calibration point on the temperature scale without having to outline a particular pre-treatment first such as reducing the particle size. As particle size appears to influence the onset of transition, inherent errors amongst users would be unavoidable. In the interest of reproducibility, samples of KNO_3-SD were also measured using the TA Instruments TA2920 producing similar heating rate dependencies $dT_e/d\beta$ to that of the Mettler Toledo DSC instrument. Although similar, the small discrepancies in the measured $T_{\beta=0}$ could have been down to discreet differences in particle size which have already shown to affect the measurement of an accurate T_e.

Table 24. ***A summary of the equilibrium temperatures for the solid-solid transition of KNO_3-SD in the α→β phase compared using two heat flux DSC systems.(sample mass, 5mg; atmosphere, argon).***

Instrument	$T_{\beta=0}$ / °C	Slope / min
Mettler Toledo DSC822^e	128.4	0.168
Thermal Instrument TA2920	129.5	0.198
Mean	129.0	
Literature	128 ± 4	-

In contrast to KNO_3 transition in the α→β phase, the measurement of the solid-solid transition through the γ→β phase has shown to be uninfluenced by slower heating rates (Fig. 51).

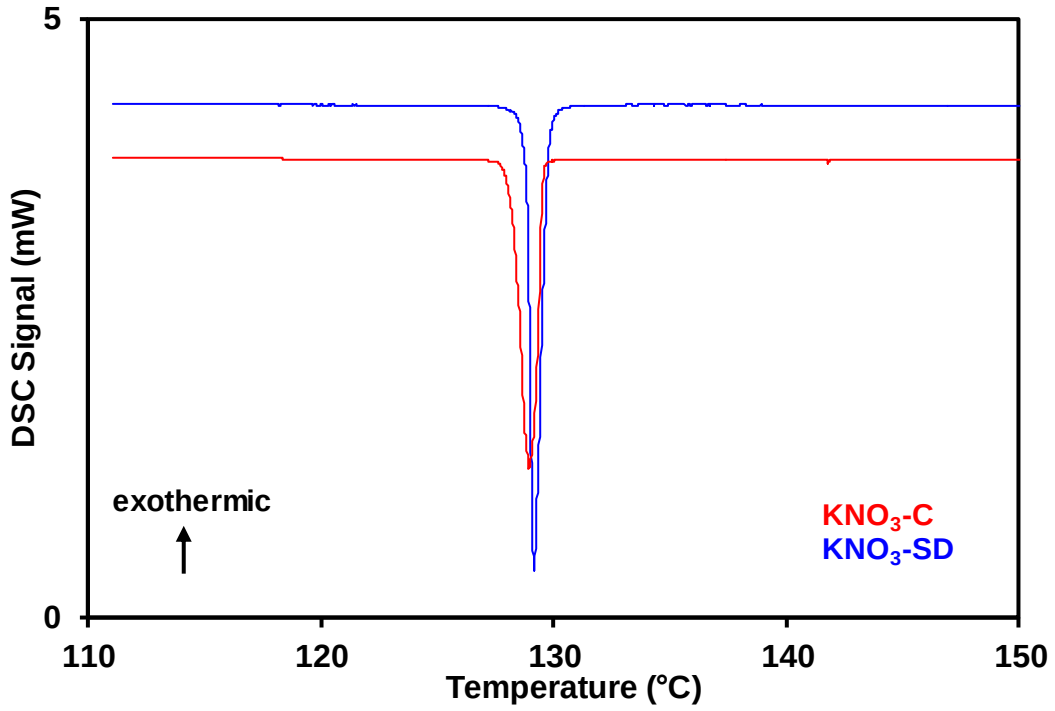

Fig. 51. ***DSC curves showing slow heating through the solid-solid transition of KNO_3 in the γ→β phase. (sample mass, 5mg; heating rate, 1°C min^{-1}; atmosphere, argon)***

The heating rate dependence $dT_e/d\beta$ of the solid-solid transition of KNO_3 in the γ→β phase for both samples were in better agreement with each other than that observed for the measured α→β phase, however, their equilibrium temperatures were not as precise as one would hope for a sample taken from the same initial batch of potassium nitrate. As with previous samples measured this could be attributed to slight variations in particle size.

Table 25. ***Equilibrium temperatures of transition measured using the $T_{\beta=0}$ method for the solid-solid transition of KNO_3 through the γ→β phase. (sample mass, 5mg; atmosphere, argon)***

Sample	$T_{\beta=0}$ / °C	$dT_e/d\beta$ (min)
KNO_3-C	128.2	0.123
KNO_3-SD	128.8	0.109

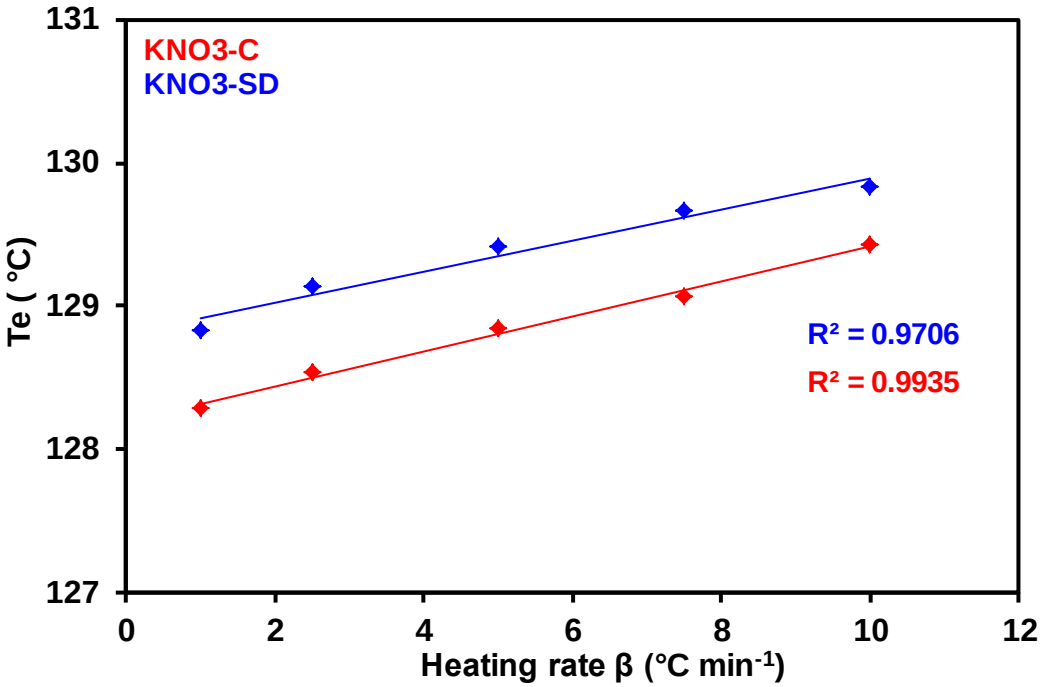

Fig. 52. ***Extrapolation to zero heating rate constructions for the solid-solid transition of KNO_3 through the γ→β phase. (sample mass, 5mg; atmosphere, argon)***

Similarly to the measurements made on the α→β , samples of KNO_3-SD were also measured using the TA Instruments TA2920 producing similar heating rate dependencies $dT_e/d\beta$ to that of the Mettler Toledo DSC instrument.

Table 26. ***Summary of the equilibrium temperature of transition for the solid-solid transition of KNO_3-SD through the γ→β phase using two heat flux DSc systems. (sample mass, 5mg; atmosphere, argon)***

Instrument	$T_{\beta=0}$ / °C	Slope / min
Mettler Toledo DSC822[e]	128.8	0.109
Thermal Instrument TA2920	129.3	0.084
Mean	129.1	
Literature	128 ± 4	-

Isothermal Stepwise Measurements on the Solid-Solid Transitions of KNO_3

Having established that the α→β behaves in a similar manner to that previously observed for the 2nd solid-solid transition of $RbNO_3$ studies using the isothermal stepwise method were not used to confirm the equilibrium temperature of transition. In addition the influence of sample size greatly influenced the onset of transition therefore further investigations would be required.

A preliminary measurement using a greatly increased temperature increment of 0.2°C was used in order to assess whether the solid-solid transition could be measured using the isothermal method, but at the cost of a lower degree of accuracy.

The resultant scan is shown in Fig.53. and shows the potential for measurement if the issue with particle sizing could be overcome.

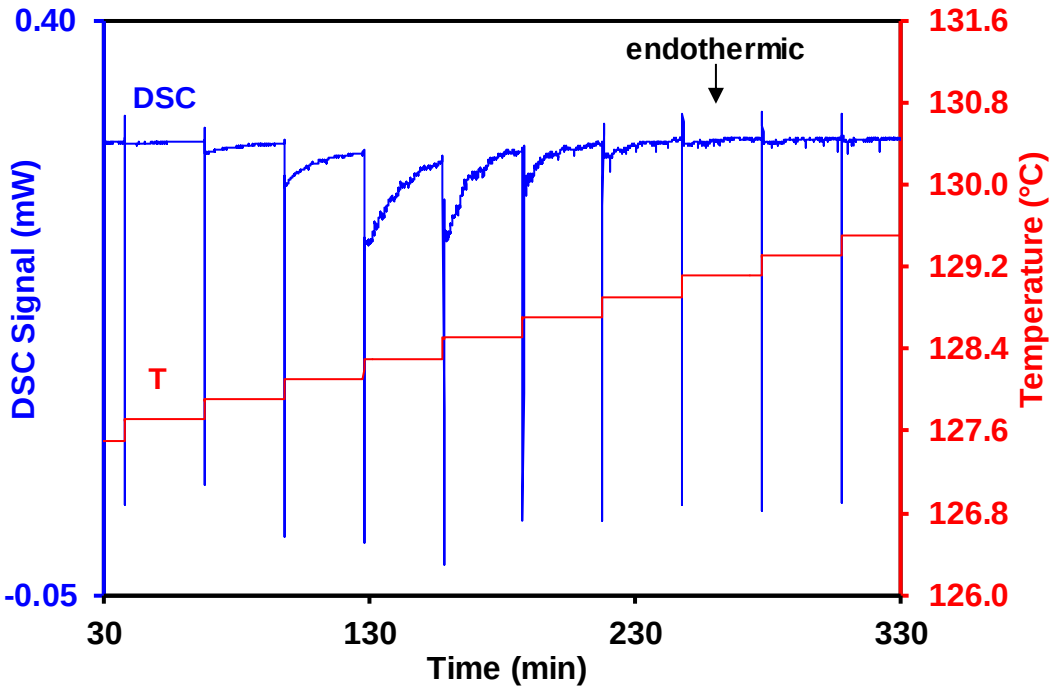

Fig. 53. ***T_{step} construction for the solid-solid transition of KNO_3-C heated through the α→β phase. (sample mass, 5mg; step size, 0.2°C; atmosphere, argon)***

4.7 Conclusions on the Accurate Temperature Determinations of KNO_3

Attempts have been made to accurately determine the equilibrium temperatures of transition for both the α→β and the γ→β phases of the solid-solid transitions of KNO_3. Preconditioning requirements of heating the sample to 300°C are required in order to measure KNO_3 in the γ phase.

A mean equilibrium temperature of transition for the γ→β phase of KNO_3 was found to be 129.1°C using the extrapolation to zero heating rate method. In order to confirm the equilibrium transition temperature, the determination of an accurate equilibrium temperature using the T_{step} method was not possible. Experiments using the 0.05°C increments generated too much noise (spikes in the DSC curve) associated with the phase conversion of individual crystals, however a preliminary experiment with 0.2°C steps showed promise for any future explorations.

Albeit known to be ferroelectric whilst in the γ phase[68, 51-52] measurements to confirm ferroelectric properties were not performed as part of this study but could be explored as part of a future project.

Section 4.5.6 shows the inability to produce a reproducible equilibrium temperature of transition due to the influence of particle size unless the proposed method of measurement in Section 4.6.3 is followed i.e. heated to 300°C. This conflict with the original method outlined for the preparation of KNO_3 for use as a reference standard[69] would require further investigations.

4.8 Potassium Perchlorate

4.8.1 Introduction

Potassium perchlorate ($KClO_4$) is a widely used oxidant in the production of pyrotechnic systems. It exhibits a reversible solid-solid phase change in the region of 300˚C prior to the onset of fusion at around 530°C. Implementing both the dynamic and stepwise heating techniques efforts have been made to determine a more accurate temperature of transition than those reported previously. By improving the accuracy of the transition temperature measurement, potassium perchlorate could be used more readily as a temperature calibrant for precision work. Current DSC calibrants of choice in the region of 300°C include the metals tin and lead.

Table 27. ***Literature Values for the Solid-Solid Transition of $KClO_4$***

First Author	Year	Temperature / °C	Ref.	Method
Vorländer	1923	299-300	70	Melting Curve
Markowitz	1961	303	71	DTA
Garn	1969	302	56	DTA
Various*	1972	299 ± 6	72	DTA
Verneker	1975	292	73	DTA
Shimokawabe	1977	312	74	DTA
Furuichi	1986	310	75	DTA
Berger	1995	301.9 ± 0.2	76	DSC
Lee	2001	303	77	DSC

**Round Robin Results by 12 international institutes*

The determination of an *accurate* temperature measurement for the phase transition of $KClO_4$ by DSC has not been well documented. Although issued as a temperature standard, previous measurements using DTA report temperature ranges of up to ±6°C[72]. By implementing the two methods of determining accurate

temperatures of transition it is hoped that a more accurate evaluation of the transition temperature of $KClO_4$ can be made.

4.8.2 Preliminary Studies

Preliminary experiments were performed on potassium perchlorate (Sigma Aldrich, 99.99%). The salt was crushed in a pestle and mortar and passed through a 150 µm sieve before being dried at 105 °C. The method of preparation of the salt was carried out due to previous recommendations that particle size has a marked effect on the transition.[78] Temperature measurements were performed using a Mettler Toledo DSC 822^e apparatus. 5 mg samples were heated in 20µL non-encapsulated aluminium crucibles in an argon atmosphere. The instrument was calibrated using a triple point stepwise measurement of high purity indium, tin and lead.

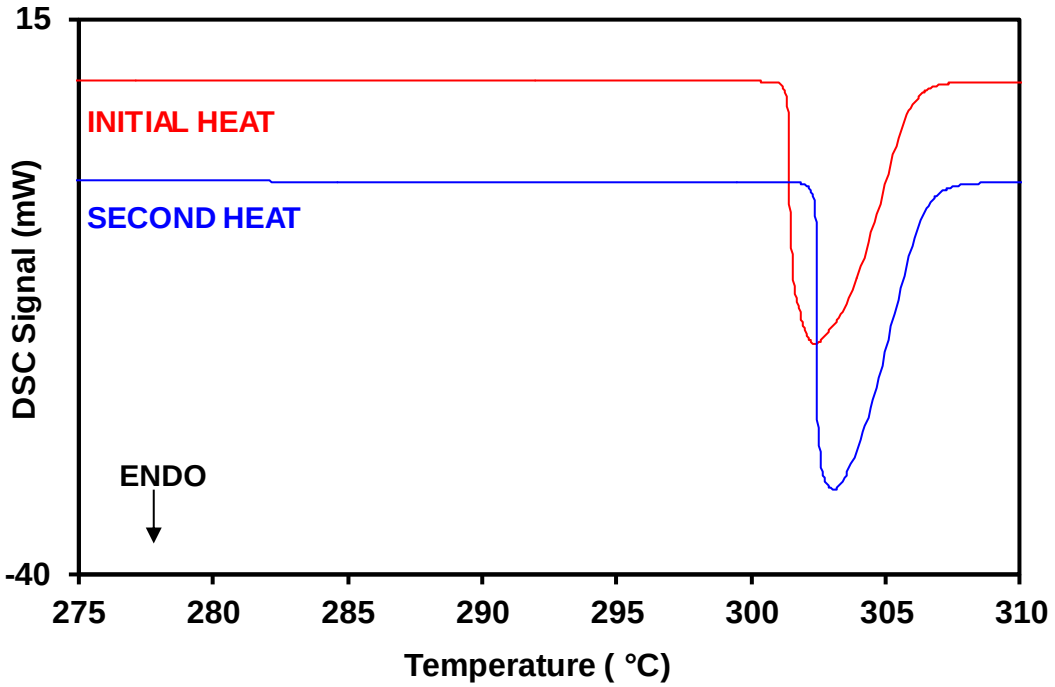

Fig. 54. ***DSC curves showing the influence of thermal history on the $KClO_4$ solid-solid transition. (sample mass, 5mg; heating rate, 10°C min^{-1}; atmosphere, argon)***

It has been noted previously that the transition temperature of potassium perchlorate showed a small increase on reheating, a possible source of error for the large range in temperatures previously reported for the transition.[72]

A DSC curve of $KClO_4$ cycled through its solid-solid transition is given in Fig. 55 and shows that the reproducibility of transition temperature T_e has a dependence on its previous thermal history. with subsequent heats producing a more reproducible transition temperature.

Table 28. ***Influence of cycling on the extrapolated onset temperature for the solid-solid transition of $KClO_4$. (sample mass, 5mg; heating rate, 10°C; atmosphere, argon)***

Experiment	T_e / °C	Enthalpy / kJ mol^{-1}
First Heat	301.32	14.06 ± 0.1
Cycles 2-12	302.50 ± 0.05	14.07 ± 0.1
All together	302.40 ± 0.34	14.06 ± 0.1

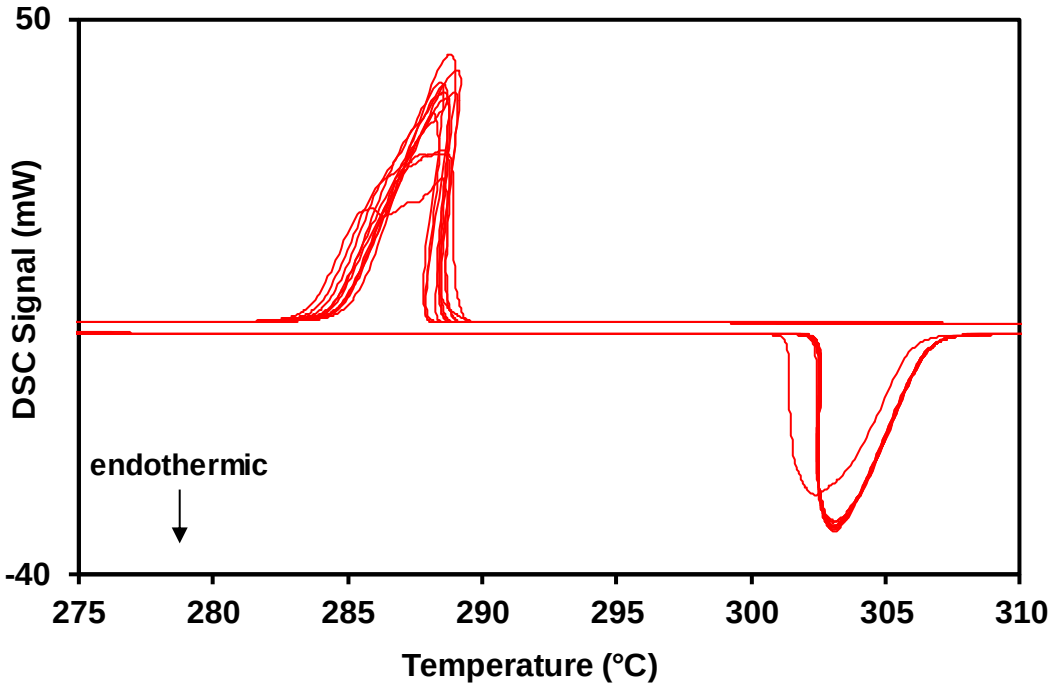

Fig. 55. ***DSC heating/cooling curves for the cycling of $KClO_4$ (sample mass, 5mg; heating/cooling rate, 10°C min^{-1}; atmosphere, argon)***

4.8.3 Determination of $T_{\beta=0}$ for $KClO_4$

Having shown that previous thermal history has an effect on the transition temperature of $KClO_4$, measurements to determine the $T_{\beta=0}$ were made on samples which had had no previous thermal history (initial heat) and those which had been heated through the transition and cooled to 240°C prior to measuring.

Table 29. ***Extrapolation to zero heating rate for the solid-solid phase transition of potassium perchlorate (sigma) (sample mass, 5 mg; atmosphere, argon)***

Experiment	$T_{\beta=0}$ / °C	$(dT_e / d\beta)$ / min
First Heating	299.7 ± 0.1	0.191
Second Heating	300.5 ± 0.1	0.221

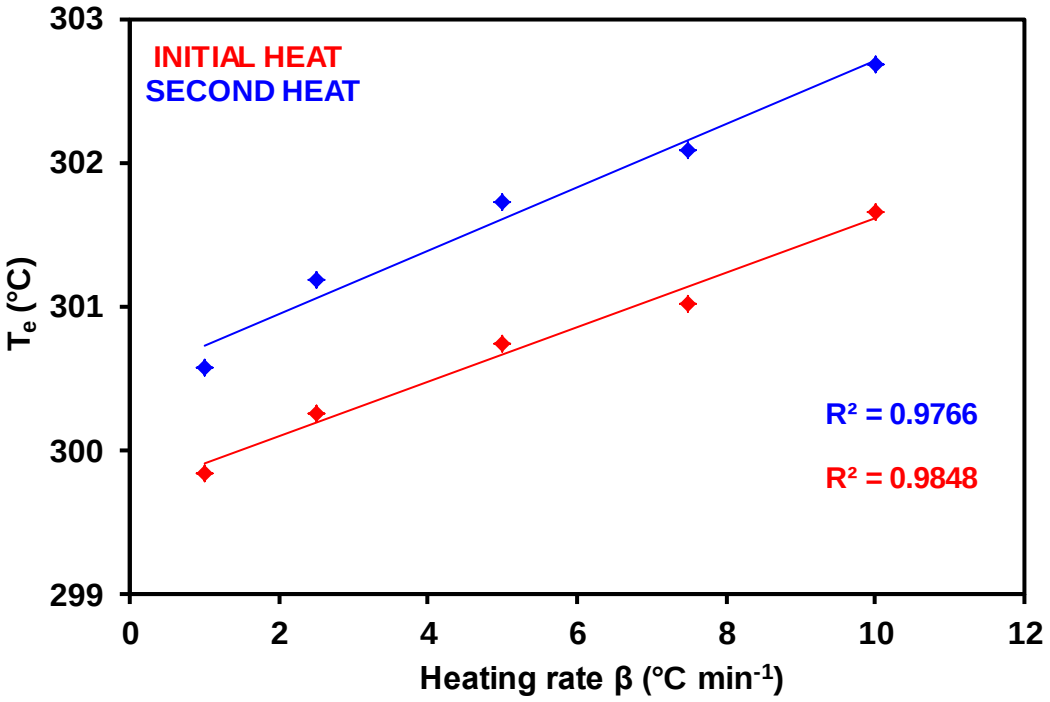

Fig. 56. ***Extrapolation to zero heating rate constructions for the solid-solid phase transition of $KClO_4$ using the Mettler DSC822^e. (sample mass, 5mg; atmosphere, argon)***

In addition, measurements were also performed using the Thermal Instruments TA2920 in order to confirm the $T_{\beta=0}$ using another DSC source.

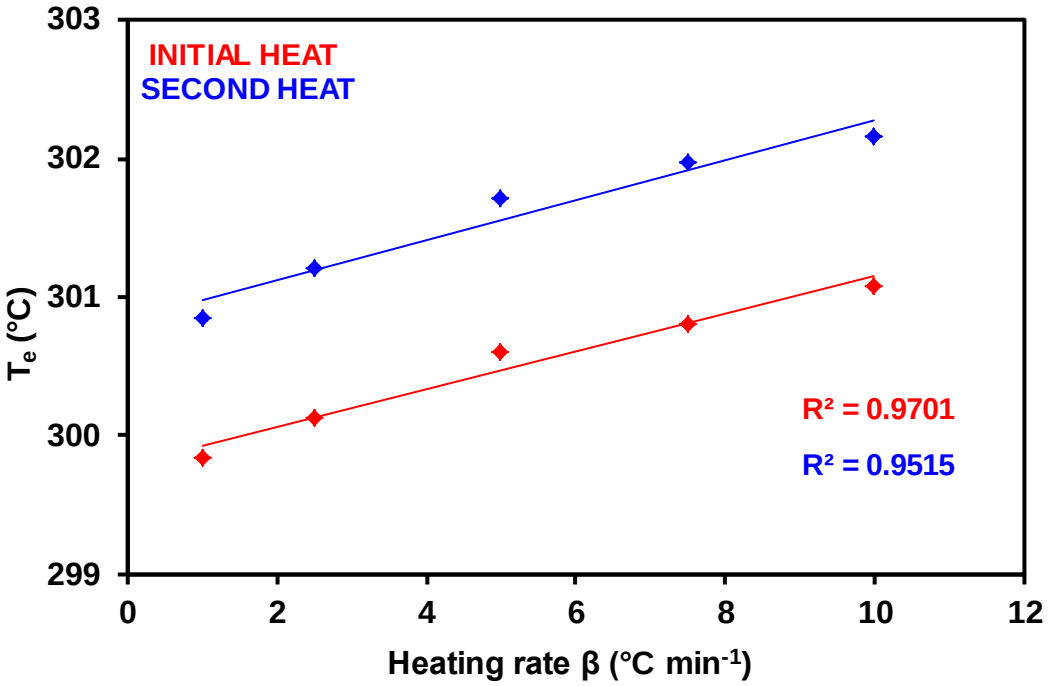

Fig. 57. ***Extrapolation to zero heating rate constructions for the solid-solid phase transition of $KClO_4$ using the TA2920 DSC. (sample mass, 5mg; atmosphere, argon)***

It can be seen that the measurements for the $T_{\beta=0}$ of both the initial and second heating of the $KClO_4$ are in good agreement using either DSC.

Table 30. ***Summary of the extrapolation to zero heating rate measurements for the solid-solid phase transition of $KClO_4$ (Sigma Aldrich) using two DSC heat-flux instruments. (sample mass, 5mg; atmosphere, argon)***

Experiment	$T_{\beta=0}$ / °C		
	Mettler Toledo DSC822^e	TA Instruments DSC2920	Difference between instruments
First Heating	299.7 ± 0.1	299.7 ± 0.1	0.0
Second Heating	300.5 ± 0.1	300.8 ± 0.1	0.3

It also shows that there is a genuine change in the equilibrium transition temperature for potassium perchlorate upon the sample having previous thermal history, with an increase of the equilibrium temperature of approximately 1 °C. In addition to temperature, enthalpy measurements were also made on both samples to determine whether that was also affected by thermal history. This however, remained constant.

Table 31. ***Enthalpy values for the solid-solid transition of potassium perchlorate (Sigma Aldrich). (sample mass, 5mg; heating rate, 3°C min^{-1}; atmosphere, argon)***

Experiment	Enthalpy / kJ mol^{-1}
First Heating	14.52 ± 0.08
Second Heating	14.51 ± 0.07

4.8.4 Determination of T_{step} for $KClO_4$

Measurements under stepwise heating conditions indicate that the solid-solid transition is slow so that the DSC trace does not return rapidly to the baseline during the isothermal period following a temperature increment. This is illustrated in Fig. 58 where the sample is left isothermally for approximately 5 hours in order to achieve a return to the baseline.

This method would not be suited for this material however, by increasing the parameters of the standard T_{step} method it is possible to achieve a reasonably accurate transition temperature for $KClO_4$. The sample was heated in 0.5°C increments, somewhat larger to the typical 0.05°C steps used in previous studies.

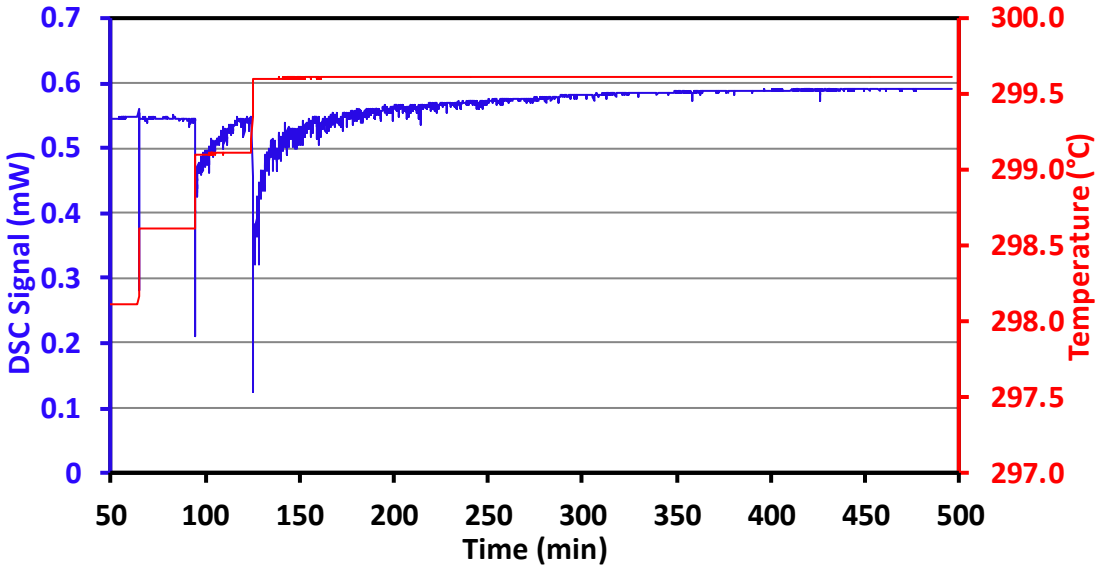

Fig. 58. ***DSC curve for the extended isothermal period in the T_{step} method for $KClO_4$ to illustrate the time required for the curve to return to its initial zero baseline. (sample mass, 5mg; step size, 0.5°C; atmosphere, argon)***

By increasing the temperature increment the T_{step} for $KClO_4$ was determined to be 300.9 ± 0.3°C which is in good agreement with those reported in Table 30.

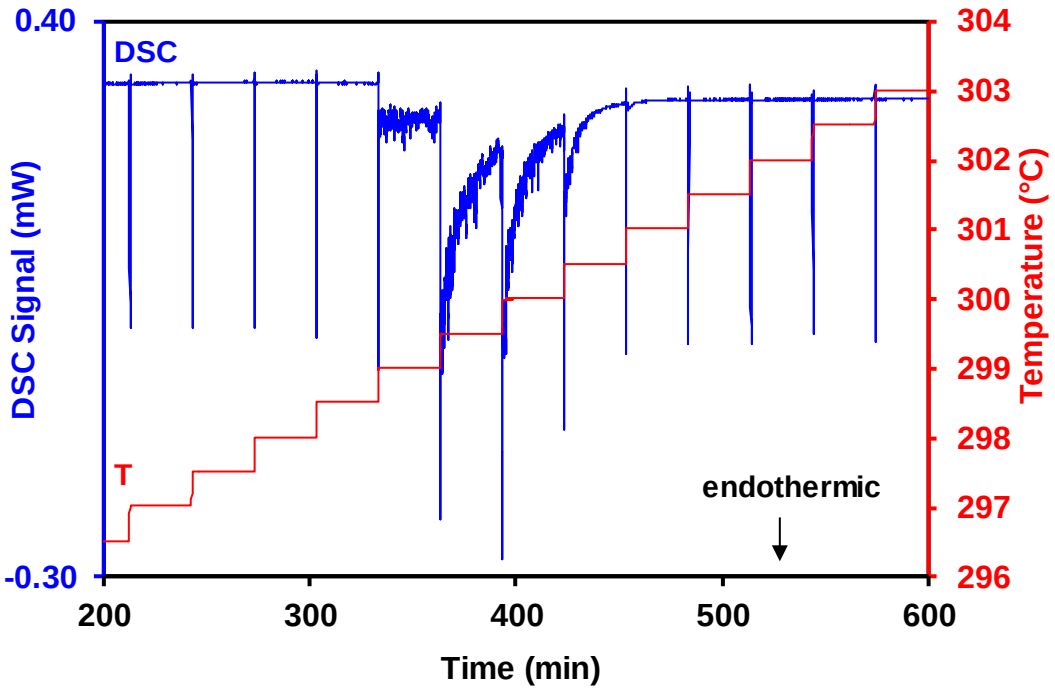

Fig. 59. ***Full DSC curve for the stepwise heating of the solid-solid phase transition of $KClO_4$ (Sigma Aldrich). (sample mass, 5mg; step size, 0.5°C; atmosphere, argon)***

4.9 Conclusions for the Accurate Determination of Temperature for the Phase Transitions of $KClO_4$

The feasibility to readily measure the temperature of transition of $KClO_4$ to a higher degree of accuracy is possible using the $T_{\beta=0}$ method. Evaluating the slight curvature at the lower heating rates in the $T_{\beta=0}$ plot indicates that $KClO_4$ would be more suited for the extended extrapolation to zero heating rates adapted for samples which decompose under slow heating rates. This is an area that could be explored in further studies.

In the case of using the T_{step} method for temperature determination it is not practical due to the slow nature of the solid-solid transformation. This was confirmed in the extended isothermal programme and although a temperature for T_{step} was determined this was not in agreement with the $T_{\beta=0}$. Had sufficient time been invested in extended isothermal periods this may have been achieved however, for the purpose of finding quick accurate temperature measurements $KClO_4$ is clearly not suited to this technique.

Chapter 5 Organics

5.1 Introduction

As discussed previously, calibration is at the heart of quantitative measurements made by DSC. Its very purpose being to link the temperature and enthalpy measurement of a sample to that of an unequivocal value defined by certified values. Calibration materials, irrespective of the compound to be investigated tend to be one, or a collective of high purity metals with indium often the favourable material of choice. Organic and inorganic calibrants for both temperature and enthalpy are less favoured due to their handling and reproducibility difficulties although in reality samples studied using low temperature DSC rarely fall into the metallurgic classification so reference has been made for the desirability of calibrating DSC equipment using “like with like” substances that have similar thermal properties to the compound to be investigated.[79]

Between ambient temperature and indium at 156.6°C there is a temperature gap in which there are no other metal substances suitable for the calibration of DSC under near equilibrium conditions. Although gallium falls within this range (29.8°C) its handling is problematic as it is reactive with most crucible types.[80]

LGC Ltd, an international leader in laboratory services, measurement standards and reference materials offers a range of organic materials intended for the purposes of checking and calibrating thermal equipment for both temperature and enthalpy. These are available as DSC standards and as temperature standards. The DSC standard materials are intended for the calibration of differential scanning calorimeters and similar instrumentation and have been certified using classical adiabatic calorimetry. Their certified melting temperatures provided are that of the final melting temperature i.e. complete liquefaction.

The temperature standard materials are for the use in the calibration and checking of apparatus used for determining melting points of samples in glass capillary tubes whereby the thermodynamic melting temperature provided is the melting point which would be observed under equilibrium conditions i.e. zero heating rate.

This chapter aims to apply the calibration methods described previously to the organic reference materials designed solely for use as DSC calibrants in the temperature range 40-150°C. Measuring both temperature and enthalpies of transition with instruments which operate using different principles of measurement, an assessment has been made of the determination of the calibration factor κ, and the temperature dependence of a range of substances when calibrated at a single reference point (indium).

The close proximity in temperature of the LGC standards indium and diphenylacetic acid has also enabled a direct assessment to be made of any differences resulting from the use of a metal or an organic substance in the calibration of DSC equipment.

In addition, discrepancies observed between certified equilibrium temperatures of two alike compounds are studied with the aim of showing how the T_{step} method can be used as a validation tool when measuring temperatures of transition under near equilibrium conditions.

5.2 A Comparison Between Indium and Diphenylacetic Acid

The close proximity in temperature of the standards indium and diphenylacetic acid provides the opportunity of making a direct assessment of any differences resulting from the use of a metal or an organic in the calibration of a DSC for temperature and enthalpy.

The certified equilibrium fusion temperature of LGC indium is 156.61 ± 0.02°C with an enthalpy of fusion of 3.296 ± 0.009kJ mol^{-1}; and for diphenylacetic acid 147.19 ± 0.03°C with an enthalpy of fusion of 31.16 ± 0.13kJ mol^{-1}.

5.2.1 Determination of Equilibrium Temperatures

Accurate temperature measurements on indium (LGC 2601) and diphenylacetic acid (LGC 2607) were determined by employing both the extrapolation to zero

heating rate and the stepwise heating methods. Temperature measurements were carried out using a Mettler Toledo DSC 822^e with the tau lag function disabled. Measurements were made using 2.5mg samples of the diphenylacetic acid and 10mg samples of indium in 40µl aluminium crucibles.

The greater mass of indium used in these experiments compared to that of diphenylacetic acid was in recognition of its considerably smaller enthalpy of fusion. Considerable care was taken to ensure good thermal contact between the sample and the crucible therefore the diphenylacetic acid was slightly crushed in the pan to increase the surface area using a glass rod before use.

The volatility of diphenylacetic acid was assessed by thermogravimetry using a Mettler Toledo TGA851^e apparatus. The sample (2.5mg) was contained in an open 20µl aluminium crucible and heated at 10°C min^{-1}. The measured mass loss at the onset of melting was about 3% and in view of this, all subsequent DSC experiments were carried out in encapsulated crucibles. Since the purpose of the work was a comparison between indium and diphenylacetic acid the same procedure was adopted for indium. No mass loss was detected.

The equilibrium fusion temperatures of indium and diphenylacetic acid were firstly measured using the extrapolation to zero heating rate method. For indium the samples were heated three times through the fusion peak in order to enable an accurate assessment to be made on the effect of pre-heating.

The values for the $T_{\beta=0}$ of indium were summarised previously in Section 3.3.1 whereby the influence of sample form on the equilibrium onset temperatures were discussed. It was found that from the agreement between the initial and subsequent fusions that it is possible to make temperature measurements using indium to a high degree of precision. However, , it was found during other studies that if the LGC indium sample was neither sufficiently thin nor firmly pressed flat into the crucible there was a significant decrease in the extrapolated onset of melting temperature from the first to second heating in the dynamic experiments.

Comparative T_{step} measurements are also discussed in Section 3.3 and show the excellent agreement between the results for both LGC and powdered indium

obtained by the two methods and clearly establishes the equality of the two methods for the determination of accurate equilibrium temperatures and thus the confidence to measure diphenylacetic acid. To determine the equilibrium fusion temperature of diphenylacetic acid using the extrapolation to zero heating rate method a new sample was used at each heating rate and was not re-heated in accordance with the recommendation stated in the materials certificate.

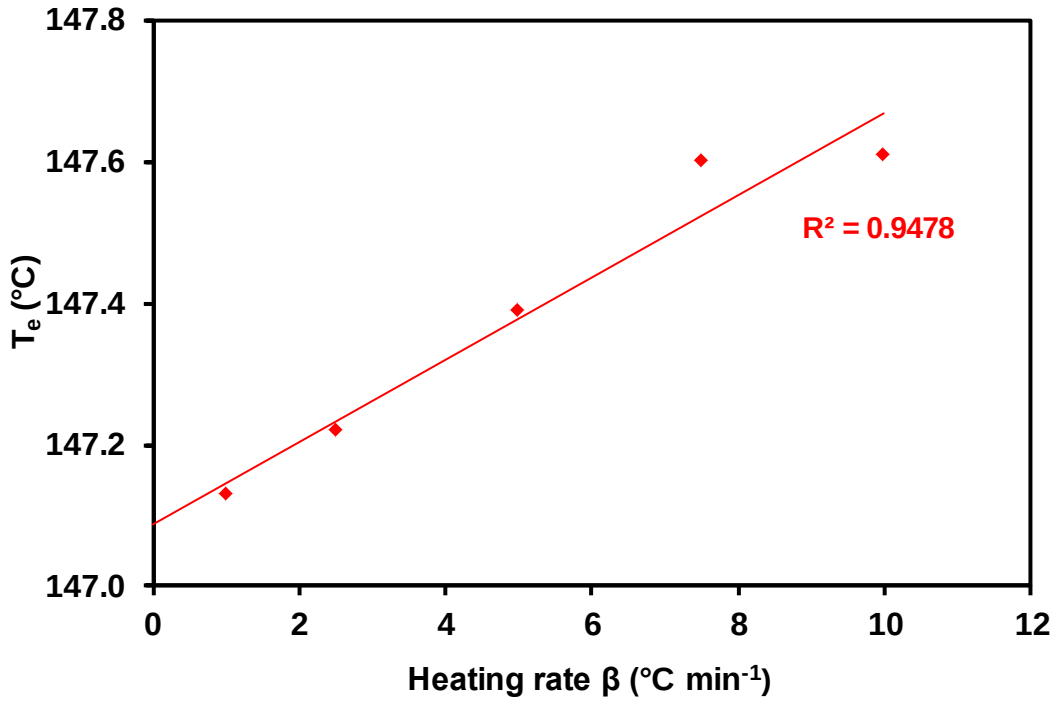

Fig. 60. ***Plot of extrapolated onset temperature against heating rate for LGC diphenylacetic acid (sample mass, 2.5mg; atmosphere, nitrogen)***

The measured extrapolated onset temperature against heating rate is shown for diphenylacetic acid (Fig. 60). The values for diphenylacetic acid were adjusted by applying calibration corrections derrived from the measurements of LGC indium measured using the same method and are summarised in Table 32 below.

Table 32. ***Summary of the measured equilibrium temperatures of fusion of diphenylacetic acid (sample mass, 2.5mg, atmosphere, nitrogen)***

	$T_{\beta=0}$ / °C	T_{step} / °C
Mean measured value	147.09 ± 0.05	147.08 ± 0.04
$(\delta T_e/\delta\beta)$/min	0.058 ± 0.008	-
Correction	0.10 ± 0.02	0.09 ± 0.03
Corrected Value	147.19 ± 0.05	147.17 ± 0.04
Certified Value	147.19 ± 0.03	147.19 ± 0.03

A mean value of 147.19 ± 0.05°C was given which was in excellent agreement with the certificate value. The equilibrium temperatures from the stepwise heating experiments on DAA agree with the certified value to within 0.02°C, well within the uncertainties. This confirms the result obtained by the extrapolation to zero heating rate experiments and establishes the equivalence between a metal and organic substance for DSC temperature calibration in a similar temperature range.

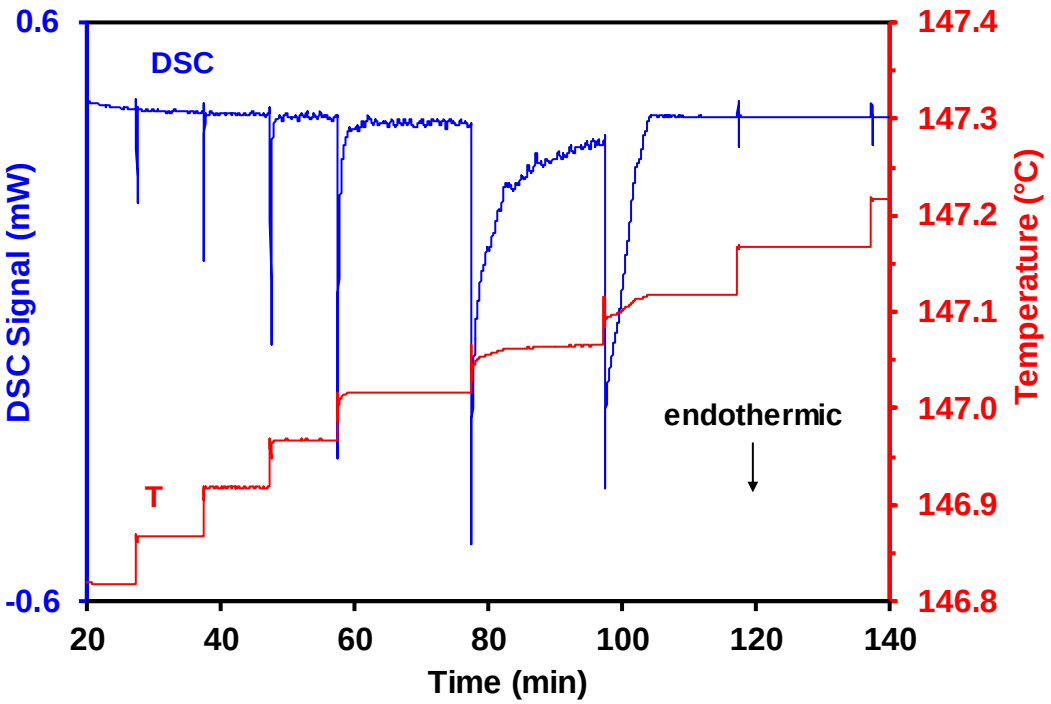

Fig. 61. ***DSC curve for the T_{step} of LGC diphenylacetic acid (sample mass, 2.5mg; step size, 0.05°C; atmosphere, nitrogen)***

Although both methods of measurement derived equivalent equilibrium temperatures the value of the gradient $dT_e/d\beta$ of 0.058 ± 0.008 min obtained for diphenylacetic acid was smaller than that for LGC indium by an amount which exceeded the combined uncertainty. However, it was in close agreement to that observed for the powdered indium. Considerable variations in $dT_e/d\beta$ for both organic and inorganic compounds have been reported[79,81] and in some instances are greater than those for metals. Results for rubidium nitrate show that even for the same compound the transitions between crystal forms can lead to very different values of $dT_e/d\beta$.[18] The lack of consistence in the values of the gradient $dT_e/d\beta$ rules out experiments under dynamic conditions for the accurate measurement of temperatures unless it is known that the gradient has the same value for both the calibrant and the compound under investigation.

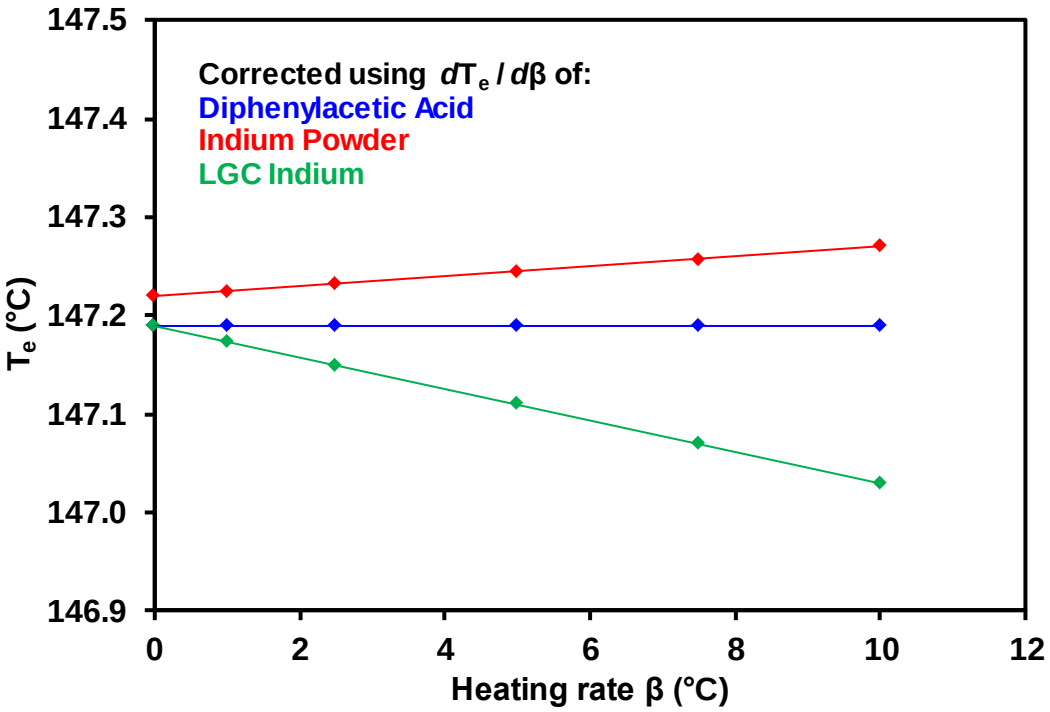

Fig. 62. **$dT_e/d\beta$** ***Temperature Corrections for Diphenylacetic Acid using Indium***

The error, albeit generally small at slower heating rates is proportional to the difference between the gradients for the calibrant and compound. Thus in this study if the indium calibration had been made at 10°C min^{-1} and the measurements

on DAA made at the same heating rate, an error of ~ 0.2°C would have resulted (Fig 62.)

5.2.2 Determination of Enthalpy

Enthalpy measurements were performed using a Perkin Elmer Diamond DSC. The samples were contained in TA Instruments low mass T_{zero} aluminium crucibles. The heating rate was 3°C min^{-1} and a flowing atmosphere of nitrogen at 20 cm^3min^{-1} was used. The sample masses were the same as those used in the temperature measurements and the same care was taken in the sample preparation. A Mettler Toledo six figure balance with a readability of 0.001 mg was used and a new sample prepared for each experiment unless otherwise stated. The greater mass of indium used in these experiments compared to that of DAA was in recognition of its considerably smaller enthalpy of fusion. The uncertainties associated with the measurements are single standard deviations unless otherwise stated.

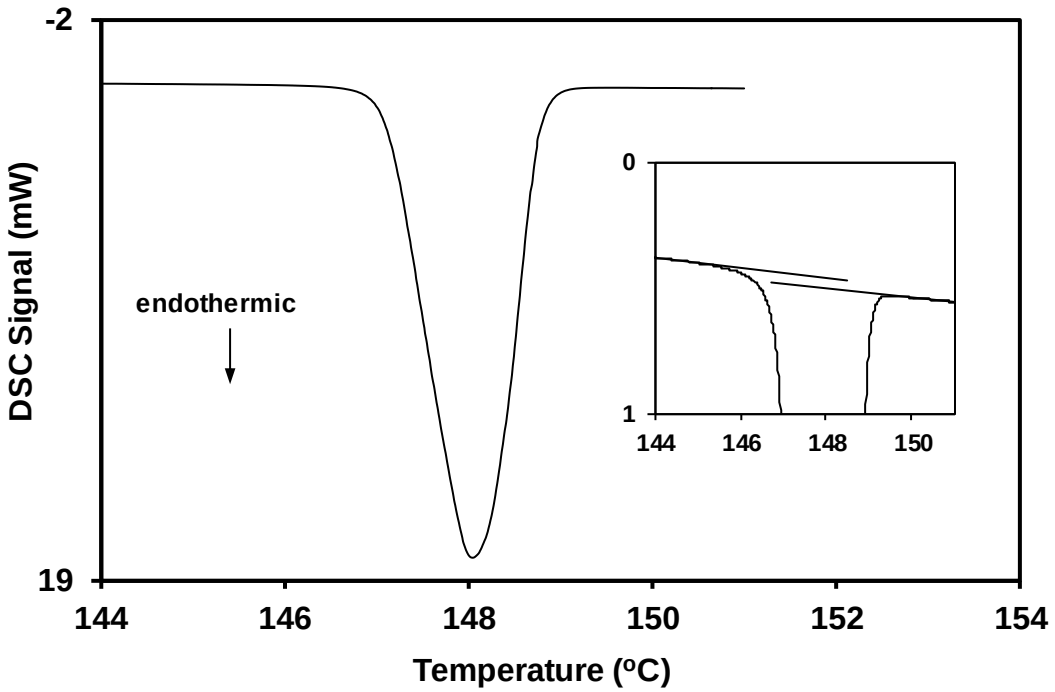

Fig. 63. ***DSC curve showing the heat capacity change during fusion for LGC diphenylacetic acid. (sample mass, 2.5mg; heating rate, 3°C min^{-1} ; atmosphere, nitrogen)***

The enthalpy of fusion of diphenylacetic acid was measured using LGC indium as the calibrant (Table 33) and the results from six determinations summarised in Table 34. Melting occurred with a small but clearly discernable change in heat capacity (Fig. 63) and the enthalpy change was calculated by representing the temperature dependence of the initial and final capacities as linear.

Table 33. ***Measurements for the enthalpy of fusion of LGC indium (sample mass, 10mg; heating rate, 3°Cmin^{-1}; atmosphere, nitrogen)***

Measurement	LGC Indium, $\Delta_{fus}H/Jg^{-1}$
First heating	28.71 ± 0.01
Second heating	28.71 ± 0.03
Third heating	28.72 ± 0.03
Mean value	28.71 ± 0.02
Certified value	28.71 ± 0.01
Calibration factor	1.000 ± 0.002

Table 34. ***Measurements for the enthalpy of fusion of diphenylacetic acid (sample mass, 2.5mg; heating rate, 3°Cmin^{-1}; atmosphere, nitrogen)***

Measurement	$\Delta_{fus}H/Jg^{-1}$
Mean measured value	146.9 ± 0.3
Calibration factor	1.000 ± 0.002
Corrected value	146.9 ± 0.4
Certified value	146.8 ± 0.6

The results were slightly dependant on the temperature range used in the calculations. Increasing the temperature range of by 0.5 and 1.0°C changed the enthalpy value from 146.81 ± 0.03 Jg^{-1} to 146.94 ± 0.13 and 147.01 ± 0.10 Jg^{-1}

respectively. The value 146.9 ± 0.3 Jg^{-1} is the mean value from the individual results together with an error that encompasses the range of the results.

Using the Perkin Elmer software, a sigmoidal baseline construction obtained a value 0.2% greater than the present value. The corrected enthalpy of fusion of diphenylacetic acid at the equilibrium temperature was found to be 146.9 ± 0.4 Jg^{-1}.

This is in excellent agreement with the certified value of 146.8 ± 0.6 Jg^{-1} and demonstrates that there is no significant difference in using an organic material for the enthalpic calibration of DSC equipment at similar temperatures.

5.3 Conclusions for the comparison of Accurate Temperature Measurements of Indium and Diphenylacetic Acid

The close proximity in temperature of the LGC Limited DSC standards indium and diphenylacetic acid, has enabled a direct assessment to be made of any differences resulting from the use of a metal or an organic substance in the calibration of DSC equipment. Following calibration with indium, the equilibrium fusion temperatures for diphenylacetic acid, measured by both the stepwise heating and extrapolation to zero heating rate methods, were found to be in excellent agreement with the certificate value. Although the enthalpy measurements with diphenylacetic acid showed a greater uncertainty than with indium, which arose from the larger heat capacity change on fusion, the results were also in agreement with the certified value.

These measurements clearly establish that indium may be used as a calibrant when making accurate DSC measurements on organic materials in the same temperature range. Indium has advantages in that it is non-volatile and as shown, can be re-melted at least 20 times without any significant change. However, measurements are often performed on samples at significantly lower temperatures than the melting point of indium and in these cases it may be advantageous to use one of the organic standards which melt in a similar temperature range.

5.4 The Use of Organic Calibration Standards for Enthalpy Calibration of DSCs in the Temperature range 42-150°C

A comparison between the use of the certified reference materials indium and diphenylacetic acid for calibrating DSCs for temperature and enthalpy has been discussed. The close proximity of the melting temperatures of the materials enabled a direct assessment to be made of any differences between the use of a metal or an organic compound in the calibration of DSC equipment.

Having demonstrated the ability to determine accurate enthalpy measurement of diphenylacetic acid using DSC at a heating rate of 3°C min^{-1} further measurements on a range of organic DSC calibration standards were made. Both indium and diphenylacetic acid have certified enthalpies of fusion determined by adiabatic calorimetry covering the range 42 – 147°C.

By exploring calibrants at temperatures lower than indium it is possible to examine the temperature dependence of the calibration factor κ and thus to investigate the possible errors arising from the common practice of performing a single point calibration such as indium.

5.4.3 Experimental

The organic DSC standards together with their equilibrium fusion temperatures and enthalpies of fusion are listed in Table 35. The uncertainties for the materials are those cited on the certificate and have a level of confidence of approximately 95%.

Table 35. ***LGC Ltd. organic DSC calibration standards.***

LGC Reference	Material	Fusion Temperature / °C	$\Delta_{fus}H_{cert}$/kJmol^{-1}
2613	Phenyl salicylate	41.79	19.18 ± 0.08
2610	Biphenyl	68.93	18.60 ± 0.11
2603	Naphthalene	80.23	18.923 ± 0.083
2604	Benzil	94.85	23.26 ± 0.10
2605	Acetanilide	114.34	21.793 ± 0.085
2606	Benzoic Acid	122.35	17.98 ± 0.04
2607	Diphenylacetic Acid	147.19	31.16 ± 0.13

As with diphenylacetic acid the volatility of the organic standards were assessed by thermogravimetry using a Mettler TG-SDTA 851^{e} apparatus. For the TG studies 2.5mg samples were contained in open 20µl aluminium crucibles and heated at 3°C min^{-1}. The mass losses were measured at the extrapolated onset temperature of melting and are listed (Table 36).

Table 36. ***Measured volatilities of organic DSC standards measured at the materials' melting temperature using the Mettler Toledo TA851^{e}. (sample mass, 2.5mg; heating rate, 3°C min^{-1}; atmosphere, nitrogen)***

LGC Reference	Material	Mass Loss / %
2613	Phenyl salicylate	0.0
2610	Biphenyl	3.7
2603	Naphthalene	41.5
2604	Benzil	0.5
2605	Acetanilide	2.9
2606	Benzoic Acid	37.5
2607	Diphenylacetic Acid	2.8

With the exception of phenyl salicylate all samples showed some mass loss with naphthalene and benzoic acid exhibiting high volatility. In view of these mass losses all of the DSC experiments were carried out with the samples in encapsulated crucibles.

The experimental procedure adopted for the enthalpy determinations was the same as that described previously for diphenylacetic acid. An empty encapsulated crucible was used as a reference and regular indium checks carried out to monitor the performance of the instrument. (Appendix 3)

The determination of the enthalpy of melting was derived using two different approaches and compared. The first method was a mathematical model based on a construction by Richardson and calculated using the expertise of Professor Peter Laye. This method was implemented by taking the raw experimental data into Microsoft Excel with 2°C intervals immediately preceding and following melting being represented by linear equations which were then used to extrapolate the data over the width of the melting peak. The area of the melting peak using a straight base line was also calculated using the experimental data expressed in Excel.

The second method utilised a more conventional approach in which the area of the fusion peak is measured using the Perkin Elmer software, Pyris. A sigmoidal baseline construction was used due to the small changes observed in heat capacity.

5.4.4 Determination of Enthalpy

The calibration factor for enthalpy obtained using the organic DSC standards is represented by γ and is defined as $\gamma=\Delta_{fus}H_{cert}/\Delta_{fus}H_{meas}$ where $\Delta_{fus}H_{meas}$ is the measured enthalpy change at the equilibrium melting temperature and $\Delta_{fus}H_{cert}$ is the certificate value.

All of the reference materials gave smooth and reproducible melting curves. The curves showed a small step change over the width of the fusion peaks consistent with a small change in heat capacity.

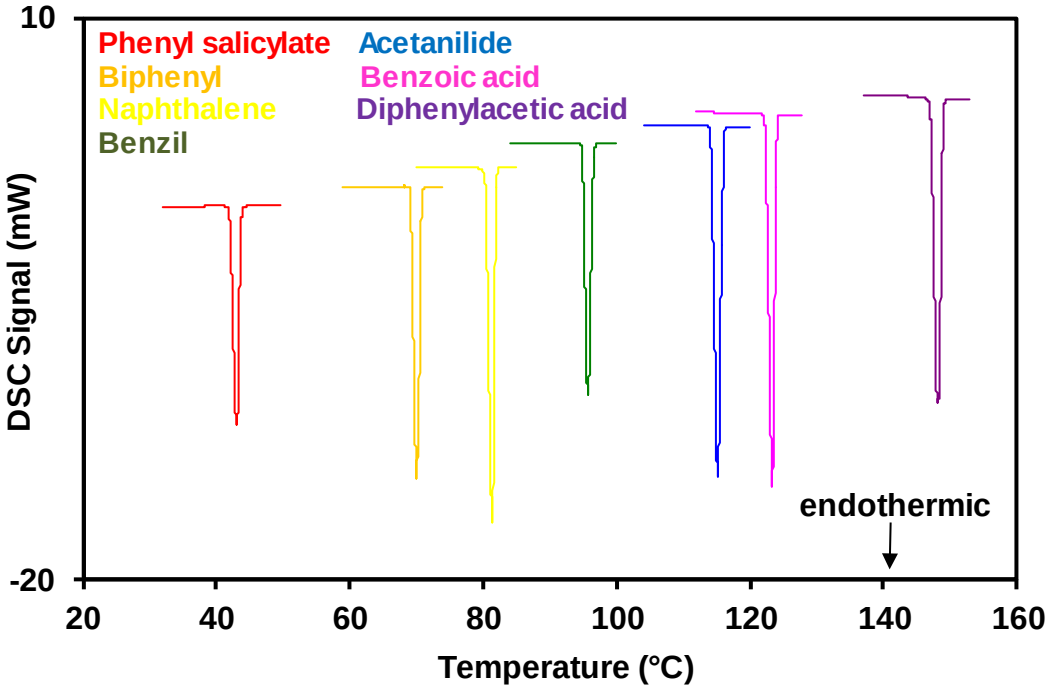

Fig. 64. ***DSC curves for the fusion peaks of organic DSC standards (sample mass, 2.5mg; heating rate, 3°C min^{-1}; atmosphere, nitrogen)***

The values of the enthalpies obtained from the area measurements are listed in Table 37. The uncertainties are estimates of the reliability of the values. They are based on single standard deviations of the means of the experimental results using

$$\sqrt{\frac{a^2}{A} + \frac{b^2}{B}}$$

Where the values are A ± a and B ± b etc. and include allowance for the uncertainty in assigning the onset temperature of melting and the error in the weighings. The

calibration factor γ calculated from the experimental enthalpies of fusion of the organic standards is presented in Table 37.

Table 37. ***Measured enthalpy change at the temperature of fusion for organic DSC standards. (sample mass, 2.5mg; heating rate, 3°C min^{-1}; atmosphere, nitrogen)***

Material	Calculated		Direct from Software	
	$\Delta_{fus}H_{meas}$/Jg^{-1}	γ	$\Delta_{fus}H_{meas}$/Jg^{-1}	γ
Phenyl salicylate	88.5 ± 0.3	1.012 ± 0.004	88.9 ± 0.4	1.008 ± 0.005
Biphenyl	120.0 ± 0.2	1.005 ± 0.004	120.1 ± 0.1	1.004 ± 0.004
Naphthalene	146.9 ± 0.2	1.005 ± 0.003	146.9 ± 0.1	1.005 ± 0.002
Benzil	110.9 ± 0.2	0.998 ± 0.003	111.1 ± 0.1	0.996 ± 0.003
Acetanilide	161.5 ± 0.4	0.997 ± 0.003	161.7 ± 0.3	0.997 ± 0.003
Benzoic Acid	147.3 ± 1.0	0.999 ± 0.007	147.3 ± 0.6	0.999 ± 0.004
Diphenylacetic Acid	146.9 ± 0.3	0.999 ± 0.007	147.3 ± 0.2	0.997 ± 0.003
Mean Calibration Factor		1.002 ± 002		1.001 ± 0.009

The values were not unduly sensitive to the assigned melting temperature in keeping with the small heat capacity change on fusion. The majority of the results showed excellent reproducibility (0.1-0.3%). Only a small error (0.2%) was introduced by using a straight base line to define the area of the melting peak. The higher uncertainty shown by the results for benzoic acid (0.7%) has potential to be associated with its greater volatility; however, the results for naphthalene showed excellent reproducibility in spite of its high volatility (ref. Table 36).

The values of γ appear to show a small increase at the lower temperatures but only the value for phenyl salicylate (1.012 ± 0.004) fell outside the combined errors. The mean values of the calibration factor over the entire temperature range was 1.002 ± 0.002 for the calculated method and 1.001 ± 0.009 for the directly measured method. An alternative interpretation of the results is possible by incorporating the indium calibration factor into the enthalpy calculations. This allows a direct comparison to be made between the experimental values for the enthalpy of fusion ($\Delta_{fus}H_{calib}$) and the certified values ($\Delta_{fus}H_{cert}$). Hence the difference $\Delta_{fus}H_{calib} - \Delta_{fus}H_{cert}$ is the error introduced by using indium as a single point calibrant. The value obtained for the indium calibration factor was 1.000 ± 0.002 and the enthalpy changes remained unchanged from those listed in Table 37 but showed a small increase in the uncertainty. The values for the error $\Delta_{fus}H_{calib}-\Delta_{fus}H_{cert}$ are listed in Table 38 together with the percentage error.

Apart from phenyl salicylate, the lowest melting material, the errors were <0.5% and were within the experimental uncertainties.

Table 38. ***Measured enthalpy change at the temperature of fusion for organic DSC standards using indium as a single point calibrant. (sample mass, 2.5mg; heating rate, 3°C min^{-1}; atmosphere, nitrogen)***

Material	Calculated $\Delta_{fus}H_{cert}$- $\Delta_{fus}H_{calib}$/Jg^{-1}	Error / %	Measured $\Delta_{fus}H_{cert}$- $\Delta_{fus}H_{calib}$/Jg^{-1}	Error / %
Phenyl salicylate	1.0 ± 0.4	1.1	0.7 ± 0.3	0.8
Biphenyl	0.6 ± 0.5	0.5	0.5 ± 0.4	0.4
Naphthalene	0.7 ± 0.5	0.5	0.7 ± 0.3	0.5
Benzil	-0.3 ± 0.4	-0.3	-0.5 ± 0.3	-0.4
Acetanilide	-0.3 ± 0.6	-0.2	-0.5 ± 0.4	-0.3
Benzoic Acid	-0.1 ± 1.0	-0.1	-0.1 ± 0.6	-0.1
Diphenylacetic Acid	-0.1 ± 0.5	-0.1	-0.4 ± 0.3	-0.3

Overall there was no significant error in using either method of determination, nor the use of indium as a single point calibrant for enthalpy measurements on the fusion of organic materials at lower temperatures.

However, it is important with all DSC equipment that the temperature dependence of the enthalpy calibration factor is investigated if accurate results are to be obtained.

5.5 Conclusions for the Enthalpy Measurements of Organic DSC Standards

The organic DSC standards provide the opportunity of calibrating DSC equipment in a temperature range for which there are no suitable metals and allow the temperature dependence of the calorimetric results to be assessed. All the materials gave reproducible fusion curves and enthalpy measurements were obtained with uncertainties of ~ 0.3% with the exception of benzoic acid where the uncertainty was 0.7%. The values of the calibration factor γ appeared to increase at the low temperatures but all the values agreed within the combined uncertainties with the exception of the result for the lowest melting temperature material phenyl salicylate (42ºC). The mean calibration factor $\gamma = 1.002 \pm 0.002$ was in agreement with the value obtained with indium (1.000 ± 0.002) and conclude that overall there was no significant error in using indium as a single point calibrant for measurements on the fusion of organic materials at lower temperatures.

I would anticipate that equipment similar to that used in the present work would show similar behaviour. However, it is important with individual DSC equipments that the temperature dependence is investigated if accurate results are to be obtained.

5.6 The Use of Stepwise Heating as a Validation Tool.

Previous studies concerning indium and diphenylacetic acid in Section 5.3 have shown that it is possible to determine both equilibrium temperatures and enthalpies of organic materials with a high level of accuracy and confidence using the DSC. The stepwise method, albeit time consuming is the preferred method of choice for accurate temperature measurements as variations in the gradient $\delta Te/\delta\beta$ for dynamic experiments can incur errors, unless it is known for sure that the calibrant and the compound under investigation have similar thermal properties.

In this study a selection of materials which have conflicting certified temperatures will be measured for accurate equilibrium temperatures using T_{step} and compared thus showing how this method lends itself for use as a validation tool.

Materials listed in Table 39 are available as both melting point temperature standards and DSC temperature standards. Their certified temperature values have been compared and in certain cases show variances of up to 0.4°C. Samples offered as certified reference materials, regardless of the intended use are in the purest form possible therefore should have unequivocal temperature of fusions.

The differences seen in the temperatures of the three materials, phenyl scalicylate, acetanilide and diphenylacetic acid are a real cause for concern and will be investigated further as it is the certified value in which the operator relies on to ensure that their instruments are accurately calibrated.

Table 39. ***Certified Temperatures for DSC and Temperature Organic Reference Standards***

Material	Certified Temperature / °C		Difference / °C
	Temperature Standard	DSC Standard	
Phenyl salicylate	41.50 ± 0.06	41.79 ± 0.03	0.29
Naphthalene	80.27 ± 0.05	80.25 ± 0.03	0.02
Benzil	94.86 ± 0.05	94.85 ± 0.02	0.01
Acetanilide	113.94 ± 0.04	114.34 ± 0.02	0.40
Benzoic Acid	122.41 ± 0.05	122.35 ± 0.03	0.06
Diphenylacetic Acid	147.05 ± 0.04	147.19 ± 0.03	0.14

5.6.1 Method of Certification

The certified temperatures obtained for the DSC standards in question were measured using adiabatic calorimetry. The T_{step} method is analogous to that used in adiabatic calorimetry and has already been shown to produce results equivalent to the certified liquefaction temperature.

In contrast, the temperature standards were certified in China and had been measured by means of interpolation. The method of temperature determination described in the certificate for the materials supplied by LGC was given as follows:

'Time temperature melting curves were produced using a primary standard platinum resistance thermometer that was traceable to the International Temperature Scale of 1990. The samples were heated using a heating rate of 0.2°C min^{-1} (±0.02°C min^{-1}) after having been held for 15 minutes at a temperature 4°C below the expected melting point. The thermodynamic melting point is the melting point that would be observed under equilibrium conditions (i.e. zero heating rate). Its value was obtained by interpolation of the liquefaction temperature and the freezing temperature observed when the molten sample was cooled at a rate of 0.2°C min^{-1}.[82]

The scanning nature of the Chinese method described above was ideal for use on the DSC and allowed a direct assessment of the method. Initial measurements on the sample with the largest temperature discrepancy, acetanilide, were made.

2.5mg samples of acetanilide were heated in encapsulated aluminium crucibles with a pin hole in the lid and measured in a flowing nitrogen atmosphere. The DSC plot is given in Fig. 65 and shows the presence of a melt however, a peak on cooling is absent, an indication of the sample "super cooling". Super cooling is a phenomenon whereby a sample can be cooled below its freezing point without the sample returning to its crystalline form without the input of energy or a source of nucleation.

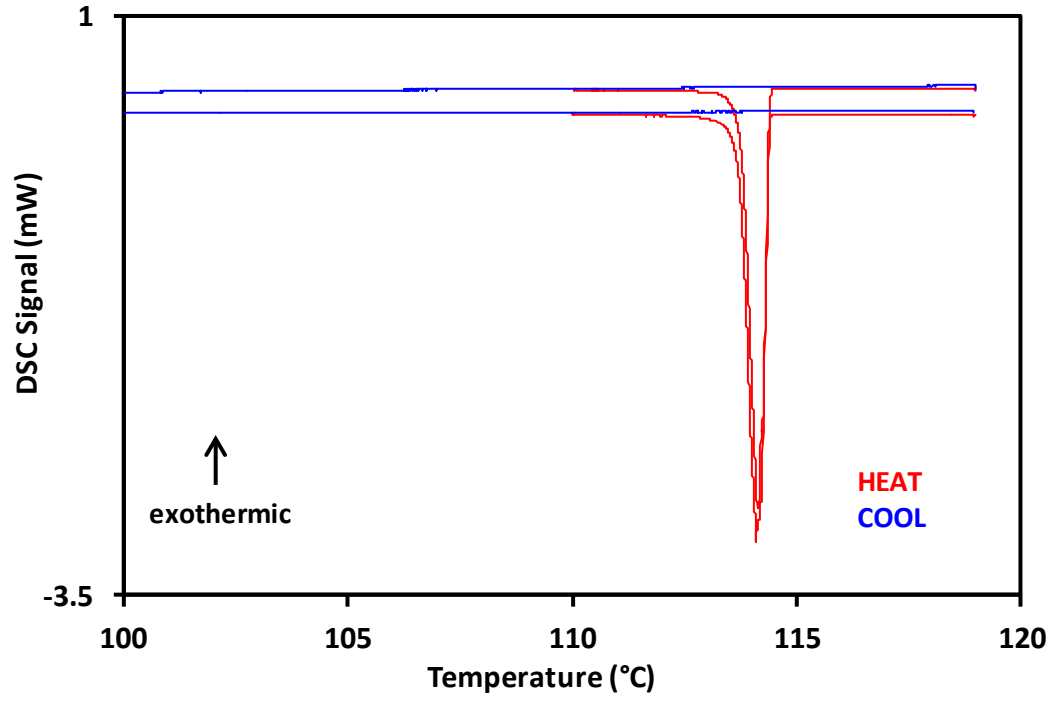

Fig. 65. ***DSC heat/cool curves for acetanilide using the method described in Section 5.6.1. (sample mass, 2.5mg; heating rate, 0.2°C min^{-1}; atmosphere, nitrogen)***

The measurements were repeated however, failure to identify a peak on cooling confirmed that this method of measurement would not be possible.

5.7 The use of Tstep as a Temperature Validation Tool

Given differences seen between the certified equilibrium temperatures for a range of organic materials in Table 39, this section aims to show how the T_{step} method can be used as a temperature validation tool for when discrepancies arise. Having established previously that the DSC standard diphenylacetic acid can be measured accurately using the T_{step} method a range of organic temperature standards whose certified equilibrium temperatures are subject to speculation will be measured and an assessment made as to whether the differences seen in the certified temperatures are actual differences or errors inherent in the method of certification.

The measurements under near equilibrium conditions were made using typical stepwise parameters outlined previously. Duplicate samples were run in encapsulated 40µL aluminium pans using a flowing nitrogen atmosphere. The results given in Table 40 confirm that when measured using the T_{step} method the DSC standards provide equivalent equilibrium temperatures to those provided on the certification.

Table 40. ***Stepwise measurements of DSC standards (sample mass, 2.5mg; step size, 0.05°C; atmosphere, nitrogen)***

Material	Equilibrium Temperature / °C				
	T_{step} Measured	Correction (Indium)	T_{step} Corrected	Certificate Value (T_{cert})	T_{Cert}-T_{step}
$DAA_{(DSC)}$	147.08 ± 0.04	0.10	147.18 ± 0.04	147.19 ± 0.03	0.01 ± 0.04
$Acetanilide_{(DSC)}$	114.18 ± 0.02	0.10	114.28 ± 0.02	114.34 ± 0.02	0.06 ± 0.02
Phenyl $Salicylate_{(DSC)}$	41.63 ± 0.02	0.10	41.73 ± 0.02	41.79 ± 0.03	0.06 ± 0.02

The equivalent results for the temperature standards are shown in Table 41.

Table 41. ***Stepwise measurement of melting point standards. (sample mass, 2.5mg; step size, 0.05°C; atmosphere, nitrogen)***

Material	Equilibrium Temperature / °C				
	T_{step} Measured	Correction (Indium)	T_{step} Corrected	Certificate Value (T_{cert})	T_{Cert}-T_{step}
$DAA_{(Mpt)}$	147.08 ± 0.03	0.10	147.18 ± 0.03	147.05 ± 0.04	-0.13 ± 0.03
$Acetanilide_{(Mpt)}$	114.11 ± 0.03	0.10	114.21 ± 0.03	113.94 ± 0.04	0.26 ± 0.03
Phenyl $Salicylate_{(Mpt)}$	41.69 ± 0.03	0.10	41.79 ± 0.03	41.50 ± 0.06	0.29 ± 0.03

It is not until you compare the equilibrium temperatures for both the DSC and the temperature standards (Table 42) that you see the effectiveness of the T_{step} method as a temperature validation tool.

Table 42. ***Comparison of measured equilibrium temperatures using the T_{step} method for DSC and temperature standards. (sample mass, 2.5mg; step size, 0.05°C; atmosphere, nitrogen)***

Material	Temperature / °C			
	T_{step} DSC Standard	T_{step} Mpt Standard	T_{step}DSC - T_{step}Mpt	Certificate Difference
DAA	147.18 ± 0.04	147.18 ± 0.03	0.00 ± 0.04	0.14 ± 0.04
Acetanilide	114.28 ± 0.02	114.21 ± 0.03	0.07 ± 0.02	0.40 ± 0.04
Phenyl Salicylate	41.73 ± 0.02	41.79 ± 0.03	0.06 ± 0.02	0.29 ± 0.06

With marginal differences shown between the equilibrium temperatures of the three materials using the accurate T_{step} method, it becomes evident that the certification values based upon a method of interpolation were inaccurate.

In addition to the measurements made the temperature dependence of the organic DSC standards under equilibrium conditions can be assessed. The values are provided in the table below.

Table 43. ***Comparison of measured equilibrium T_{step} temperatures for DSC and temperature standards for materials certified using triple point measurements. (sample mass, 2.5mg; step size, 0.05°C; atmosphere, nitrogen)***

Material	Temperature / °C			
	T_{step} DSC	Correction (Indium)	T_{step} Corrected	T_{cert} - T_{step}
DAA	147.08 ± 0.04	0.10	147.18 ± 0.04	0.01
Acetanilide	114.18 ± 0.02	0.10	114.28 ± 0.02	0.06
Benzil	94.73 ± 0.02	0.10	94.83 ± 0.02	0.02
Naphthalene	80.03 ± 0.01	0.10	80.13 ± 0.01	0.10
Phenyl Salicylate	41.63 ± 0.02	0.10	41.73 ± 0.02	0.06

5.8 Conclusions for the use of the T_{step} Method as a Validation Tool

The uncertainty of the equilibrium temperatures of materials intended for use as calibration standards provided an opportunity to explore the use of the T_{step} method as a means to validate equilibrium temperatures of two different batches of a material. Initial equilibrium values provided on the certification gave dissimilarities of up to 0.40°C, a significant error and uncertainty for when calibrating

instrumentation. Subsequent measurements utilising the T_{step} method provided confirmation that the two materials had the same equilibrium temperatures and shows that the method has potential for use as a validation tool when situations of ambiguity arise. In addition the temperature dependence under equilibrium conditions could be determined and showed little change over a 100°C span.

Chapter 6 Determination of Equilibrium Temperatures for Materials Susceptible to Decomposition at Slow Heating Rates.

6.1 Introduction

The thermal properties of the highly energetic oxidants potassium and rubidium dinitramides [$MN(NO_2)_2$ where M= K or Rb] are of a growing interest due to their potential use in pyrotechnic compositions. Previous studies have shown that equilibrium temperature values for solid-solid transitions of inorganic materials of pyrotechnic interest can be measured with a high degree of accuracy using DSC.[83] However, it has been found that during slow heating rates some oxidants, in particular dinitramides, decompose below their melting points making it impossible to determine accurate equilibrium melting temperatures using either the stepwise heating technique or the standard extrapolation to zero heating rate method.[84-85] In circumstances such as these whereby slower heating rates cause undesirable effects on the sample, methodologies which incorporate much faster heating rates should be explored.

The lightweight furnace design of the power compensated systems such as those used in the Perkin Elmer Diamond DSC have shown that by achieving heating rates of over 500°C min^{-1} it is possible to accentuate transitions that would be potentially lost when measured using more conventional slower heating rates (HyPer DSC).[86] The use of fast heating rates does not inhibit the samples response but can affect and inhibit kinetically controlled transitions.[87]

Due to the more robust nature of the heatflux DSC measuring cell and higher thermal mass furnace design, achieving heating rates of less than 100°C min^{-1} are more realistic. Previous studies have already concluded that equilibrium temperatures can be calculated using the regression analysis of a straight line at slower heating rates (1-10°C). The aim of this section of work is to see if the extrapolation to zero heating rate method can be modified to implement faster heating rates in the range 10-50°C min^{-1} in order to overcome problems of decomposition.

6.2 Method Validation

The extrapolation to zero heating rate method has been adapted to include the range of heating rates 10-50°C min^{-1} instead of the typical 1-10°C min^{-1}. Preliminary measurements were made on the DSC temperature standards indium, benzil and diphenylacetic acid supplied by LGC Ltd in order to bracket the melting range of the dinitramides to be studied. Measurements were made using a Mettler DSC 822^e with 2.5mg samples encapsulated in aluminium crucibles with a pin hole in the lid. A flowing atmosphere of argon at 80 cm^3min^{-1} was used. The instrument was calibrated using the T_{step} of high purity LGC Indium prior to use. To distinguish between the equilibrium temperature values for the two extrapolation methods, $T_{\beta=0.FHR}$ will be used herein to distinguish the fast heating rate method from the standard extrapolation to zero heating rate method. The extrapolated onset temperatures at the faster heating rates for the DSC standards are plotted in Figs 63 to 65 and show that even at the faster heating rates a linear regression is still achievable without showing any signs of curvature (an indication of slower response time to temperature input).

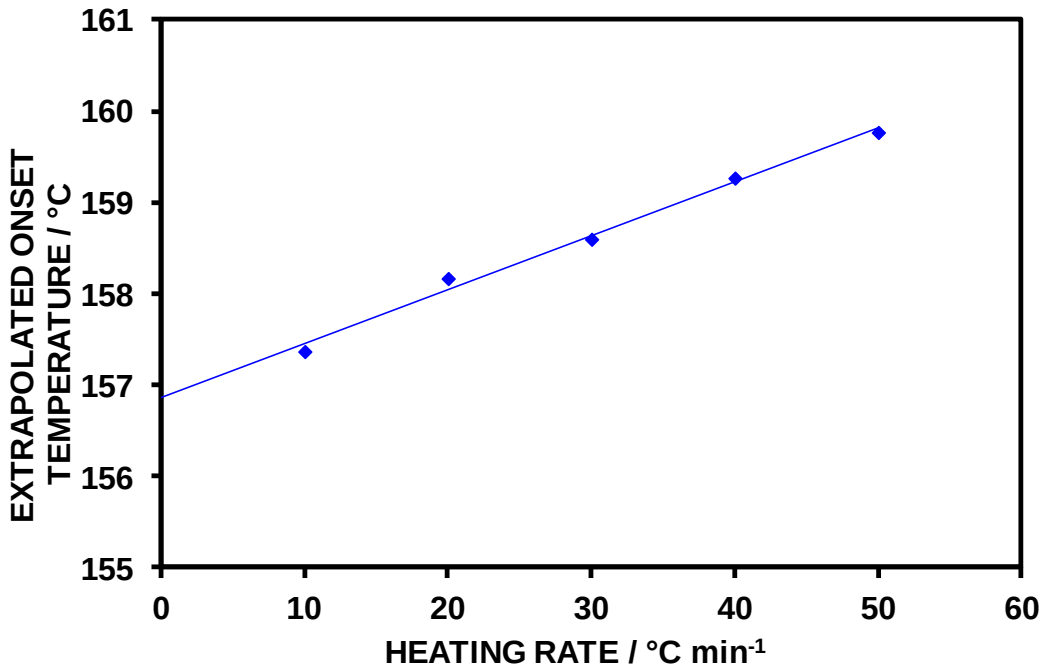

Fig. 66. ***Plot of extrapolated onset temperature against heating rate for the fast heating of LGC indium. (sample mass, 10mg; atmosphere, nitrogen)***

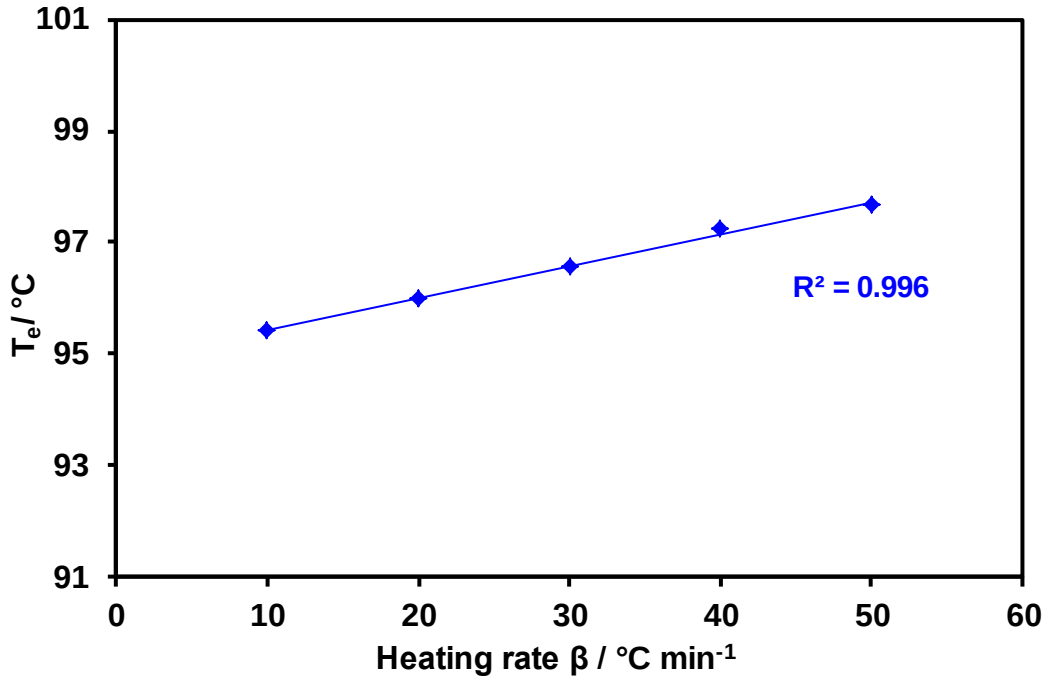

Fig. 67. ***Plot of extrapolated onset temperature against heating rate for the fast heating of LGC benzil. (sample mass, 2.5mg; atmosphere, nitrogen)***

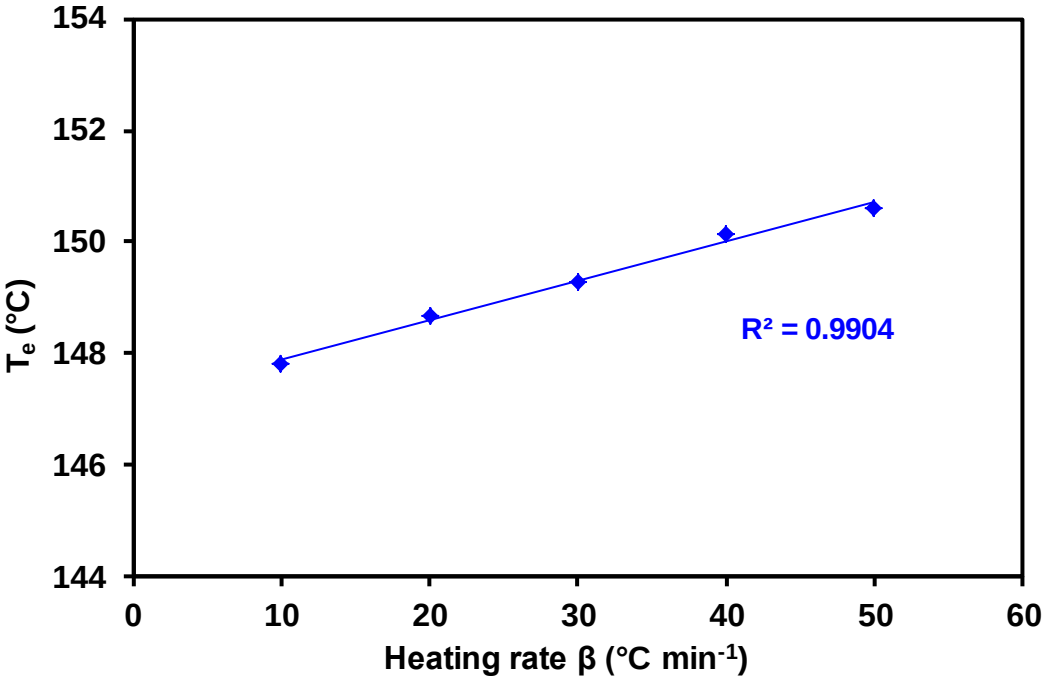

Fig. 68. ***Plot of extrapolated onset temperature against heating rate for the fast heating of LGC diphenylacetic acid. (sample mass, 2.5mg; atmosphere, nitrogen)***

Comparison of the measured $T_{\beta=0.\,FHR}$ values with the certified equilibrium values for these materials has enabled the fast heating rate method to be validated and confirms that the fast heating rate method enables relatively accurate equilibrium temperature values to be determined for benzil and diphenylacetic acid.

Whilst not as close as the organic materials the value obtained for indium is within 0.2 °C of the certified value. The reason for the slight difference in the indium temperature values unknown, however, to achieve a value of ± 0.2 °C of the certificate is significantly better than determinations at such high heating rates which would traditionally be reported in the region of ± 1-5°C of the measured value.

Table 44. ***Equilibrium fusion temperatures measured using $T_{\beta=0.FHR}$ method for LGC ltd DSC standards. (sample mass, 2.5mg; atmosphere, nitrogen)***

DSC Standard	Temperature / °C		Difference / °C
	Measured	Certificate	
Benzil	94.85 ± 0.07	94.85	0.00
DPA	147.17 ± 0.13	147.19	0.02
Indium	156.78 ± 0.12	156.61	0.17

6.3 The Use of the $T_{\beta=0}$. FHR Method to Determine Equilibrium Temperatures of Dinitramides

The thermal properties of the highly energetic oxidants potassium and rubidium dinitramides are of a growing interest due to their potential use in pyrotechnic compositions. Unlike the other oxidants studied in this thesis, the low temperature fusion of the dinitramide salts are susceptible to decomposition when heated at slow heating rates.[85]

The amount of pre-melt decomposition occurring increases in magnitude the slower the heating rate becomes (Fig. 69).

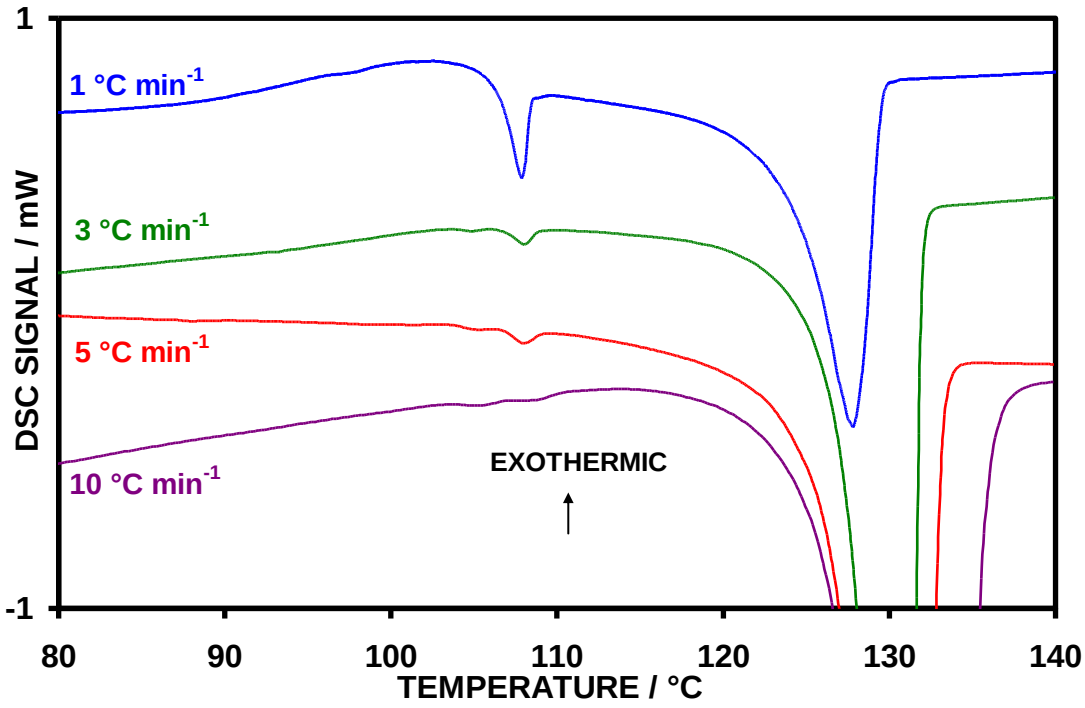

Fig. 69. ***DSC curves showing the decomposition of KDN-1 under slow heating. (sample mass, 2.5mg; atmosphere, nitrogen)***

The appearance of this pre-melt decomposition means that both the T_{step} and the $T_{\beta=0}$ methods are impractical for any accurate determinations of the fusion.

Having validated the fast heating rate method equilibrium fusion temperature measurements have been carried out on potassium dinitramides KDN-1, KDN-2 and KDN Bofors and on the rubidium dinitramides RbDN-1 and RbDN-2.

Samples of both potassium and rubidium dinitramide have been measured using the fast heating rate method described. Potassium dinitramide is an extremely photosensitive compound that decomposes readily when left out on the open bench, therefore all samples; including rubidium dinitramide were stored and prepared in a dark environment.

6.4 Results

6.4.1 Potassium Dinitramide

A DSC curve for KDN-1 (with exception of KDN-2) at 10°C min^{-1} is shown in Fig. 70. The fusion of KDN occurs at ~130°C and is proceeded by the decomposition in the liquid state.[88-100]

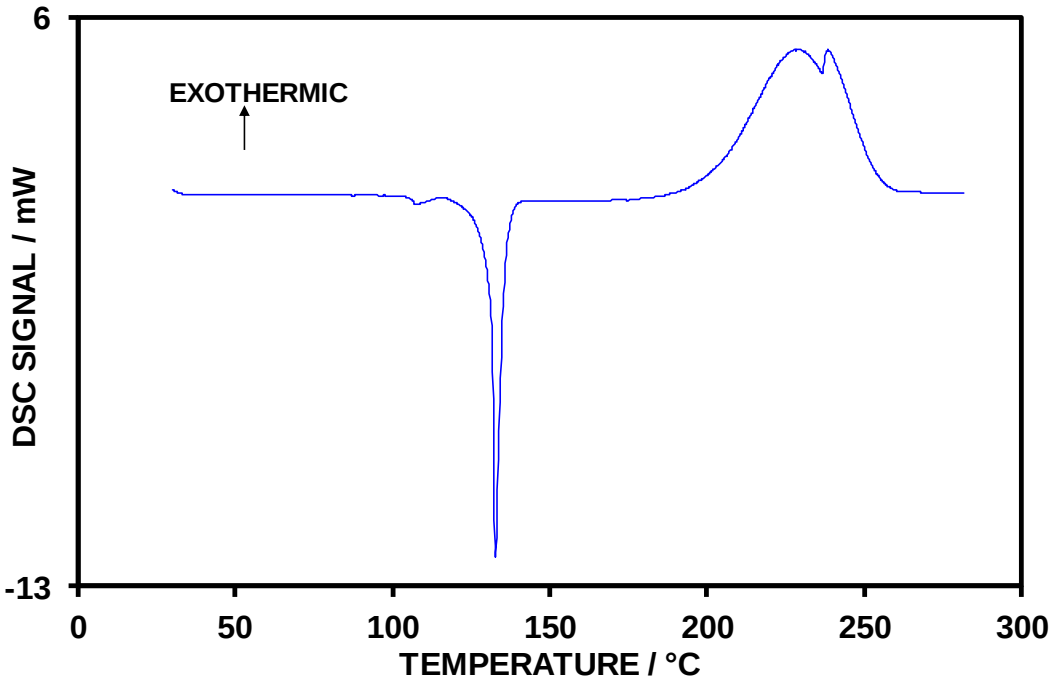

Fig. 70. ***DSC curve for KDN-1 (sample mass, 2.5mg; heating rate, 10°C min^{-1}; atmosphere, nitrogen)***

Measurements were made on three variants of potassium dinitramide and their extrapolated onset temperatures compared (Fig. 71). It can be seen that each sample of dinitramide has a different heating rate dependence and their resultant slopes provided in Table 45.

Table 45. ***Equilibrium fusion temperatures measured for KDN using $T_{\beta=0.FHR}$. (sample mass, 2.5mg; atmosphere, nitrogen)***

Sample	Equilibrium Temperature / °C	Slope / min
KDN-1	129.1 ± 0.0	0.0774
KDN Bofors	128.6 ± 0.1	0.0561
KDN-2*	127.4 ± 0.1	0.1017

* Results at 10 °C min^{-1} have been omitted

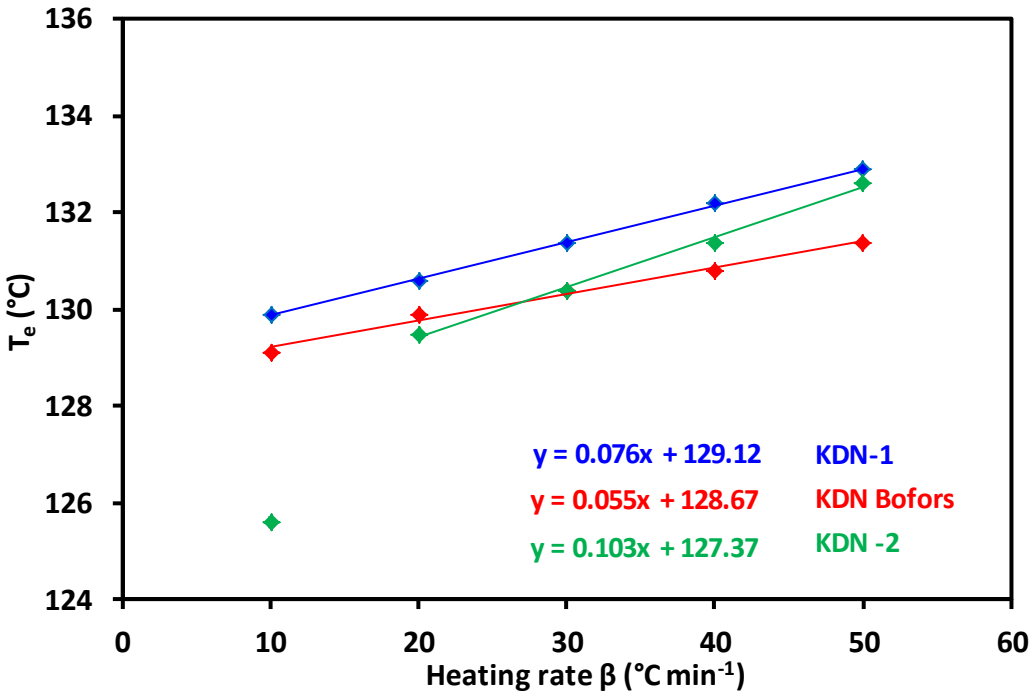

Fig. 71. ***Plot of extrapolated onset temperature versus heating rate for the fast heating $T_{\beta=0}$ of potassium dinitramide. (sample mass, 2.5mg; atmosphere, nitrogen)***

The consistently low T_e values measured for KDN-2 at 10 °C min^{-1} indicates that some decomposition may be occurring at this heating rate and thus $T_{\beta=0.FHR}$ has been determined from heating rates in the range 20 to 50 °C min^{-1}. The DSC plot showing the fusion of KDN-2 is given in Fig. 72.

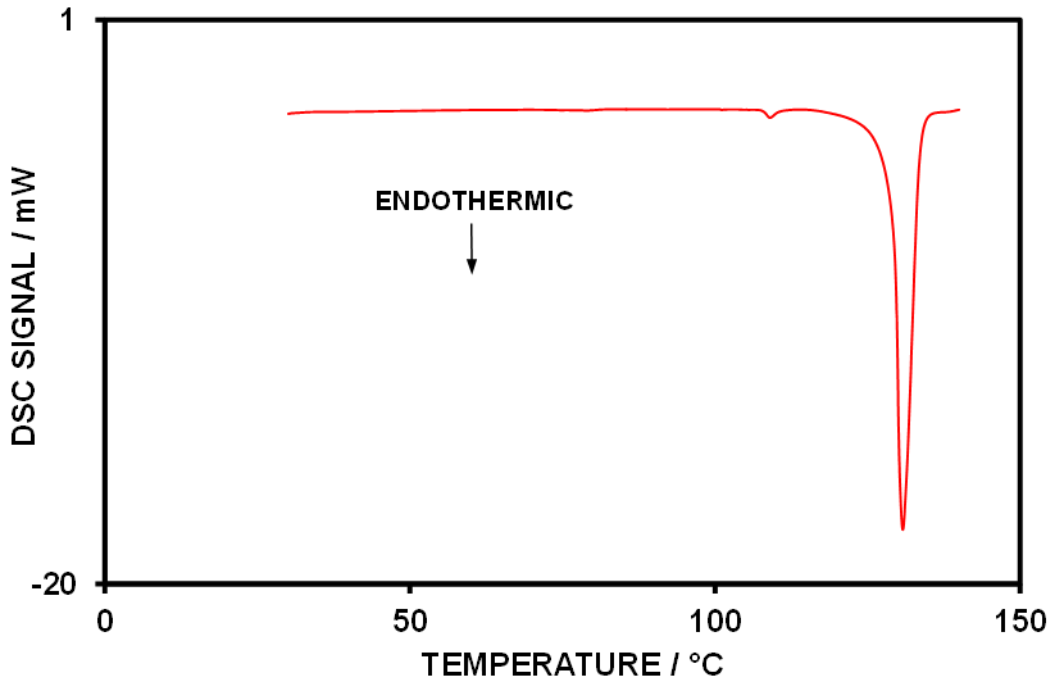

Fig. 72. ***DSC curve for KDN-2 (sample mass, 2.5mg; heating rate, 10°C min^{-1}; atmosphere, nitrogen)***

6.4.2 Rubidium Dinitramide

The thermal properties of the energetic oxidant rubidium dinitramide (RbDN) are of interest due to its potential use in pyrotechnics. To date only limited studies have been carried out on this material.

DSC studies by Babkin[99]. Cliff & Smith[96] obtained similar results in their DSC studies and reported a small endothermic peak at 85 °C and the melting of the sample at 104 °C. A two stage exothermic decomposition reaction was observed with peaks at 141 °C and 230 °C. In contrast, Berger[84] found from DSC and TG studies that the melting peak for rubidium dinitramide at 106 °C was followed by a single stage exothermic decomposition reaction with a peak maximum at 234 °C.

In order to resolve these conflicting observations measurements have been made using the fast heating rate method to investigate further, similar to the study on potassium dinitramide (Section 6.3).

A typical DSC curve for RbDN-1 at 10°C min^{-1} is shown. DSC studies on rubidium dinitramide in both crystal and powder form show that following the fusion peak at 107°C an exothermic decomposition reaction was given similar to its potassium counterpart.

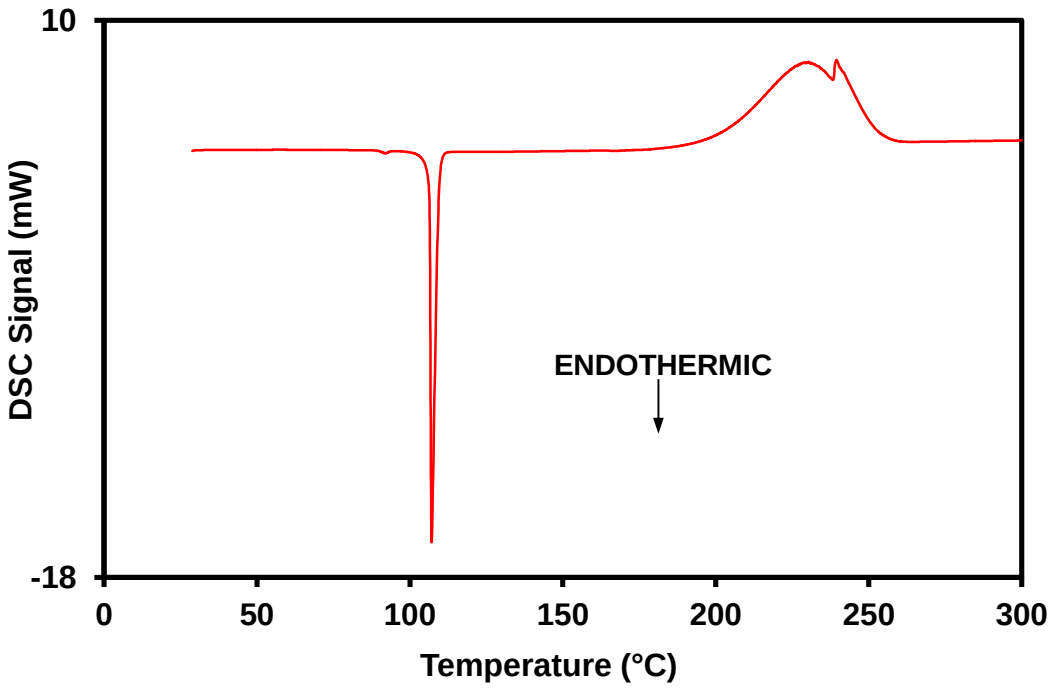

Fig. 73. ***DSC curve for RbDN-1. (sample mass, 2.5mg; heating rate, 10°C min^{-1}; atmosphere, nitrogen)***

Measurements were made on two variants of rubidium dinitramide and their extrapolated onset temperatures compared. An example of an extrapolation to zero heating is shown in Fig. 74 with the comparative data provided in Table 46.

Table 46. ***Measured equilibrium fusion temperatures for RbDN using $T_{\beta=0.FHR}$ method. (sample mass, 2.5mg; atmosphere, nitrogen)***

Sample	Equilibrium Temperature / °C	Slope / min
RbDN-1	105.9 ± 0.2	0.0582
RbDN-2	103.4 ± 0.1	0.0635

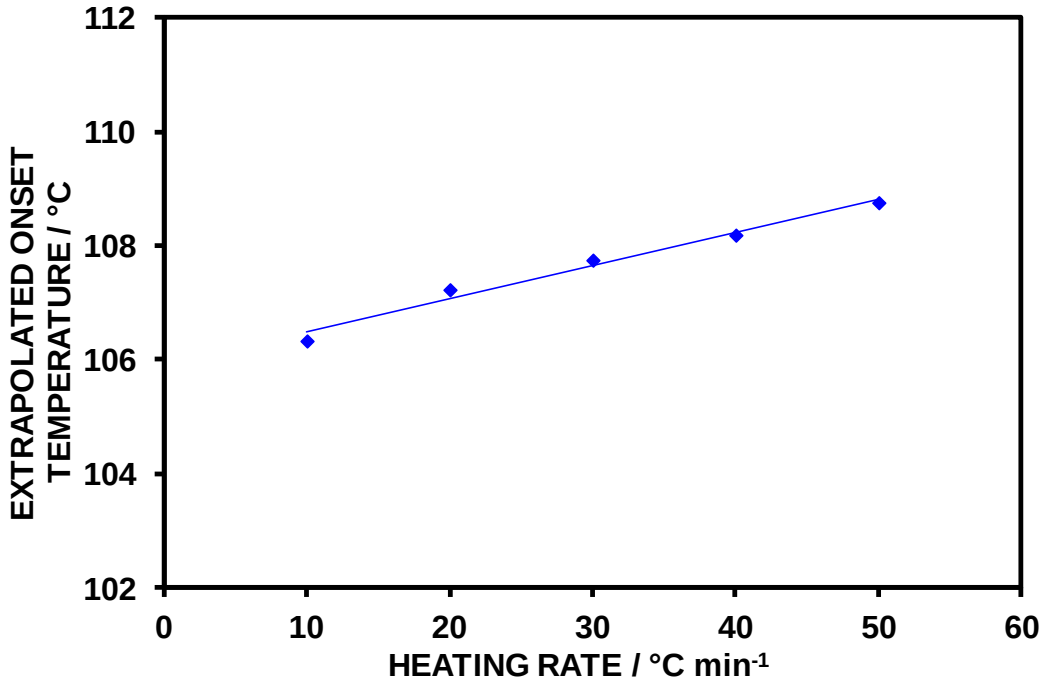

Fig. 74. ***Plot of extrapolated onset temperature against heating rate for the fast heating of RbDN-1. (sample mass, 2.5mg; atmosphere, nitrogen)***

6.5 Conclusions for the determination of equilibrium temperatures of materials susceptible to decomposition at slower heating rates.

The methods extrapolation to zero heating rate and stepwise heating have been shown to produce accurate equilibrium temperature of transition using DSC. For some materials such as the dinitramide salts, this is an inappropriate method of determining the equilibrium transition temperature due to decomposition which occurs when heated at slow temperature rates less than10°C min^{-1}.

As the isothermal stepwise heating method would not be suitable for determining equilibrium temperatures, an extended extrapolation to zero heating rate method was developed. Using both organic and metal calibrants the heating rates for the extrapolation to zero heating were extended to include the range 10°C – 50°C min^{-1} to provide equilibrium temperatures similar to those indicated on the certificate provided. Having established confidence in the extended method, measurements

were made on both rubidium and potassium dinitramides to provide a more accurate equilibrium temperature of transition.

Whilst no direct comparison can be made between samples due to the differences in the methods of their chemical preparation and purities the method has shown promise for determining accurate temperatures for samples which undergo decomposition under slow heating rates.

Chapter 7 Summary of Work

7.1 Overall Conclusions for the Determination of Accurate Temperatures and Enthalpies

There are two methods for which the accurate equilibrium temperature of a material can be determined using DSC. The first method utilises the DSC in its traditional scanning mode, whilst the alternative method adopts a stepwise isothermal programme similar to that used in classic calorimetry measurements.

Whilst both methods have shown to produce concurring results, for transitions which occur over a broad temperature range the determination of equilibrium temperatures using the isothermal method is not suitable when higher degrees of accuracy are sought. An example highlighting such can be seen when accurately determining the equilibrium onset temperatures of the three solid-solid phase transitions of $RbNO_3$ in Section 4.3. In this example both the 1st and 3rd transitions are measurable to accuracies of ± 0.05°C using the isothermal technique, however, the determination of an accurate equilibrium onset temperature of the 3rd transition relies solely on those results obtained from the extrapolation to zero heating rate method due its broad and distorted peak shape under slow heating rates.

Of the two methods, the isothermal stepwise method of determining accurate equilibrium temperatures is more favourable as less sample runs are required overall to achieve a definitive temperature value (1:4) than those required in the construction of an extrapolation, however, the process can be extremely time consuming. In order to avoid unnecessary time and sample wastage when measuring accurate equilibrium temperatures of unfamiliar transitions an assessment can be made as to which method is suitable for use by initially running the sample at a relatively slow heating rate such as 1°C min^{-1} and observing any peak distortions that may occur.

7.2 Future Work

The exploration of equilibrium temperatures using DSC is exhaustive and has potential to achieve accurate temperature results similar to those obtained from classic calorimetry techniques such as adiabatic calorimetry. Having shown that measurements can be made to a higher degree of accuracy on materials such as $RbNO_3$ and KNO_3 it would be of interest to extend this to cover a wide range of inorganic salts for which accurate values are not available at present.

The main drawback of the DSC method is in the differences seen in the heating rate dependencies of materials especially when compared to a calibrant. Future developments may include mapping out the heating rate dependencies of a wide range of metal calibrants in their various forms and exploring how they may influence the temperature measurements of other samples including a detailed investigation of the effect of crucible type and material, atmosphere and sample mass on the temperature measurements carried out under equilibrium conditions. It will be of particular interest to investigate if alumina crucibles give the same values as aluminium crucibles. This would enable temperature calibration using gallium.

Having shown that it is possible to obtain extended extrapolation to zero heating rate measurements using faster heating rates in the lower temperature regions (sub 300°C), it may also be of interest to adapt this method of measurement to include higher temperatures above 600°C; however this would ultimately be reliant on whether there is a direct correlation between the alumina and aluminium sample pans.

Appendix 1. References

1. T. Lever, P. Haines, J. Rouquerol, E.L. Charsley, P.V. Eckeren, D.J. Burlett, *Pure and Applied Chemistry,* 2014, **86(4),** 545-553.
2. M. Richardson, E.L. Charsley, in *Handbook of Thermal Analysis and Calorimetry*. M.E. Brown (ed.) Elsevier Science B.V. 1998, ch.13, pp.547-575.
3. P.H. Willcocks, N.R. Bosley, A. Broadhurst, I.D. Luscombe, *Journal of Thermal Analysis and Calorimetry,* 1999, **56**, 1413-1418.
4. T. Carnelley, W. Carleton-Williams, *Journal of the Chemical Society Transactions,* 1880, **37**, 125-127.
5. S. Spiel, L.H. Berkelheimer, J.A. Pask, B. Davies, *Differential thermal analysis – Its application of clays and other aluminous minerals*. U.S. Bureau of Mines. [Technical paper] 1945.
6. W.W. Wendlandt, P.K. Gallagher, *Thermal Characterization of Polymeric Materials*,E. Turi (ed.) Academic Press Inc. 1981.
7. H. Bunjes, T. Unrah, *Advanced Drug Delivery Reviews*, 2007, **59**, 379-402.
8. M.J. O'Neill, *Analytical Chemistry*, 1964, **36(7)**, 1238-1245.
9. Perkin Elmer Inc. PYRIS Diamond DSC datasheet Online, http://www-omcs.materials.ox.ac.uk/uploads/diamond%20dsc%20tech%20sheet.pdf. (acessed 15th September 2015)
10. D. Chen, A. Green, D. Dollimore, *Thermochimica Acta*, 1996, **284,** 429-433.
11. D.V. Malakhov and M.K. Abou Khatwa, *Journal of Thermal Analysis and Calorimetry*, 2007, **87(2)**, 595-599.
12. R. Riesen, *Choosing the right baseline*, Thermal Analysis Information for Users. User Com 25, Mettler Toledo AG. [Technical paper], 2007
13. E.L. Charsley, P.G. Laye, V. Palakollu, J.J. Rooney, B. Joseph, *Thermochimica Acta,* 2006, **446**, 29-32.
14. G.W.H. Höhne, *Journal of Thermal Analysis*, 1991, **37**, 1987-2000.
15. H.Preston-Thomas, *Metrologia,* 1990, **27**, 3-10.
16. H. Staub, W. Perron, *Analytical Chemistry*, 1974. **46**, 128-130.
17. M.J. Richardson, *Thermochimica Acta,* 1997, **300**, 15-28.

18. E.L. Charsley, P.G. Laye, H.M. Markham, J.O. Hill, B. Berger, T.T. Griffiths, *Thermochimica Acta,* 2008, **469**, 65-70.
19. R.E. Bedford, G. Bonnire, H. Maas, F. Paverse, *Metologica,* 1984, **20**, 145-155.
20. A. Shimkin, *Thermochimica Acta*, 2013, **566**, 71-76.
21. D.G. Archer, *Journal of Thermal Analysis and Calorimetry*, 2006, **85(I)**, 131-134.
22. G. Della Gatta, M.J. Richardson, S.M.Sarge, S.Stølen, *Pure and Applied Chemistry*, 2006, **78(7)**, 1455-1476.
23. G. Hakvoort, C.M. Hol, P.J. van Ekeren, *Journal of Thermal Analysis and Calorimetry*, 2002, **69**, 333-338.
24. M. Schubnell, *Journal of Thermal Analysis,* 2000, **61**, 91-98.
25. Mettler Toledo. The MultiSTAR DSC sensor family Online, http://us.mt.com/us/en/home/supportive_content/product_documentation/datasheets/DS_MultiSTAR/_jcr_content/download/file/file.res/51724386B_V09.10_MultiSTAR_DSC_Sensor_DB_e.pdf (acessed September 15th 2015)
26. TA Instruments. DSC 2920 CE Operating manual Online, http://www.geminibv.nl/labware/differential-scanning-calorimeter/dsc2920ce.pdf (accessed September 15th 2015)
27. E. L. Charsley, A. C. F. Kamp, *Thermal Analysis*, Ed. H. G. Wiedemann, Birkhauser Verlag, Vol.1,1972, 499-513.
28. Mettler Toledo. Online, http://ca.mt.com/ca/fr/home/phased_out_products/PhaseOut_Ana/TGA_SDTA851e_Thermogravimetric_Analyzer.html (acessed 15th September 2015)
29. A.A. Van Dooren, B.W. Müller, *Thermochimica Acta*, 1983, **66**,161-186.
30. LGC Ltd. Certificate of measurement. Online, http://www.lgcstandards.com/medias/sys_master/pdfs/pdfs/h41/h69/8928438747166/LGC2610-ST-WB-CERT-1775118-1-1-1.pdf (accessed April 2006)
31. A.A. Van Dooren, B.W. Müller, *Thermochimica Acta*, 1981, **49**, 151-161.
32. Perkin Elmer Inc. Online, http://www.perkinelmer.co.uk/Catalog/Gallery.aspx?ID=Sample Pans

and Cups&PID=Thermal Analysis Consumables&refineCat=Consumables Category&N=189 139 78933 4293911495&TechNVal=4293911495 (accessed 15th September 2015)

33. DSC CONSUMABLES Inc. Online, http://www.dscconsumables.com/category/TA-Instruments.html (accessed: 15th September 2015)
34. Mettler Toledo. Thermal analysis crucibles, Online, http://int.mt.com/int/en/home/products/Laboratory_Analytics_Browse/TA_Family_Browse/ta_consumable_browse.html (accessed September 2015)
35. E.L. Charsley, J.O. Hill, P. Nicholas, S.B. Warrington, *Thermochimica Acta*, 1992, **195**. 65-71.
36. A.P. Rostowski, *Russian Journal of Physical Chemistry*, 1930, **62**, 2067.
37. V.E. Plyuschchev, I.B. Markina, L.P. Shklover, *Zhurnal Neorganicheskoi Khimii,* 1956, **1**, 1613.
38. A. Mustajoki, *Annales Acadmiæ Scientarium Fennicæ*, 1958, **A VI**, 3.
39. A. Arell, M. Varteva, *Annales Acadmiæ Scientarium Fennicæ*, 1961, **A VI**, 1.
40. R.N. Brown, A.C. McLaren, *Acta Crystallographica,* 1962, **15,** 974.
41. K.J. Rao, C.N.R. Rao, *Journal of Material Science*, 1966, **1(3)**, 238-248.
42. P.I. Protsenko, L.S. Grin'ko, L.N. venerovskaya, V.A. Lyutsedarskii, *Russian Journal of Applied Chemistry*, 1973, **46,** 2568.
43. E.A. Secco, R.A. Secco, *Physical Chemistry Chemical Physics,* 1999, **1(21)**, 5011-5016.
44. M. Hichri, C. Favotto, H. Zamali, Y. Feutelais, B. Legendre, *Journal of Thermal Analysis and Calorimetry,* 2002, **69(2)**. 509-518
45. S. Wacharine, D. Hellali, H. Zamali, J. Rogez, M. Jemal, *Journal of Thermal Analysis and Calorimetry*, 2012, **107(2)**, 477-481.
46. H. Jendoubi, D. Hellali, H. Zamali, M. Jemal, *Journal of Thermal Analysis and Calorimetry*, 2013, **111**, 877-883.
47. E.L. Charsley, J.P. Davies, E. Glöggler, N. Hawkins, G.W.H. Höhne, T. Lever, K. Peters, M.J. Richardson, I. Rothemund, A. Stegmayer, *Journal of Thermal Analysis*, 1993, **40**, 1405-1414.

48. G.W. H. Höhne, K.H. Breuer, W. Eysel, *Thermochimica Acta,* 1983, **69**, 145-151.
49. G.W.H. Höhne, W. Eysel, K.H. Breuer, *Thermochimica Acta,* 1985, **94**. 199-204.
50. H.G. McAdie, *Journal of Thermal Analysis,* 1971, **3**, 79-102.
51. F. Roget, C. Favotto, J. Rogez, *Solar Energy*, 2013, **95**, 155-169.
52. C. Martin, T. Bauer, H. Müller-Steinhagen, *Applied Thermal Engineering*. 2013, **56**, 159-166.
53. J. Lopez, Z. Acem, E. Palomo Del Barrio, *Applied Thermal Engineering,* 2010, **30**, 1586-1593.
54. R. Murugan, P.J. Huang, A. Ghule, H. Chang, *Thermochimica Acta,* 2000, **346**, 83-90.
55. S. Gordon, C. Campbell, *Analytical Chemistry*, 1955, **27(7)**, 1102-1109.
56. P. Garn, *Analytical Chemistry*, 1969, **41(3)**, 447-456.
57. P.W. Bridgman, *Proceedings of the American Academy of Arts and Sciences*, 1916, **51**, 581-625.
58. V.V. Deshpande, M.D. Karkhanavala, U.R.K. Rao, *Journal of Thermal Analysis,* 1974, **6**, 613-621.
59. E.Y. Wang, *Journal of the Electrochemical Society*, 1976, **123**, 435-437.
60. D.J. Rojers, G.J. Janz, *Journal of Chemical & Engineering Data*, 1982, **27**, 424-428.
61. R.W. Carling, *Thermochimica Acta,* 1983, **60(3)**, 265-275.
62. Y. Takahashi, R. Sakamoto, M. Kamimoto, *International Journal of Thermophysics*, 1988, **6**, 1081-1090.
63. M.J. Westphal, J.W. Wood, R.D. Redlin, T. Ashworth, *Journal of Applied Physics*, 1993, **73**, 7302-7310.
64. H. Zamali, M. Jemal, *Journal of Phase Equilibria,* 1995, **16**, 235-238.
65. M. Guizani, H. Zamali, M. Jemal, *Comptes rendus de l'Académies des Sciences*, 1998, **1**, 787-789.
66. A.A. Van Dooren, B.W. Müller, *Thermochimica Acta*, 1981, **49**, 175-183.
67. A.A. Van Dooren, B.W. Müller, *Thermochimica Acta,* 1981, **49**, 185-197.
68. S. Sawada, S. Normura, *Journal of the Physical Society of Japan*, 1958, 13, 1594.

69. NBS-ICTA standard reference material. Online, https://www-s.nist.gov/srmors/certificates/archive/758.pdf (accessed September 2015)
70. D. Vorlander, E. Kaascht, *Berichte der Deutschen Chemischen Gesellschaft (A and B series)*, 1923, **56**, 1157-1162.
71. M.M. Markowitz, D.A. Boryta, R.F. Harris, *Journal of Physical Chemistry*, 1961, **65**, 261-263.
72. P. Garn, H.G. McAdie, O. Menis, *Selection of Differential Thermal Analysis Temperature Standards Through a Cooperative Study,* ed. L.M. Kushner, NBS Special Publication. 1972, SRM 758,759,760.
73. V.R. Pai Verneker, K. Rajeshwar, *Thermochimica Acta,* 1975, **13**, 293-304.
74. M. Shimokawabe, R. Furuichi, T. Ishii, *Thermochimica Acta,* 1977, **21**, 273-284.
75. R. Furuichi, Y. Tsusaka, T. Ishii, T. Okutani, *Thermochimica Acta,* 1986, **97**, 295-302.
76. B. Berger, A.J. Brammer, E.L. Charsley, *Thermochimica Acta,* 1995, **269/270**, 639-648.
77. J-S. Lee, C-K. Hsu, *Thermochimica Acta,* 2001, **367-368**, 367-370.
78. K.J. Rao, G.V. Subba, C.N.R. Rao, *Transactions of the Faraday Society*, 1967, **63**, 1013-1022.
79. P. Skoglund, Å. Fransson, *Thermochimica Acta,* 1996, **276**, 27-39.
80. D.G. Archer, *Journal of Chemical and Engineering Data*, 2002, **47(2)**, 304-309.
81. G.W.H. Höhne, H.K. Cammenga, W. Eysel, E. Gmelin, W. Hemminger, *Thermochimica Acta*, 1990, **160(1)**, 1-12.
82. LGC Ltd., Certificate of Measurement LGC2404, LGC2406,and LGC2411 1997-2000.
83. E. Charrier, E.L. Charsley, P.G. Laye, H.M. Markham, B. Berger, T.T. Griffiths, *Thermochimica Acta,* 2006, **445**, 36-39.
84. E.L. Charsley, P.G.Laye, H.M. Markham, J.J. Rooney, B. Berger, T.T Griffiths, M.P. Wasko, Thermal Studies on Rubidium Dinitramide, in: 35th International Pyrotechnics Seminar, Fort Collins USA, 2008, 331.

85. P.C. P. Gabbot, T.Mann, P. Royall, S. Shergill, *Americal Laboratory,* 2003, **37**, 17-21.
86. C. McGregor, M.H. Saunders, G. Buckton, R.D, *Thermochimica Acta,* 2004, **417,** 231-237.
87. F.I. Dubovitskii, G.A. Volkov, V.N. Grebennikov, G.B. Manelis, G.M. Nazin, *Doklady Akademii Nauk,* 1996, **347(6),** 763-765.
88. F.I. Dubovitskii, G.A. Volkov, V.N. Grebennikov, G.B. Manelis, G.M. Nazin, *Doklady Akademii Nauk*, 1996, **348(2),** 205-206.
89. J.C. Oxley, J.L. Smith, W. Zheng, E. Rogers, M.D. Coburn, *Journal of Physical Chemistry A,* 1997, **101(31),** 5646-5652.
90. A.S. Tompa, R.F. Boswell, P. Skahan, C. Gotzmer, *Journal of Thermal Analysis*, 1997, **49(3),** 1161-1170.
91. M.D. Cliff, D.P. Edwards, M.W. Smith, Alkali metal dinitramides. Properties, thermal behaviour, and decomposition products. *International Annual Conference of ICT, 29th Energetic Materials.* 1998, **24**, 1-24.
92. J.R. Dawe, M.D. Cliff, Metal dinitramides: new novel oxidants for the preparation of boron based flare compositions. *International Pyrotechnics Seminar*, 1998, **24**, 789-810.
93. M.D. Cliff, M.W. Smith, *Journal of Energetic Materials*, 1999, **17(1),** 69-86.
94. M. Lei, Z.Z. Zhang, Y.H. Kong, Z.R. Liu, C.H. Zhu, Y.H. Shao, P. Zhang, *Thermochimica Acta*, 1999, **335(1-2),** 105-112.
95. M. Lei, Y.H. Kong, Z.R. Liu, C.M. Yin, B.Z. Wang, Y. Wang, P. Zhang, *Thermochimica Acta,* 1999, **335(1-2),** 113-120.
96. M.D. Cliff, M.W. Smith, D.P. Edwards, *Propellants, Explosives, Pyrotechnics*, 1999, **24(1),** 43-45.
97. C. Yin, Z. Liu, Y. Kong, F. Zhao, Y. Wang, M. Lei,Y. Luo, P. Zhang, Y. Shao, S. Li, *Progress in Astronautics and Aeronautics,* 2000, **185,** 425-437.
98. E.L. Charsley , P.G. Laye, H.M. Markham, J.J. Rooney, B. Berger, P. Folly, R.P. Claridge, T.T. Griffiths, Thermal studies on potassium dinitramide in the liquid state. *ICT 32nd International Pyrotechnic Seminar, Karlsrueh,* 2005, 34.

99. S.B. Babkin, A.N. Pavlov, G.M. Nazin,*Russian Chemical Bulletin,* 1997, **46(11),** 1844-1847.
100. B. Berger, H. Bircher, M. Studer, M. Wälchli, *Propellants, Explosives, Pyrotechnics,* 2005, **30** 184-190.

Appendix 2. Published Work

During the programme of work a number of paper have been submitted and published in Thermochimica Acta, an international journal which has an impact factor of 2.184. The publications are as follows and full texts are included:

a) E.L. Charsley, P.G. Laye, H.M. Markham, J.O. Hill, B. Berger, T.T. Griffiths. "Determination of the equilibrium temperatures and enthalpies of the solid-solid transitions of rubidium nitrate by differential scanning calorimetry" Published in Thermochimica Acta 2008, 469(1-2) pages 65-70.

b) E.L. Charsley, P.G. Laye, H.M. Markham, T. Le Goff. "Calibration of differential scanning calorimeters: A comparison between indium and diphenylacetic acid" Published in Thermochimica Acta 2010, 497(1-2) pages 72-76.

c) E.L. Charsley, P.G. Laye, H.M. Markham. "The use of organic calibration standards in the enthalpy calibration of differential scanning calorimeters" Published in Thermochimica Acta 2012, 539 pages 115-117.

Available online at www.sciencedirect.com
ScienceDirect
Thermochimica Acta 469 (2008) 65–70
thermochimica acta
www.elsevier.com/locate/tca

Determination of the equilibrium temperatures and enthalpies of the solid–solid transitions of rubidium nitrate by differential scanning calorimetry

E.L. Charsley [a,*], P.G. Laye [a], H.M. Markham [a], J.O. Hill [b], B. Berger [c], T.T. Griffiths [d]

[a] *Centre for Thermal Studies, University of Huddersfield, Queensgate, Huddersfield HD1 3DH, UK*
[b] *Department of Chemistry, La Trobe University, Bundoora, Victoria 3086, Australia*
[c] *Armasuisse, Feuerwerkerstrasse 39, CH-Thun 2, Switzerland*
[d] *QinetiQ Ltd., Fort Halstead, Sevenoaks, Kent TN14 7BP, UK*

Received 7 November 2007; accepted 21 December 2007
Available online 3 January 2008

Abstract

The equilibrium temperatures of the three solid–solid phase transitions of high purity rubidium nitrate have been measured accurately by stepwise heating and by the extrapolation to zero heating rate method. Mean values of $164.9 \pm 0.1\,^{\circ}C$ (transition 1), $222.2 \pm 0.5\,^{\circ}C$ (transition 2) and $284.0 \pm 0.1\,^{\circ}C$ (transition 3) were obtained using two different types of heat flux DSC instruments. The enthalpies of transitions 1 and 2 were determined using both heat flux and power compensated DSC instruments. The mean values were $3.83 \pm 0.02\,kJ\,mol^{-1}$ (transition 1) and $3.14 \pm 0.03\,kJ\,mol^{-1}$ (transition 2). For transition 3 the shape of the DSC curve prevented an unequivocal determination of the enthalpy. Values obtained using two alternative interpretations of the DSC peak shape are discussed in the text.
© 2007 Elsevier B.V. All rights reserved.

Keywords: Rubidium nitrate; DSC; Transition; Temperature; Enthalpy

1. Introduction

Rubidium nitrate exhibits three reversible solid–solid phase transitions prior to fusion, which takes place at about 310 °C. These are:

- Transition 1 (160–166 °C): trigonal to CsCl (cubic)
- Transition 2 (219–228 °C): CsCl (cubic) to rhombohedral
- Transition 3 (278–291 °C): rhombohedral to NaCl (cubic)

The temperatures shown in brackets represent the ranges of the literature values [1–9]. These are listed in Table 1 and show that even in the most recent publications there are discrepancies of several degrees between the reported temperatures. The reason for the poor agreement is uncertain. $RbNO_3$ is reported to be stable to temperatures well above the transition temperatures and although thermal history was found to influence the temperature of transition 2, transitions 1 and 3 were reported to be free from such effects [10]. In view of the discrepancies in the literature values we have determined accurate values for the equilibrium transition temperatures by means of DSC. In addition, we have measured the enthalpies of the transitions. Previous enthalpy measurements are rather few in number and are summarised in Table 2 [3,4,6,8,11,12].

There are two possible approaches to the accurate measurement of equilibrium temperatures of melting or solid-state transitions by DSC. In one, the extrapolated onset temperature of the peak (T_e) is measured at a number of heating rates (typically from 1 to $10\,^{\circ}C\,min^{-1}$) and the equilibrium temperature is obtained by extrapolating the results to zero heating rate [13]. In the other approach the equilibrium temperature is obtained from the final step of a stepwise heating programme in which the temperature is raised in small increments (0.1 or 0.05 °C) with isothermal periods between the increments. In this method the melting or transition takes place under near-equilibrium conditions

* Corresponding author. Tel.: +44 1484 473178; fax: +44 1484 473179.
E-mail address: e.l.charsley@hud.ac.uk (E.L. Charsley).

0040-6031/$ – see front matter © 2007 Elsevier B.V. All rights reserved.
doi:10.1016/j.tca.2007.12.008

Table 1
Literature values for the temperature of the solid–solid phase transitions of rubidium nitrate

First author	Year	Temperature (°C)			Reference	Method
		Transition 1	Transition 2	Transition 3		
Rostkowski	1930	166	229	–	1	Heating curve
Plyushchev	1956	164	219	291	2	Heating curve
Mustajoki	1958	160	218	281	3	Calorimetry
Arell	1961	164.4	219.2–220.7	–	4	Calorimetry
Brown	1962	160	220	290	5	Microscopy
Rao	1966	166	228	278	6	DTA
Protsenko	1973	164	220	285	7	DTA
Secco	1999	166	222	285	8	DSC
Hichri	2002	164	227	282	9	DSC

[14]. The procedure is similar to that adopted in adiabatic calorimetry and is easy to implement using modern DSC equipment.

A study of organic melting point temperature standards established that the melting temperatures obtained by the extrapolation to zero heating rate method corresponded to the near-equilibrium values [15]. Both methods were applied to the measurement of the equilibrium temperature of the solid-state transition of $CsNO_3$ and identical values were achieved [16].

For enthalpy determinations the conventional approach is to measure the area enclosed by the transition peak and a linear baseline. However, delineation of the base line becomes less straightforward when contributions from changes in heat capacity become significant. Richardson [14] has commented on the changes in heat capacity that accompany the transitions in $RbNO_3$. These are both positive (transition 1) and negative (transitions 2 and 3). Various DSC base line constructions have been discussed by Hemminger and Sarge [17]. The DSC software supplied by the instrument manufacturers has a number of constructions with the aim of eliminating the effect of the change in heat capacity on the measured transition enthalpy.

We have adopted the approach recommended by Richardson [14] in which the overall enthalpy change ΔH is expressed in terms of the isothermal enthalpy change at an assigned temperature $\Delta H(T)$ and contributions from the initial and final heat capacities where $\Delta H(T) = \Delta H - C_i(T - T_1) - C_f(T_2 - T)$. C_i and C_f are the initial and final heat capacities and T_1 and T_2 are the initial and final temperatures over which the area is to be calculated. In accordance with Richardson's recommendation the thermal analysis curves should be plotted with heat capacity and temperature as the ordinate and abscissa, respectively. In common with other base line constructions this procedure is not without difficulty in assigning the temperatures T_1 and T_2. However, in principle the procedure leads to thermodynamically valid enthalpies of transition.

2. Experimental

The rubidium nitrate (Alfa Aesar) used in these studies had a purity of 99.975% and was crushed with a pestle and mortar and dried at 105 °C before use. The calibration materials (LGC Limited) were high purity samples (99.995%) of indium, tin and lead. The certified values for both the equilibrium temperature and enthalpy of melting of these materials, which were obtained using adiabatic calorimetry, are shown in Table 3.

The temperature determinations were carried out using a Mettler Toledo 822^e heat flux DSC (operated with the 'tau lag' correction disabled) and a TA Instrument 2920 heat flux DSC. The Mettler Toledo DSC was also used for the enthalpy measurements together with a PerkinElmer Diamond power compensated DSC.

The DSC instruments were calibrated for temperature using the stepwise heating method with temperature increments of 0.05 °C and either 10 or 20 min isothermal periods between the increments. The measurements were performed on 5 mg samples in non-hermetically sealed aluminium crucibles. The temperature of melting of the metals was normally found to be reproducible to within a single temperature step.

The enthalpy calibration was carried out using a sample mass of 10 mg and a heating rate of 3 °C min^{-1}. For both the tem-

Table 2
Literature values for the enthalpies of the solid–solid phase transitions of rubidium nitrate

First author	Year	Enthalpy (kJ mol^{-1})			Reference	Method
		Transition 1	Transition 2	Transition 3		
Mustajoki	1958	3.90	3.21	0.96	3	Calorimetry
Arell	1961	3.86	3.24	–	4	Calorimetry
Rao	1966	3.97	2.72	1.26	6	DTA
Höhne	1983	3.82	3.15	1.37	11	DSC*
Höhne	1985	3.82	3.13	1.27	12	DSC‡
Secco	1999	4.00	3.29	1.47	8	DSC

* Unweigted mean from 2 instruments.
‡ Unweigted mean from round-robin study. Value for Transition 3 obtained using linear baseline.

Table 3
LGC limited temperature/enthalpy standards

Material	Reference number	Melting temperature (°C)	Enthalpy of fusion (kJ mol^{-1})
Indium	LGC 2601	156.61 ± 0.02	3.296 ± 0.009
Tin	LGC 2609	231.92 ± 0.02	7.187 ± 0.011
Lead	LGC 2608	327.47 ± 0.02	4.765 ± 0.012

perature and enthalpy calibration using lead the crucibles were pre-oxidised by heating in air at 550 °C for 2 h to minimise reaction between the sample and crucible.

The stepwise temperature and enthalpy measurements on rubidium nitrate were carried out under the same conditions as for the calibration materials. The measurements were made in triplicate using a new sample for each determination. The extrapolation to zero heating rate measurements were performed over the range 1–10 °C min^{-1} and a new sample was used at each heating rate.

The atmosphere used for the experiments was argon (80 cm^3 min^{-1}). Regular performance checks were carried out during the programme of work to ensure consistency in the results.

The calibration factors for temperature and enthalpy at the transition temperatures were obtained by linear interpolation between the values measured at the melting temperatures of the reference materials. In applying Richardson's method for the determination of enthalpies of transition of rubidium nitrate we have adopted a linear temperature extrapolation of the initial and final heat capacities. The assigned temperature was the measured equilibrium transition temperature. A small correction for thermal lag was incorporated into the calculations. The heat capacity ordinate was calculated from the instrument signal and the measured heating rate. The variation of the enthalpy calibration factor across the temperature breadth of the peaks was <0.2%.

3. Results and discussion

3.1. Determination of equilibrium transition temperatures

A DSC curve for rubidium nitrate obtained at a heating rate of 10 °C min^{-1} shows three sharp peaks for the solid–solid transitions (Fig. 1). The influence of heating rate on the peak for transition 1 is shown in Fig. 2. It can be seen that the peak is well-defined over the range of heating rates studied. In contrast, the peak for transition 2 become less well-defined and increasingly noisy as the heating rate was reduced. This is exemplified in Fig. 3 which shows the peak obtained at a heating rate of 1 °C min^{-1}. The peaks for this transition were smoothed using the software supplied by the instrument manufacturers to facilitate the evaluation of T_e.

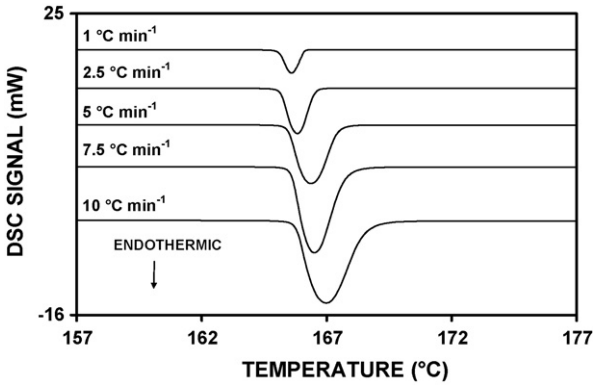

Fig. 2. Influence of heating rate on the DSC curves for transition 1 of rubidium nitrate (sample mass, 5 mg; atmosphere, argon).

Transition 3 appeared to give a well-defined peak. However, when plotted at higher sensitivity it became clear that there was a slow increase in the heat capacity C_p before the main peak, with small peaks superimposed at about 265 and 275 °C (Fig. 4). These peaks were observed in all our experiments and appeared to increase slightly in magnitude in repeated cycles of the sample through the transitions. Thermogravimetric measurements showed that they were not associated with a mass change. The significance of these superimposed peaks is not clear and they have been ignored in obtaining the enthalpy values.

The equilibrium transition temperatures obtained by extrapolating the values of T_e to zero heating rate are shown in Table 4. The uncertainties are the standard deviations and include the uncertainty in the calibration factor. The measurements for transition 1 and transition 3 showed excellent reproducibility and the values obtained using the two DSC instruments were in close

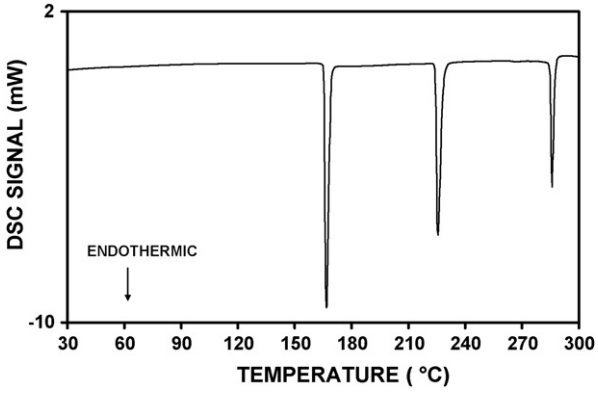

Fig. 1. DSC curve showing the solid–solid transitions of rubidium nitrate (sample mass, 5 mg; heating rate, 10 °C min^{-1}; atmosphere, argon).

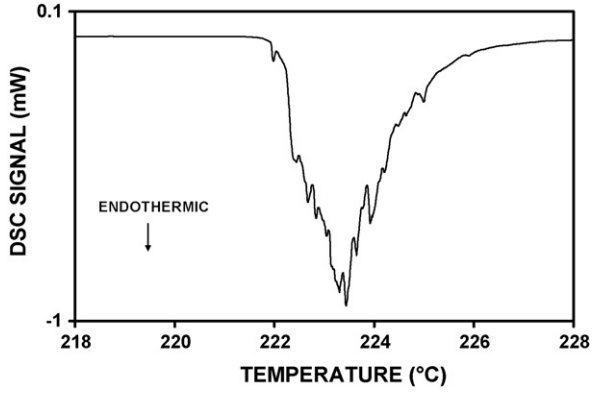

Fig. 3. DSC curve for transition 2 of rubidium nitrate (sample mass, 5 mg; heating rate, 1 °C min^{-1}; atmosphere, argon).

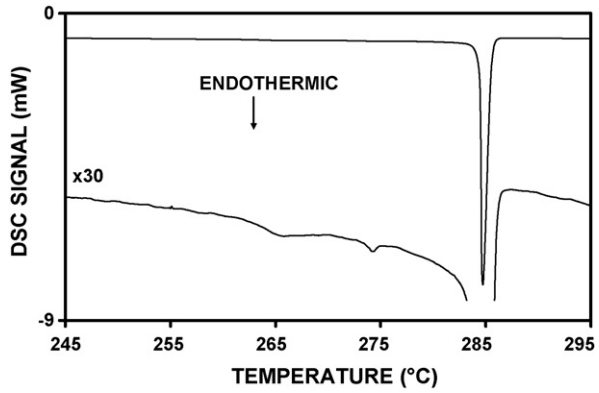

Fig. 4. DSC curve for transition 3 of rubidium nitrate (sample mass, 10 mg; heating rate 10 °C min^{-1}; atmosphere, argon).

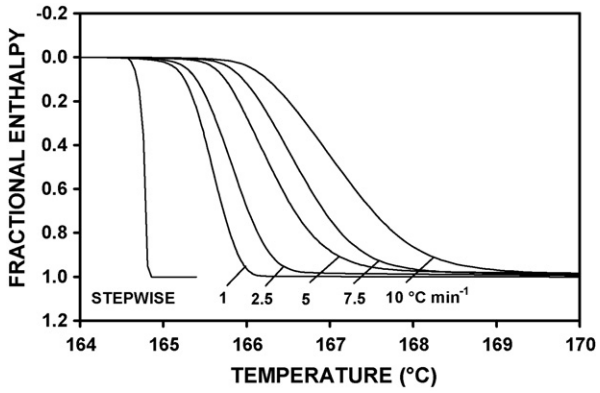

Fig. 6. Plot of fractional enthalpy against temperature for transition 1 of rubidium nitrate obtained under stepwise and linear heating conditions.

Table 4
Equilibrium temperature for the solid–solid phase transitions of rubidium nitrate obtained using the extrapolation to zero heating rate method

Instrument	Equilibrium temperature (°C)		
	Transition 1	Transition 2	Transition 3
Mettler DSC 822[e]	164.95 ± 0.05	221.7 ± 0.4	283.98 ± 0.04
TA DSC 2920	164.86 ± 0.03	222.7 ± 0.5	284.07 ± 0.07
Mean	164.91 ± 0.03	222.2 ± 0.5	284.03 ± 0.04

agreement. The mean values given in Table 4 are the weighted means with the corresponding uncertainties. The temperatures obtained for transition 2 showed greater variability, which is not unexpected in view of the difficulty in measuring T_e for this transition. In this case we have calculated the mean and assigned an error, which encompasses the results from the two instruments.

The gradients of the curves obtained by plotting T_e against the heating rate β for the three transitions showed large differences which were well outside the experimental uncertainties. The mean values of $dT_e/d\beta$ from the two instruments were 0.079 ± 0.003 min (transition 1); 0.27 ± 0.03 min (transition 2) and 0.11 ± 0.02 min (transition 3). These marked variations within a single compound illustrate the potential errors in calibration at a single heating rate when the calibrant and sample may have significantly different heating rate dependencies.

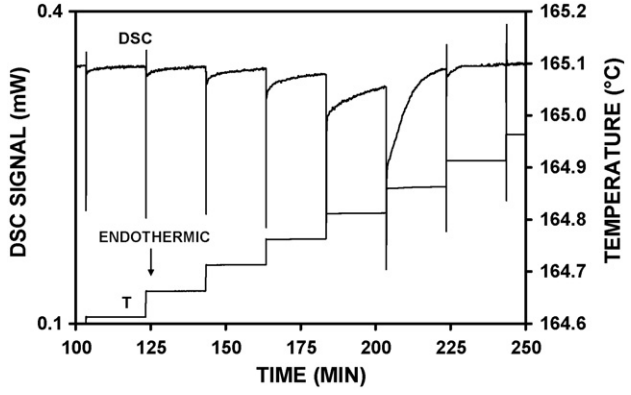

Fig. 5. DSC curve for transition 1 of rubidium nitrate obtained under stepwise heating conditions (sample mass, 5 mg; step size, 0.05 °C; atmosphere, argon).

The DSC curve from a typical stepwise experiment for transition 1 is shown in Fig. 5. Plotting the incremental enthalpy against temperature enabled a direct comparison to be made between results from the stepwise and the linear heating rate methods. This is illustrated in Fig. 6 and demonstrates the very narrow temperature range over which the transition takes place under stepwise heating conditions compared with heating under linear conditions. The temperatures obtained for transitions 1 and 3 are summarised in Table 5. The results for the two instruments were in agreement and the overall uncertainty exemplifies the excellent reproducibility that can be obtained using this technique. It was not possible to measure transition 2 using the stepwise technique because the DSC curves were too diffuse and noisy.

The results for transitions 1 and 3 in Tables 4 and 5 clearly show the close agreement between the temperatures obtained by the two experimental approaches. This provides further confirmation that the extrapolated onset temperature at zero heating rate corresponds to the temperature at near-equilibrium conditions. The overall values from the two approaches are 164.9 ± 0.1 °C (transition 1) and 284.0 ± 0.1 °C (transition 3) where the uncertainties have been rounded to a single decimal place. For transition 2 we have the value 222.2 ± 0.5 °C from the extrapolation to zero heating rate method.

Our temperatures for transitions 1 and 3 fall between the values reported by Secco and Secco [8] and Hichri et al. [9] which are also based on measurements by DSC. These authors claim uncertainties of ±2 and ±1 °C, respectively in their temperature measurements. Our results show a 10-fold improvement in precision with values that can be traced to the certified reference

Table 5
Equilibrium temperature for the solid–solid phase transitions of rubidium nitrate obtained using the isothermal stepwise heating DSC method

Instrument	Equilibrium temperature (°C)	
	Transition 1	Transition 3
Mettler DSC 822[e]	164.90 ± 0.03	283.79 ± 0.03
TA DSC 2920	165.02 ± 0.04	283.84 ± 0.04
Mean	164.96 ± 0.03	283.82 ± 0.03

temperatures and unlike the previous DSC measurements our values relate to thermodynamic equilibrium. For comparative purposes we have used our heating rate coefficients to adjust our values to correspond to the heating rates used in the previous measurements. At the heating rate of 10 °C min^{-1} used by Secco and Secco [8] our values become 165.7 °C (transition 1), 224.9 °C (transition 2) and 285.1 °C (transition 3). The agreement between the values of Secco and Secco and our calculated values is particularly striking for transitions 1 and 3.

The temperatures obtained by Mustajoki [3] are of obvious interest since they originate from calorimetric measurements of heat capacity as a function of temperature. The result for transition 1 is in marked contrast to that obtained by the other authors with the exception of Brown and McLaren [5] who claimed only that their value was about 160 °C. The value of 164.4 °C obtained by Arell and Varteva [4] by differential calorimetry, using a heating/cooling method, is close to that of the present work.

3.2. Determination of transition enthalpies

Table 6 shows our results for the transition enthalpies measured using the approach adopted by Richardson [14]. There was no significant difference between the results from the Mettler Toledo and PerkinElmer instruments which is of particular interest in view of their different operating principles.

For transitions 1 and 2 there is broad agreement between the published values and those obtained in the present work, with the exception of the result of Rao and Rao [6] for transition 2. As previously mentioned we have assumed a linear dependence of heat capacity on temperature. However, any errors are likely to be small since the sharpness of the peaks for transitions 1 and 2 limits the extent of the heat capacity extrapolations. We have included in the uncertainty an estimate of the sensitivity of the results to the assignment of temperatures T_1 and T_2. The uncertainty in our results is about 1% which is similar to that given by Mustajoki [3], Arell and Vateva [4] and Höhne et al [11] (1–1.5%). The uncertainty reported by Secco and Secco [8] was slightly greater (3%).

The accuracy of the measurement of the enthalpy of transition 3 is reduced by the slow increase in C_p heat capacity before the main peak which introduces considerable uncertainty in the assignment of T_1. The presence of pre-transition C_p curvature is not without parallel in other systems [14]. In the present work the initial temperature T_1 has been assigned to a temperature before the onset of the C_p curvature. A further cause of uncertainty is in the assignment of T_2 due to the lack of a well-defined linear baseline following the transition peak. By using a treatment common to all the curves we have obtained results reproducible to about 3%. The values shown in Table 6 exclude the contribution from the small superimposed peaks (∼0.03 kJ mol^{-1})

Table 6
Enthalpy values for the solid–solid phase transitions of rubidium nitrate

Instrument	Enthalpy (kJ mol^{-1})		
	Transition 1	Transition 2	Transition 3
Mettler DSC 822[e]	3.83 ± 0.04	3.15 ± 0.04	1.74 ± 0.06[a]
PerkinElmer Diamond	3.82 ± 0.02	3.13 ± 0.05	1.72 ± 0.06[a]
Mean	3.83 ± 0.02	3.14 ± 0.03	1.73 ± 0.04[a]

[a] These values were obtained by assigning T_1 to a temperature before the onset of C_p curvature (see text).

The presence of a systematic error in our results cannot be ruled out. If we set T_1 to a temperature following the superimposed peaks we obtain an enthalpy of transition of 1.56 ± 0.03 kJ mol^{-1} which is closer to the value of 1.47 kJ mol^{-1} obtained by Secco and Secco [8]. We have no explanation for the very low value reported by Mustajoki [3].

The point has been already been made that the aim in using Richardson's method for enthalpy measurements is to obtain values which have thermodynamic validity. Thus our enthalpies of transition are determined at the equilibrium transition temperatures. It is of interest to compare these values with those obtained using commercial software. We obtained mean values of 3.83 ± 0.02 kJ mol^{-1} (transition 1), 3.12 ± 0.02 kJ mol^{-1} (transition 2) and 1.73 ± 0.03 kJ mol^{-1} (transition 3) using Mettler Toledo 'integral tangential' software and PerkinElmer 'sigmoidal' base line constructions. These values are based on iterative procedures in which the initial and final temperatures are assigned and are virtually the same as those obtained using Richardson's method. However, the use of a conventional straight base line construction would lead to a significant difference in the results for transitions 1 and 3 which would be outside the errors in the present results.

4. Conclusions

Accurate values for the equilibrium temperatures of the three solid–solid phase transitions in high purity rubidium nitrate have been measured by two different experimental methods using two different types of heat flux DSC instruments. Transitions 1 and 3 showed good reproducibility and gave overall mean values of 164.9 ± 0.1 and 283.9 ± 0.1 °C, respectively. These values show a significant improvement in precision over those published previously. The DSC peak for transition 2 was less well-defined at lower heating rates and the equilibrium temperature could not be measured using the stepwise technique. A value of 222.2 ± 0.5 °C was obtained by extrapolating T_e to zero heating rate measurements.

The enthalpies of the transitions have been measured at the equilibrium temperatures using both heat flux and power compensation DSC instruments. For transitions 1 and 2 there was good agreement for the two sets of results and mean values of 3.83 ± 0.02 and 3.14 ± 0.03 kJ mol^{-1}, respectively were obtained. For transition 3 there is considerable uncertainty in the results because of the slow increase in the heat capacity before the main transition peak. When the pre-transition region (excluding the small superimposed peaks) is included we obtained the value 1.73 ± 0.04 kJ mol^{-1}, whereas if this region is excluded a value of 1.56 ± 0.03 kJ mol^{-1} is obtained. Similar results were given for the enthalpies of the three transitions using the dedicated software supplied by the instrument manufacturers.

Acknowledgement

We should like to thank James Rooney of the Centre for Thermal Studies for his skilled technical assistance. This work was supported by WPE as part of an MOD Research Programme under a Technical Arrangement between the UK and Switzerland.

References

[1] A.P. Rostowski, J. Phys. Chem. Soc. Russ. 62 (1930) 2067.
[2] V.E. Plyushchev, I.B. Markina, L.P. Shklover, Zhur. Neorg. Khimii. 1 (1956) 1613.
[3] A. Mustajoki, Ann. Acad. Sci. Fenn A 6 (9) (1958) 3.
[4] A. Arell, M. Varteva, Ann. Acad. Sci. Fenn A VI (58) (1961) 1.
[5] R.N. Brown, A.C. McLaren, Acta Cryst. 15 (1962) 974.
[6] K.J. Rao, C.N.R. Rao, J. Mater. Sci. 1 (1966) 238.
[7] P.I. Protsenko, L.S. Grin'ko, L.N. Venerovskaya, V.A. Lyutsedarskii, Russ. J. Appl. Chem. 46 (1973) 2568.
[8] E.A. Secco, R.A. Secco, Phys. Chem. Chem. Phys. 1 (1999) 5011.
[9] M. Hichri, C. Favotto, H. Zamali, Y. Feutelais, B. Legendre, A. Sebaoun, M. Jemal, J. Therm. Anal. Calorim. 69 (2002) 509.
[10] E.L. Charsley, J.P. Davies, E. Glöggler, N. Hawkins, G.W.H. Höhne, T. Lever, K. Peters, M.J. Richardson, I. Rothemund, A. Stegmayer, J. Therm. Anal. 40 (1993) 1405.
[11] G.W.H. Höhne, K.-H. Breuer, W. Eysel, Thermochim. Acta 69 (1983) 145.
[12] G.W.H. Höhne, W. Eysel, K.-H. Breuer, Thermochim. Acta 94 (1985) 199.
[13] G.W.H. Höhne, H.K. Cammenga, W. Eysel, E. Gmelin, W. Hemminger, Thermochim. Acta 160 (1990) 1.
[14] M.J. Richardson, Thermochim. Acta 300 (1997) 15.
[15] E.L. Charsley, P.G. Laye, V. Palakollu, J.J. Rooney, B. Joseph, Thermochim. Acta 446 (2006) 29.
[16] E. Charrier, E.L. Charsley, P.G. Laye, H.M. Markham, B. Berger, T.T. Griffiths, Thermochim. Acta 445 (2006) 36.
[17] W. Hemminger, S.M. Sarge, J. Therm. Anal. 37 (1991) 1455.

Thermochimica Acta 497 (2010) 72–76

Contents lists available at ScienceDirect

Thermochimica Acta

journal homepage: www.elsevier.com/locate/tca

Calibration of differential scanning calorimeters: A comparison between indium and diphenylacetic acid

E.L. Charsley[a,*], P.G. Laye[a], H.M. Markham[a], T. Le Goff[b]

[a] Centre for Thermal Studies, University of Huddersfield, Queensgate, Huddersfield HD1 3DH, UK
[b] LGC Limited, Queens Road, Teddington, Middlesex TW11 OLY, UK

ARTICLE INFO

Article history:
Received 28 June 2009
Received in revised form 14 August 2009
Accepted 21 August 2009
Available online 31 August 2009

Keywords:
DSC
Calibration
Indium
Diphenylacetic acid

ABSTRACT

The close proximity in melting temperature of the LGC Limited DSC standards indium and diphenylacetic acid, has enabled a direct assessment to be made of any differences resulting from the use of a metal or an organic compound in the calibration of DSC equipment. Following calibration with indium, the equilibrium fusion temperatures for diphenylacetic acid, were determined by both the stepwise heating and extrapolation to zero heating rate methods. The results were in excellent agreement with the certificate values and established that indium may be used as a calibrant when making accurate DSC measurements on organic materials in the same temperature range and that it has the advantage that it is non-volatile and can be used a number of times without significant change. Similar agreement was obtained in the measurement of the enthalpy of fusion, although the larger heat capacity change on fusion of diphenylacetic acid resulted in a greater uncertainty than with indium.

© 2009 Elsevier B.V. All rights reserved.

1. Introduction

Calibration is at the heart of quantitative measurements by differential scanning calorimetry. Its purpose is to link the temperature and enthalpy (or heat flow) measurements to their 'true' values. In view of its crucial importance it is hardly surprising that there have been many publications dealing with the methodology of calibration and the choice of calibrants. Comprehensive discussions include those by Höhne et al. [1], Richardson and Charsley [2] and Della Gatta et al. [3].

There are two approaches to the accurate measurement of equilibrium temperatures of fusion by DSC. The method proposed by Höhne et al. [4] utilises the differential scanning calorimeter in its conventional dynamic mode and derives the equilibrium temperature by measuring the extrapolated onset temperature of the fusion peak over a range of heating rates and extrapolating the results to zero heating rate. An alternative method advocated by Richardson [5] uses stepwise heating through the fusion peak with isothermal periods between the steps. In this method the melting takes place under near-equilibrium conditions and the equilibrium fusion temperature is identified with the temperature of the final step. In a previous study of organic melting point temperature standards we established that the melting temperatures obtained by the extrapolation to zero heating rate method corresponded to the near-equilibrium values [6].

In principle, the measurement of enthalpy of fusion is more straightforward than that of temperature. The enthalpy is obtained from the peak area with results which should be independent of the heating rate. In practice, complications may arise: Richardson and Charsley [2] have pointed out that the area of the fusion peak extends over a temperature range and will contain contributions from both the enthalpy of fusion and the change in heat capacity. For metals the change in heat capacity is negligible but for the fusion of organic compounds it may become significant when making measurements of the highest accuracy. The elimination of the heat capacity component has been discussed in connection with the enthalpies of transition of rubidium nitrate [7].

The most frequently used DSC calibrants are metals with melting temperatures and enthalpies measured by adiabatic calorimetry under near-equilibrium conditions: indium is often the chosen calibrant. However, reference has been made to the desirability of calibrating equipment using substances that have the similar thermal properties to the compound to be investigated [8]. Price [9] has reported a different trend between temperature calibrations carried out with metals and organic compounds.

LGC Limited offers a range of organic and metal DSC standards whose temperatures and enthalpies of fusion have been determined by adiabatic calorimetry [10]. The close proximity in temperature of the standards indium (156.61 °C) and diphenylacetic acid (147.19 °C) provides the opportunity of making a direct assessment of any differences resulting from the use of a metal or an organic in the calibration of a DSC for temperature and enthalpy.

We have therefore carried out an accurate comparison of the equilibrium temperatures and the enthalpies of fusion of the two

* Corresponding author. Tel.: +44 01484 473178; fax: +44 01484 473179.
E-mail address: e.l.charsley@hud.ac.uk (E.L. Charsley).

0040-6031/$ – see front matter © 2009 Elsevier B.V. All rights reserved.
doi:10.1016/j.tca.2009.08.010

materials. The temperatures have been measured using both the extrapolation to zero heating rate and stepwise heating methods. The enthalpy of fusion at the equilibrium temperature has been determined by making allowance for the change in heat capacity using a procedure similar to that recommended by Richardson [11].

In addition, the influence of the form of the indium on both the temperature and enthalpy measurements has been investigated by comparing the results obtained from the LGC sample, which was supplied as small pellets, with those from high purity indium powder. The advisability of pre-melting indium samples before carrying out calibration measurements has also been assessed. The purpose of pre-melting is to improve the reliability of subsequent measurements by bringing about better thermal contact between the sample and the crucible. Metal calibrants are frequently pre-melted before use, but with many samples pre-melting is not an option.

2. Experimental

Indium was supplied by LGC Limited (LCC2601) and was in the form of 'tear-drop' shaped pellets 2–3 mm in diameter. It had a certified equilibrium fusion temperature of 156.61 ± 0.02 °C and an enthalpy of fusion of 3.296 ± 0.009 kJ mol^{-1} (28.71 ± 0.08 J g^{-1}). Indium powder was obtained from Alfa Aesar (Puratronic, 99.999% purity). In the present paper we will refer to the two samples of indium as 'LGC' and 'powder' respectively. Diphenylacetic acid (LCC2607) had a certified equilibrium fusion temperature of 147.19 ± 0.03 °C and an enthalpy of fusion of 31.16 ± 0.13 kJ mol^{-1} (146.8 ± 0.6 J g^{-1}).[1]

The volatility of the diphenylacetic acid was assessed by thermogravimetry using a Mettler TG 851 apparatus. The sample (2.5 mg) was contained in an open 20 μl aluminium crucible and heated at 10 °C min^{-1}. The measured mass loss at the onset of melting was about 3%. In view of this mass loss all subsequent DSC experiments were carried out with samples in encapsulated crucibles. Since the purpose of the present work was a comparison between indium and diphenylacetic acid the same procedure was adopted for indium. No mass loss was detected in the DSC experiments.

Temperature measurements were carried out using the Mettler DSC 822^e with the 'tau lag' disabled. The measurements were made using 2.5 mg of the diphenylacetic acid and 10 mg of the LGC and powdered indium in Mettler 40 μl aluminium crucibles. An atmosphere of nitrogen was maintained in the apparatus (80 cm^3 min^{-1}). Considerable care was taken to ensure good thermal contact between the sample and the crucible. For LGC indium a thin section of the pellet was pressed flat between glass plates and then pressed into the crucible. The indium powder and diphenylacetic acid were evenly distributed in the crucible. Diphenylacetic acid was lightly crushed before use.

The extrapolated onset temperature measurements were performed at five different heating rates within the range 1–10 °C min^{-1} and a new sample was used at each heating rate. The stepwise heating experiments were made with 0.05 °C temperature steps and 10–20 min isothermal periods between the steps. The fusion temperature was identified with the temperature of the final step of the fusion process. The measurements were made in triplicate with a new sample for each experiment unless indicated otherwise.

The enthalpy measurements were performed using a PerkinElmer Diamond DSC. The samples were contained in TA Instruments low mass Tzero aluminium crucibles. The heating rate was 3 °C min^{-1} and an atmosphere of nitrogen was maintained in the apparatus (20 cm^3 min^{-1}). The sample masses were the same as those used in the temperature measurements and the same care was taken to ensure good thermal contact between the sample and crucible. A new sample was used for each experiment unless indicated otherwise. The greater mass of indium used in these experiments compared to that of diphenylacetic acid was in recognition of its considerably smaller enthalpy of fusion. The uncertainties associated with the present measurements are single standard deviations unless otherwise stated.

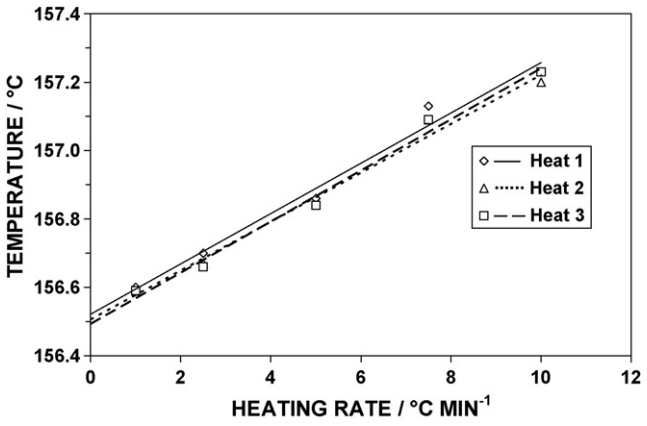

Fig. 1. Plot of extrapolated onset temperature against heating rate for LGC indium (sample mass, 10 mg; atmosphere, nitrogen).

3. Symbols

T_e represents the experimental extrapolated onset temperature. Unless otherwise stated all other temperatures are equilibrium values. $T_{\beta=0}$ and T_{step} are the experimental values obtained from the extrapolated onset and stepwise heating methods respectively. $\Delta_{fus}H$ is the experimental enthalpy of fusion at the melting temperature. β is the heating rate (°C min^{-1}).

4. Results and discussion

4.1. Equilibrium temperature measurements

The results of the extrapolation to zero heating rate experiments on LGC indium are plotted in Fig. 1. Each of the 5 samples studied was heated 3 times through the fusion peak in order to enable an accurate assessment to be made of the effect of pre-heating. An excellent linear correlation was found between T_e and the heating rate. The values for $T_{\beta=0}$ and the slopes of the lines are given in Table 1.

The agreement between the initial and subsequent fusion experiments within the limits of experimental error show that it is possible to make temperature measurements using indium to a

Table 1
Equilibrium temperature of fusion of LGC indium measured by the extrapolation to zero heating rate method.

Experiment	$T_{\beta=0}$/°C	$(dT_e/d\beta)$/min
First heating	156.52 ± 0.03	0.074 ± 0.006
Second heating	156.51 ± 0.03	0.072 ± 0.005
Third heating	156.49 ± 0.03	0.075 ± 0.004
Mean value	156.51 ± 0.02	0.074 ± 0.003
Certified value	156.61 ± 0.01[a]	–
Calibration correction	0.10 ± 0.02	–

[a] Single standard deviation.

[1] The uncertainties associated with the certified values for indium and quoted on the certificate provide a level of confidence of approximately 95%. For diphenylacetic acid the uncertainties are an estimate of the total uncertainty and take into account both random and systematic error.

Table 2
Equilibrium temperature of fusion of indium powder measured by the extrapolation to zero heating rate method.

Experiment	$T_{\beta=0}$/°C	$(dT_e/d\beta)$/min
First heating	156.50 ± 0.02	0.054 ± 0.003
Second heating	156.48 ± 0.02	0.053 ± 0.003
Third heating	156.47 ± 0.01	0.053 ± 0.002
Mean value	156.48 ± 0.01	0.053 ± 0.002

Table 3
Equilibrium temperature of fusion of LGC indium and indium powder measured by the stepwise heating method.

Experiment	LGC, T_{step}/°C	Powder, T_{step}/°C
First heating	156.52 ± 0.05	156.50 ± 0.03
Second heating	156.51 ± 0.05	156.52 ± 0.05
Mean value	156.52 ± 0.04	156.51 ± 0.03
Certified value	156.61 ± 0.01[a]	–
Calibration correction	0.09 ± 0.04	–

[a] Single standard deviation.

high degree of precision without recourse to pre-melting. However, it was found that if the indium sample was neither sufficiently thin nor firmly pressed flat into the crucible there was a significant decrease in the melting temperature from the first to second heating in the dynamic experiments. Therefore, where possible, pre-melting the sample would seem to be a sensible precaution.

Corresponding extrapolation to zero heating rate experiments were carried out on indium powder and the results are summarised in Table 2. It can be seen that the equilibrium fusion temperature is unchanged by melting and that the value agrees well with that obtained for the LGC sample. The magnitude of the gradients $dT_e/d\beta$ from the extrapolation to zero heating rate experiments for the powder is significantly smaller than those obtained for the LGC sample. Thermomicroscopy showed that the indium powder did not coalesce after fusion and retained its powdery nature. This accounts for the value of $dT_e/d\beta$ remaining unchanged on re-melting the sample rather than becoming similar to that of the LGC sample which was in the form of a single piece.

The results of the stepwise measurements on the LGC indium and indium powder are summarised in Table 3. An uncertainty corresponding to half the step height (0.025 °C) has been included in the results. The sharpness of the melting in stepwise heating is clear from the plot for LGC indium in Fig. 2 which shows the melting curve for the concluding temperature steps. Melting is seen to occur almost entirely over a single temperature step. The equilibrium temperatures for the two forms of indium are in excellent agreement and the values are unchanged by re-melting.

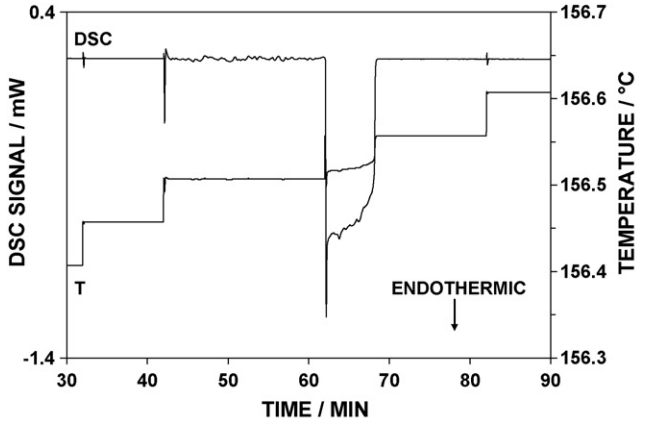

Fig. 2. DSC curve for LGC indium obtained under stepwise heating conditions (sample mass, 10 mg; step size, 0.05 °C; atmosphere, nitrogen).

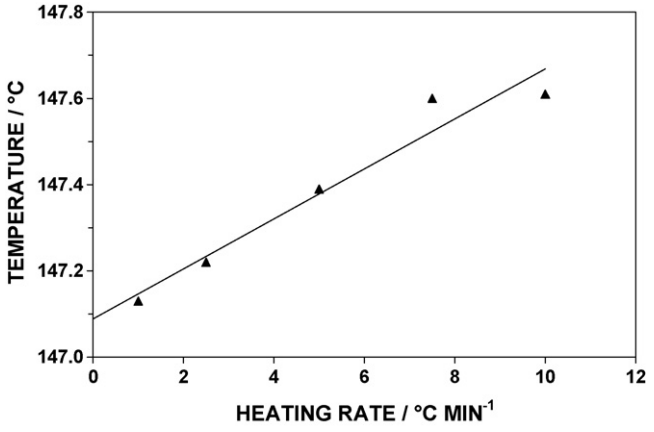

Fig. 3. Plot of extrapolated onset temperature against heating rate for LGC diphenylacetic acid (sample mass, 2.5 mg; atmosphere, nitrogen).

The agreement between the results for LGC indium and indium powder obtained by extrapolation to zero heating rate and stepwise heating clearly establishes the equality of the two methods for the determination of accurate equilibrium temperatures. This extends to a metal the agreement which was reported previously for organic melting point standards [6] and solid-solid phase transitions in rubidium and caesium nitrates [7,12]. The uncertainty in the results from the two methods is similar, although in the case of the stepwise heating it is dominated by the allowance made for the step height. This uncertainty can be reduced by decreasing the step height at the expense of more time consuming experiments.

The equilibrium fusion temperature of diphenylacetic acid was determined using the extrapolation to zero heating rate method. A new sample was used at each heating rate and was not re-heated in accordance with the recommendation in the certificate. The plot of T_e against heating rate is shown in Fig. 3 and the value for $T_{\beta=0}$ and the slope of the line are given in Table 4. The measured value was adjusted by applying the calibration correction obtained from the extrapolation to zero heating rate experiments on LGC indium (Table 1). A mean value of 147.19 ± 0.05 °C was given which is in excellent agreement with the certified value.

The value of the gradient $dT_e/d\beta$ of 0.058 ± 0.008 min obtained for diphenylacetic acid was smaller than that for LGC indium (0.074 ± 0.005 min) by an amount which exceeded the combined uncertainty. However, values of $dT_e/d\beta$ for both organic and inorganic compounds show considerable variation [4,8] and in some instances are greater than those for the metals. Our results for rubidium nitrate [7] show that even for the same compound the transitions between different crystal forms can lead to very different values of $dT_e/d\beta$.

The lack of consistency in the values of the gradient $dT_e/d\beta$ rules out experiments under dynamic conditions for the accurate measurement of temperatures unless it is known that the gradient has

Table 4
Determination of the equilibrium temperature of fusion of diphenylacetic acid by the extrapolation to zero heating rate and stepwise heating methods.

	$T_{\beta=0}$/°C	T_{step}/°C
Mean measured value	147.09 ± 0.05	147.08 ± 0.04
$(dT_e/d\beta)$/min	0.058 ± 0.008	–
Correction	0.10 ± 0.02	0.09 ± 0.03
Corrected value	147.19 ± 0.05	147.17 ± 0.04
Certified value	147.19 ± 0.03	147.19 ± 0.03

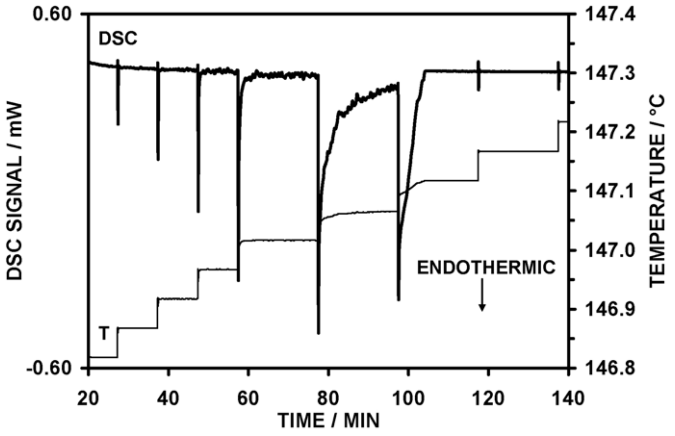

Fig. 4. DSC curve for LGC diphenylacetic acid obtained under stepwise heating conditions (sample mass, 2.5 mg; step size, 0.05 °C; atmosphere, nitrogen).

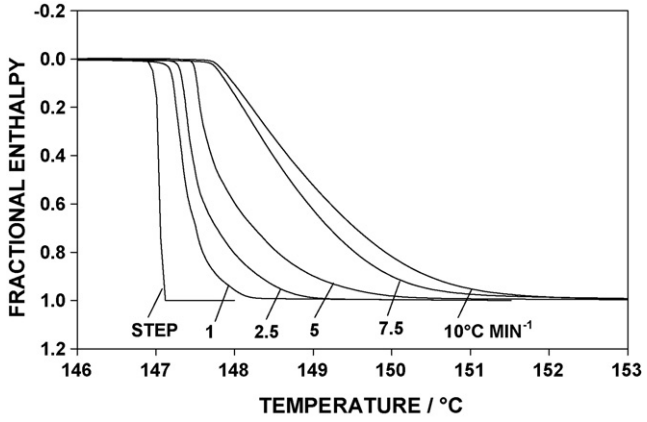

Fig. 5. Plot of fractional enthalpy against temperature for diphenylacetic acid obtained under stepwise and linear heating conditions (sample mass, 2.5 mg; atmosphere, nitrogen).

the same value for both the calibrant and the compound under investigation. The error, albeit generally small for modest heating rates, is proportional to the difference between the gradients for the calibrant and compound. Thus in the present case if the indium calibration had been made at 10 °C min^{-1} and the measurements on diphenylacetic acid made at the same heating rate, an error of ~0.2 °C would have resulted.

A typical DSC plot for the stepwise melting of diphenylacetic acid is shown in Fig. 4. The reduced temperature range of melting under stepwise heating is clearly evident in the incremental enthalpy plot in Fig. 5, where the stepwise and the linear heating rate DSC curves are compared. The equilibrium temperatures from the stepwise heating experiments on diphenylacetic acid are summarised in Table 4. The mean corrected value agrees with the certified value to within 0.02 °C, well within the uncertainties. This confirms the result obtained by the extrapolation to zero heating rate experiments and establishes the equivalence between a metal and an organic substance for DSC temperature calibration in a similar temperature range.

4.2. Enthalpy measurements

Typical DSC curves from the enthalpy measurements on LGC indium and indium powder are given in Fig. 6 and show the broader nature of the peaks for the powder sample. The determination of the enthalpy of fusion was simplified by the negligible heat capacity change on melting. The results in Table 5 were obtained using the

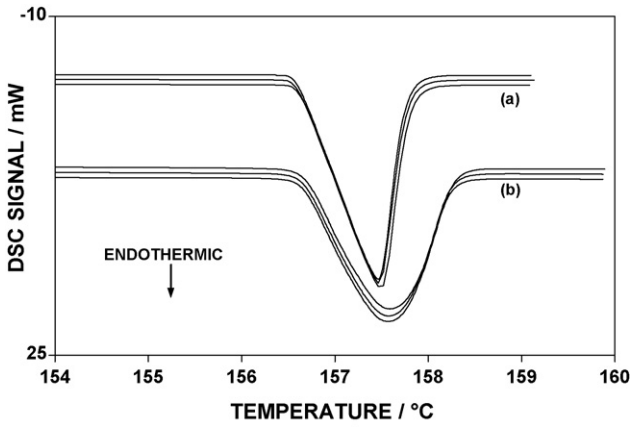

Fig. 6. DSC curves for (a) LGC indium and (b) indium powder showing effect of re-heating samples on the enthalpy of fusion (sample mass, 10 mg; heating rate, 10 °C min^{-1}; atmosphere, nitrogen).

Table 5
Measurements of the enthalpy of fusion of LGC indium and indium powder.

	LGC, $\Delta_{fus}H$/J g^{-1}	Powder, $\Delta_{fus}H$/J g^{-1}
First heating	28.71 ± 0.01	28.50 ± 0.06
Second heating	28.71 ± 0.03	28.49 ± 0.05
Third heating	28.72 ± 0.03	28.48 ± 0.05
Mean value	28.71 ± 0.02	28.49 ± 0.03
Certified value	28.71 ± 0.01[a]	–
Calibration factor	1.000 ± 0.002	–

[a] Single standard deviation.

PerkinElmer software and show excellent reproducibility. There was no change in the enthalpy on heating the samples for a second and third time. In a further series of experiments the LGC sample was cycled 20 times through its melting temperature at 10 °C min^{-1}. No change in enthalpy was observed.

There is a clear difference between the enthalpy results for the LGC and powder samples. The enthalpy of the indium powder is about 0.8% less than that of the LGC sample which is greater than the combined uncertainties in the results. The presence of an oxide coating on the powder seems a likely explanation for the discrepancy even though the sample used in the present work was from a previously unopened bottle. Such a coating might vary from one sample to another and with the length and conditions of storage. Therefore the use of indium powder, even of high purity, as a calibrant together with the assumption that the enthalpy of fusion is that of a solid sample may lead to a small systematic error in subsequent measurements.

The enthalpy of fusion of diphenylacetic acid was measured using LGC indium as the calibrant. The results from six determinations are summarised in Table 6. Melting occurred with a small but clearly discernable change in heat capacity and the enthalpy change was calculated by representing the temperature dependence of the initial and final capacities as linear (Fig. 7). The results were slightly dependent on the temperature range used

Table 6
Determination of the enthalpy of fusion of diphenylacetic acid.

	$\Delta_{fus}H$/J g^{-1}
Mean measured value	146.9 ± 0.3
Calibration factor	1.000 ± 0.002
Corrected value	146.9 ± 0.4
Certified value	146.8 ± 0.6

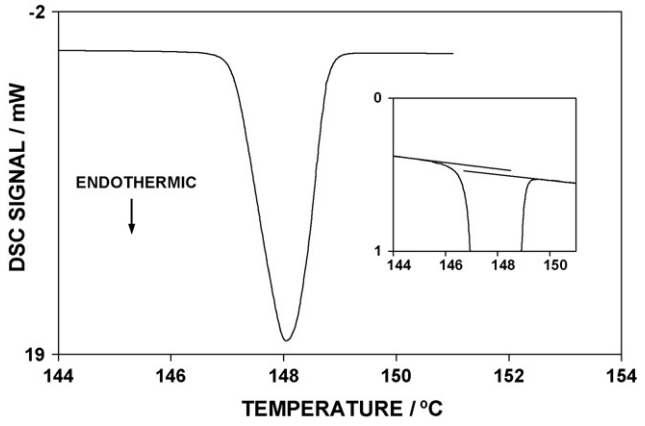

Fig. 7. DSC curves for LGC diphenylacetic acid showing heat capacity change on fusion (sample mass, 2.5 mg; heating rate, 10 °C min^{-1}; atmosphere, nitrogen).

in the calculations. Increasing the temperature range of by 0.5 and 1.0 °C changed the enthalpy value from $146.81 \pm 0.03\,J\,g^{-1}$ to 146.94 ± 0.13 and $147.01 \pm 0.10\,J\,g^{-1}$ respectively. The value in Table 6 ($146.9 \pm 0.3\,J\,g^{-1}$) is the mean value from the individual results together with an error that encompasses the range of the results. We have also used the PerkinElmer software for a sigmoidal baseline construction and obtained a value 0.2% greater than the present value.

The corrected enthalpy of fusion of diphenylacetic acid at the equilibrium temperature was found to be $146.9 \pm 0.4\,J\,g^{-1}$. This is in excellent agreement with the certified value of $146.8 \pm 0.6\,J\,g^{-1}$ and demonstrates that there is no significant difference in using a metal or an organic material for the enthalpic calibration of DSC equipment at similar temperatures.

5. Conclusions

The close proximity in temperature of the LGC Limited DSC standards indium and diphenylacetic acid, has enabled a direct assessment to be made of any differences resulting from the use of a metal or an organic substance in the calibration of DSC equipment. Following calibration with indium, the equilibrium fusion temperatures for diphenylacetic acid, measured by both the stepwise heating and extrapolation to zero heating rate methods, were found to be in excellent agreement with the certificate value. Although the enthalpy measurements with diphenylacetic acid showed a greater uncertainty than with indium, which arose from the larger heat capacity change on fusion, the results were also in agreement with the certified value.

These measurements clearly establish that indium may be used as a calibrant when making accurate DSC measurements on organic materials in the same temperature range. Indium has advantages in that it is non-volatile and as we have shown, can be re-melted at least 20 times without any significant change. However, measurements are often performed on samples at significantly lower temperatures than the melting point of indium and in these cases it may be advantageous to use one of the organic standards which melt in a similar temperature range. Work is at present in progress using these standards to assess the magnitude of the temperature dependence of the errors in temperature and enthalpy if only a single point calibration is performed using indium [13].

References

[1] G. Höhne, W. Hemminger, H.-J. Flammersheim, Differential Scanning Calorimetry, Springer-Verlag, Berlin/Heidelberg/New York, 2003.
[2] M.J. Richardson, E.L. Charsley, in: M.E. Brown (Ed.), Handbook of Thermal Analysis and Calorimetry, vol.: Principles and Practice, Elsevier Science B.V, Amsterdam, 1998 (Chapter 13).
[3] G. Della Gatta, M.J. Richardson, S.M. Sarge, S. Stølen, Pure Appl. Chem. 78 (2006) 1455.
[4] G.W.H. Höhne, H.K. Cammenga, W. Eysel, E. Gmelin, W. Hemminger, Thermochim. Acta 160 (1990) 1.
[5] M.J. Richardson, in: D. Maglic, A. Cezairliyan, V.E. Peletsky (Eds.), Compendium of Thermophysical Property Measurement Methods, Plenum Press, New York, 1992, p. 519.
[6] E.L. Charsley, P.G. Laye, V. Palakollu, J.J. Rooney, B. Joseph, Thermochim. Acta 446 (2006) 29.
[7] E.L. Charsley, P.G. Laye, H.M. Markham, J.O. Hill, B. Berger, T.T. Griffiths, Thermochim. Acta 469 (2008) 65.
[8] P. Skoglund, Å. Fransson, Thermochim. Acta 276 (1996) 27.
[9] D.N. Price, J. Therm. Anal. 45 (1995) 1285.
[10] Reference Materials for Physical Properties 2008/2009, LGC Limited, Teddington, 2008, p. 6.
[11] M.J. Richardson, Thermochim. Acta 300 (1997) 15.
[12] E. Charrier, E.L. Charsley, P.G. Laye, H.M. Markham, B. Berger, T.T. Griffiths, Thermochim. Acta 445 (2006) 36.
[13] E.L. Charsley, P.G. Laye, H.M. Markham, T. Le Goff, Thermochim. Acta, in preparation.

Thermochimica Acta 539 (2012) 115–117

Contents lists available at SciVerse ScienceDirect

Thermochimica Acta

journal homepage: www.elsevier.com/locate/tca

Short communication

The use of organic calibration standards in the enthalpy calibration of differential scanning calorimeters

E.L. Charsley[a,*], P.G. Laye[a], H.M. Markham[b]

[a] Centre for Thermal Studies, IPOS, University of Huddersfield, Queensgate, Huddersfield HD1 3DH, UK
[b] Department of Chemical and Biological Sciences, University of Huddersfield, Queensgate, Huddersfield HD1 3DH, UK

ARTICLE INFO

Article history:
Received 22 February 2012
Received in revised form 23 March 2012
Accepted 30 March 2012
Available online 6 April 2012

Keywords:
DSC
Calibration
Enthalpy
Indium
Organic certified reference materials

ABSTRACT

The LCG Limited organic DSC calibration standards have been used to carry out the enthalpy calibration of a power compensated DSC in a temperature range (42–147 °C) for which suitable metal standards are not available. The mean calibration factor was in agreement with the value obtained using indium, thus demonstrating that there was no significant error in using indium as a single point calibrant for measurements on the fusion of organic materials at lower temperatures.

© 2012 Elsevier B.V. All rights reserved.

1. Introduction

A comparison between the use of the certified reference materials indium and diphenylacetic acid for calibrating differential scanning calorimeters for temperature and enthalpy was discussed in a previous paper [1]. The close proximity of the melting temperatures of the materials enabled a direct assessment to be made of any differences between the use of a metal or an organic compound in the calibration of DSC equipment. The measurements established clearly that indium could be used to calibrate for both temperature and enthalpy when making accurate DSC measurements on organic materials at a similar temperature.

We have now extended the enthalpy measurements to the other organic DSC calibration standards marketed by LGC Limited. The materials have certified enthalpies of fusion determined by adiabatic calorimetry. The melting temperatures cover the range 42–147 °C. This has allowed us to examine the temperature dependence of the calibration factor for enthalpy and hence for the possible presence of systematic errors arising from the common practice of performing a single point calibration using indium.

The enthalpies of fusion have been measured using Richardson's construction [2] in which explicit allowance is made for the change in heat capacity over the width of the fusion peak. The method has been illustrated in a number of publications and allows the enthalpy to be determined for the melting process at the equilibrium melting temperature. The results have been compared with those obtained using the more conventional approach in which the area of the fusion peak is delineated by a straight base line drawn from the start to finish of the peak.

2. Experimental

Indium was obtained from LGC Limited (LG2601) and had a certified enthalpy of fusion of $3.296 \pm 0.009\,kJ\,mol^{-1}$ ($28.71 \pm 0.08\,J\,g^{-1}$). The organic standards together with their equilibrium fusion temperatures and enthalpies of fusion are listed in Table 1. The uncertainties for the materials are those cited on the certificate and have a level of confidence of approximately 95%.

The volatility of the organic standards was assessed by thermogravimetry using a Mettler TG-SDTA 851[e] apparatus. The samples (2.5 mg) were contained in an open 20 μl aluminium crucible and heated at $3\,°C\,min^{-1}$. The mass losses were measured at the extrapolated onset temperature of melting and the results are listed in Table 2. With the exception of phenyl salicylate all the samples showed some mass loss with naphthalene and benzoic acid exhibiting high volatility. In view of these mass losses all the DSC experiments were carried out with the samples in encapsulated crucibles. The same procedure was adopted for indium. No mass loss was detected in the subsequent experiments.

The enthalpy measurements were made with a PerkinElmer Diamond DSC with 2.5 mg of the organic calibrants and 10 mg of indium weighed using a 'six figure' balance with a readability of

* Corresponding author. Tel.: +44 01484 473178.
E-mail address: e.l.charsley@hud.ac.uk (E.L. Charsley).

0040-6031/$ – see front matter © 2012 Elsevier B.V. All rights reserved.
http://dx.doi.org/10.1016/j.tca.2012.03.028

Table 1
LGC Limited organic DSC calibration standards.

LGC reference	Standard	Fusion temperature/°C	$\Delta_{fus}H_{cert}$/kJ mol^{-1}
2613	Phenyl salicylate	41.79	19.18 ± 0.08
2610	Biphenyl	68.93	18.60 ± 0.11
2603	Naphthalene	80.23	18.923 ± 0.083
2604	Benzil	94.85	23.26 ± 0.10
2605	Acetanilide	114.34	21.793 ± 0.085
2606	Benzoic acid	122.35	17.98 ± 0.04
2607	Diphenylacetic acid	147.19	31.16 ± 0.13

0.001 mg. The samples were encapsulated in TA Instruments low mass Tzero aluminium crucibles and care was taken to ensure a uniform distribution of the sample over the base of the crucible. A new sample was used for each measurement without preheating and triplicate measurements were performed. The heating rate was 3 °C min^{-1} and an atmosphere of nitrogen was maintained in the equipment (20 cm^3 min^{-1}). An empty encapsulated crucible was used as a reference. Regular checks were carried out using indium to monitor the performance of the instrument.

The determination of the enthalpy of melting by Richardson's method was implemented by copying the experimental data into Microsoft Excel. The experimental data over 2 °C intervals immediately preceding and following melting were represented by linear equations which were used to extrapolate the data over the width of the melting peak. The area of the melting peak using a straight base line was also calculated using the experimental data expressed in Excel.

3. Symbols

The calibration factor for enthalpy obtained using the organic DSC standards is represented by γ and is defined as $\gamma = \Delta_{fus}H_{cert}/\Delta_{fus}H_{meas}$ where $\Delta_{fus}H_{meas}$ is the measured enthalpy change at the equilibrium melting temperature and $\Delta_{fus}H_{cert}$ is the certificate value.

4. Results and discussion

All the reference materials gave smooth and reproducible melting curves. The curves showed a small step change over the width of the fusion peaks consistent with a small change in heat capacity. The values of the enthalpies obtained from the area measurements using Richardson's construction are listed in Table 3. The uncertainties are our estimates of the reliability of the values. They are based on single standard deviations of the means of the experimental results and include an allowance for the uncertainty in assigning the onset temperature of melting and the error in the weighings. The values were not unduly sensitive to the assigned melting temperature in keeping with the small heat capacity change on fusion. The majority of results showed excellent reproducibility (0.1–0.3%). Only a small error (0.2%) was introduced by using a straight base line to define the area of the melting peak. It is tempting to suggest that the higher uncertainty shown by the results for benzoic acid (0.7%) was associated with its greater volatility (Table 2) but the results for naphthalene showed excellent reproducibility in spite of its high volatility.

Table 2
Mass loss of organic DSC standards measured at the melting temperature in open crucibles.

Standard	Mass loss/%
Phenyl salicylate	0.0
Biphenyl	3.7
Naphthalene	41.5
Benzil	0.5
Acetanilide	2.9
Benzoic acid	37.5
Diphenylacetic acid	2.8

Table 3
Calorimetric results obtained using the organic DSC standards.

Standard	$\Delta_{fus}H_{cert}$/J g^{-1} [a]	$\Delta_{fus}H_{meas}$/J g^{-1}	γ
Phenyl salicylate	89.53 ± 0.19	88.5 ± 0.3	1.012 ± 0.004
Biphenyl	120.6 ± 0.4	120.0 ± 0.2	1.005 ± 0.004
Naphthalene	147.64 ± 0.33	146.9 ± 0.2	1.005 ± 0.003
Benzil	110.6 ± 0.3	110.9 ± 0.2	0.998 ± 0.003
Acetanilide	161.24 ± 0.32	161.5 ± 0.4	0.997 ± 0.003
Benzoic acid	147.2 ± 0.2	147.3 ± 1.0	0.999 ± 0.007
Diphenylacetic acid	146.8 ± 0.3	146.9 ± 0.3	0.999 ± 0.003

[a] The errors for the DSC standards are shown as single standard deviations to facilitate comparison with the experimental results.

Table 4
Calorimetric results obtained for the organic DSC standards using indium as a single point calibrant.

Standard	$\Delta_{fus}H_{calib}$/J g^{-1}	$\Delta_{fus}H_{cert} - \Delta_{fus}H_{calib}$/J g^{-1}	Error/%
Phenyl salicylate	88.5 ± 0.3	1.0 ± 0.4	1.1
Biphenyl	120.0 ± 0.3	0.6 ± 0.5	0.5
Naphthalene	146.9 ± 0.4	0.7 ± 0.5	0.5
Benzil	110.9 ± 0.3	−0.3 ± 0.4	−0.3
Acetanilide	161.5 ± 0.5	−0.3 ± 0.6	−0.2
Benzoic acid	147.3 ± 1.0	−0.1 ± 1.0	−0.1
Diphenylacetic acid	146.9 ± 0.4	−0.1 ± 0.5	−0.1

% error = $100 \times (\Delta_{fus}H_{cert} - \Delta_{fus}H_{calib})/(\Delta_{fus}H_{cert})$.

Table 3 shows the calibration factor γ calculated from the experimental enthalpies of fusion of the organic standards. The uncertainties have been obtained by combining the errors in the present work with those associated with the certificate values. The values of γ appear to show a small increase at the lower temperatures but only the value for phenyl salicylate (1.012 ± 0.004) fell outside the combined errors. The mean value of the calibration factor γ over the entire temperature range was 1.002 ± 0.002.

An alternative interpretation of the results is possible by incorporating the indium calibration factor into the enthalpy calculations. This allows a direct comparison to be made between the experimental values for the enthalpy of fusion ($\Delta_{fus}H_{calib}$) and the certified values. Hence the difference $\Delta_{fus}H_{calib} - \Delta_{fus}H_{cert}$ is the error introduced by using indium as a single point calibrant. In the present work the value obtained for the indium calibration factor was 1.000 ± 0.002 (the value of unity is fortuitous) and the enthalpy changes remain unchanged from the values listed in Table 3 but showed a small increase in the uncertainty. The values for the error $\Delta_{fus}H_{calib} - \Delta_{fus}H_{cert}$ are listed in Table 4, together with the percentage error: $\% = 100 \times (\Delta_{fus}H_{calib} - \Delta_{fus}H_{cert})/\Delta_{fus}H_{cert}$. Apart from phenyl salicylate, the lowest melting material, the errors were <0.5% and were within the experimental uncertainties. Thus for the present apparatus it is possible to use indium as a single point DSC enthalpy calibrant when carrying out quantitative measurements on organic materials with significantly lower melting temperatures.

5. Conclusions

The organic DSC standards provide the opportunity of calibrating DSC equipment in a temperature range for which there are no suitable metals and allow the temperature dependence of the calorimetric results to be assessed. All the materials gave reproducible fusion curves and enthalpy measurements were obtained with uncertainties of ~0.3% with the exception of benzoic acid where the uncertainty was 0.7%.

The values of the calibration factor γ appeared to increase at the low temperatures but all the values agreed within the combined uncertainties with the exception of the result for the lowest melting temperature material phenyl salicylate (42 °C). The mean calibration factor $\gamma = 1.002 \pm 0.002$ was in agreement with the value obtained with indium (1.000 ± 0.002) and we conclude that overall there was no significant error in using indium as a single point calibrant for measurements on the fusion of organic materials at lower temperatures.

We would anticipate that equipment similar to that used in the present work would show similar behaviour. However, it is important with all DSC equipment that the temperature dependence of the performance is investigated if accurate results are to be obtained.

Acknowledgements

We would like to thank LGC Limited for the provision of the DSC Standards and Dr John Warren for helpful comments. We also thank James Rooney of the Centre for Thermal Studies for his skilled technical assistance.

References

[1] E.L. Charsley, P.G. Laye, H.M. Markham, T. Le Goff, Thermochim. Acta 497 (2010) 72.
[2] M.J. Richardson, Thermochim. Acta 350 (1997) 15.

Appendix 3. Secondary Calibration Data

During the measurement of accurate temperatures and enthalpies secondary checks at regular intervals were performed using a sample of high purity indium at both a linear heating rate of 3°C min^{-1} and under near equilibrium conditions using the stepwise method. For both the HF-DSC and PC-DSC their secondary temperature and enthalpy checks are provided in the following figures and show that over the course of 1500 runs little deviation in the temperatures measured were seen. The enthalpy measurements were erratic over time when measured using the HF-DSC system however, were remarkably consistent when measured using the PC-DSC system.

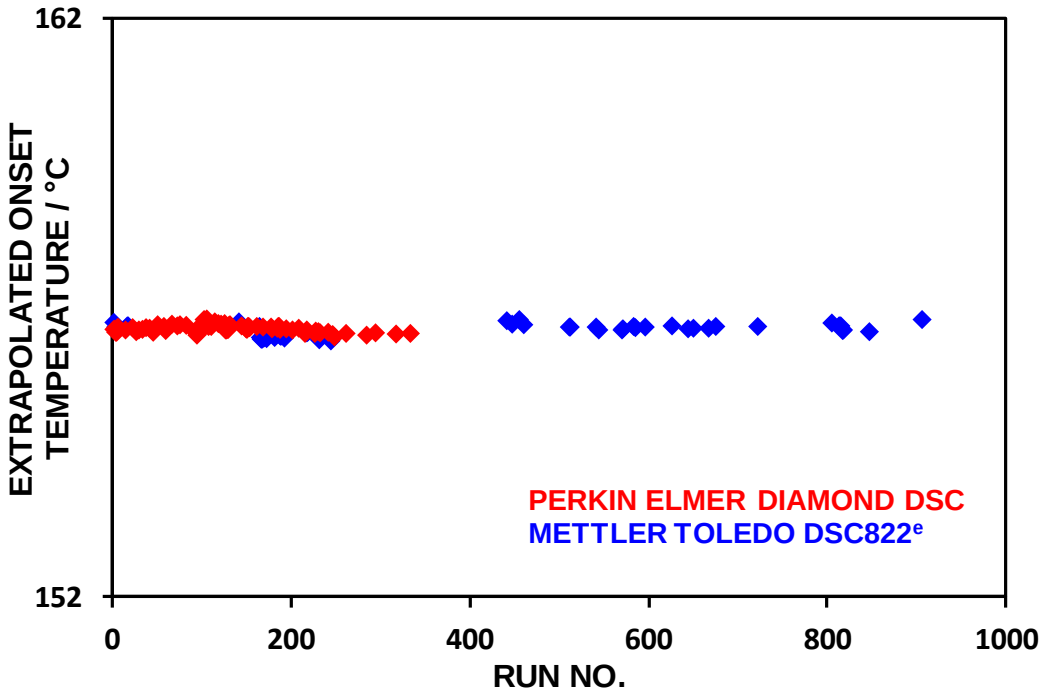

Fig. 75. ***Secondary Temperature Calibration Checks Using LGC Indium at 3°C min^{-1}***

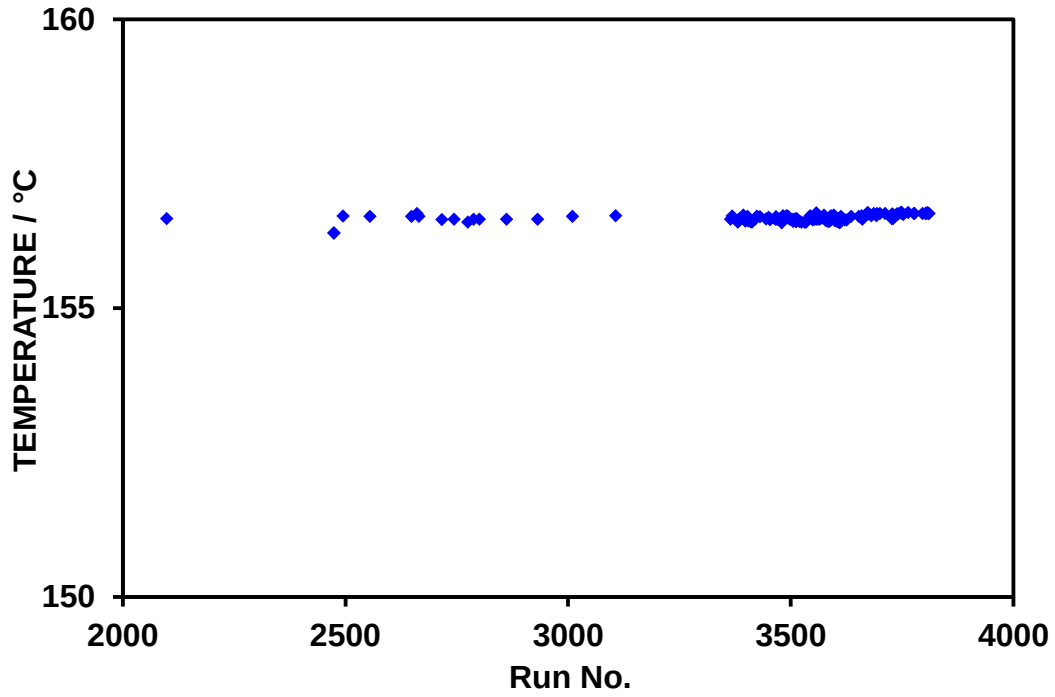

Fig. 76. ***Mettler Toledo DSC822^e Secondary Temperature Calibration Checks Using Stepwise LGC Indium***

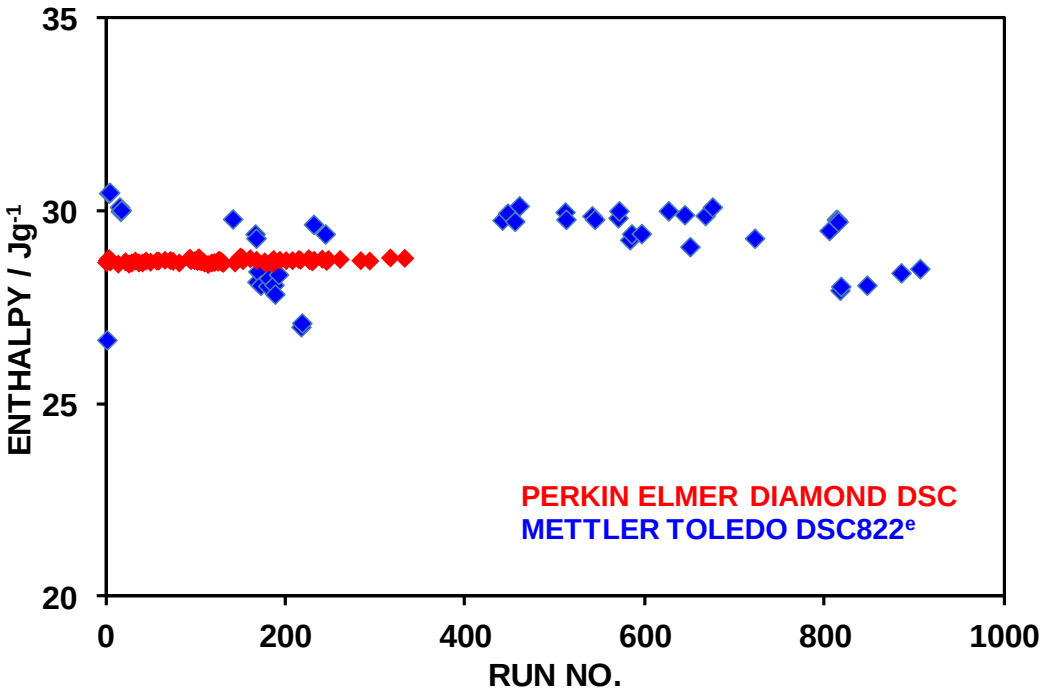

Fig. 77. ***Enthalpy Calibration Checks Using LGC Indium***